


Crossover from the macroscopic fluctuation theory to the Kardar-Parisi-Zhang equation controls the large deviations beyond Einstein's diffusion

Alexandre Krajenbrink ^{*}

Quantinuum, Terrington House, 13–15 Hills Road, Cambridge CB2 1NL, United Kingdom

Pierre Le Doussal[†]

Laboratoire de Physique de l'École Normale Supérieure, CNRS, ENS & PSL University, Sorbonne Université, Université de Paris, 75005 Paris, France

 (Received 26 April 2022; accepted 21 December 2022; published 27 January 2023)

We study the crossover from the macroscopic fluctuation theory (MFT), which describes one-dimensional stochastic diffusive systems at *late times*, to the weak noise theory (WNT), which describes the Kardar-Parisi-Zhang (KPZ) equation at *early times*. We focus on the example of the diffusion in a time-dependent random field, observed in an atypical direction which induces an asymmetry. The crossover is described by a nonlinear system which interpolates between the derivative and the standard nonlinear Schrodinger equations in imaginary time. We solve this system using the inverse scattering method for mixed-time boundary conditions introduced by us to solve the WNT. We obtain the rate function which describes the large deviations of the sample-to-sample fluctuations of the cumulative distribution of the tracer position. It exhibits a crossover as the asymmetry is varied, recovering both MFT and KPZ limits. We sketch how it is consistent with extracting the asymptotics of a Fredholm determinant formula, recently derived for sticky Brownian motions. The crossover mechanism studied here should generalize to a larger class of models described by the MFT. Our results apply to study extremal diffusion beyond Einstein's theory.

DOI: [10.1103/PhysRevE.107.014137](https://doi.org/10.1103/PhysRevE.107.014137)

I. INTRODUCTION

A. Overview and model

For one-dimensional stochastic systems with a diffusive scaling at large time, such as the symmetric exclusion process (SEP), the macroscopic fluctuation theory (MFT) [1] provides a powerful framework to describe the large deviations of the density and current [2]. Upon introduction of an asymmetry or driving, such as in the asymmetric exclusion process (ASEP) [3], the diffusive scaling breaks down above some scale, and the large-scale behavior of the model is usually described by the Kardar-Parisi-Zhang (KPZ) universality class [4]. A paradigmatic member of this class is the KPZ equation [5], which can be obtained as the continuum limit of the ASEP with a weak asymmetry [6]. The large deviations for the KPZ equation at short time can be described using the so-called weak noise theory (WNT) [7–9]. It is a close cousin of the MFT; both reduce the calculation of large-deviation rate functions to solving saddle-point partial nonlinear differential equations, not always an easy task. A natural question is to understand, in presence of a small but relevant asymmetry, the nature of the crossover from the MFT to the WNT. We can expect that it should be somewhat subtle since the MFT describes the large deviations at large time, while the WNT

describes the large deviations for the KPZ equation at short time.

Recently, exact solutions of the WNT equations were obtained by us [10,11]. It required to extend the inverse scattering method of Refs. [12,13] to mixed-time boundary conditions on the so-called $\{P, Q\}$ system, a close cousin of the nonlinear Schrodinger equation (NLS). In this paper we show on an example that the crossover from the MFT to the WNT can be realized as the crossover from the derivative nonlinear Schrodinger equation (DNLS) [14] to the NLS equation. We focus on a model for the diffusion of a particle (also called a tracer) at position $y(\tau)$ convected by a centered Gaussian random field $\eta(y, \tau)$ which is white noise in time and short-range correlated in space, described by a Langevin equation,

$$\frac{dy(\tau)}{dt} = \sqrt{2}\eta(y(\tau), \tau) + \chi(\tau), \quad (1)$$

where χ is a standard white noise in time. In this paper we consider the limit where $\eta(y, \tau)$ is white noise also in space. Equivalently, the probability density function (PDF) for the particle position in a given realization of η , $q_\eta(y, \tau) = \langle \delta(y(\tau) - y) \rangle_\chi$, obeys the Fokker-Planck equation

$$\partial_\tau q_\eta(y, \tau) = \partial_y^2 q_\eta(y, \tau) - \partial_y(\sqrt{2}\eta(y, \tau)q_\eta(y, \tau)). \quad (2)$$

This model, and its discrete random walk versions, has been revisited recently [15–20]. The typical behavior is rather dull, and is given by the random field average $\bar{q}_\eta(y, \tau)$ which yields standard diffusion $y \sim \sqrt{\tau}$. However, in the space-time directions which are *atypical* for the random walk, e.g.,

^{*}alexandre.krajenbrink@quantinuum.com

[†]pierre.ledoussal@phys.ens.fr

$y \sim v\tau$, it exhibits interesting sample to sample fluctuations related to the KPZ class [15]. In fact, in the small v regime (more precisely for $y \sim \tau^{3/4}$), it maps to the KPZ equation itself (as predicted in Refs. [16,18] and proved in Ref. [20], see also Ref. [17]). These predictions found interesting applications in quantum models with noise, for the study of observables dominated by atypical trajectories [21]. They also lead to interesting predictions for extremal diffusions [15,16,20,22], i.e., for the position of the maximum of N independent particles, see below. It turns out that Eq. (2) also arises from a lattice gas model of heat transfer, the Kipnis-Marchioro-Presutti (KMP) model [23], to which the MFT has been applied [1,24–36]. Hence, we anticipate a crossover from the MFT to the WNT when focusing on less and less typical directions. It is an interesting and open question to understand how the large-time large deviations of this model match the short-time large deviations of the KPZ equation.

In this paper we show that this crossover is described by the so-called interpolating system, see Eq. (11) below. Using inverse scattering methods we provide the solution for this system and obtain the large deviation function of a particular observable. At the end we sketch how the result agrees with the asymptotic behavior of a Fredholm determinant formula for this observable obtained in Ref. [19] for a related model of sticky Brownian motions.

B. Observables of interest

We consider a particle which is at position $y = 0$ at time $\tau = 0$ and study the statistics of the probability $Z(Y, T)$ (quenched w.r.t. η) that at time $\tau = T$ it is found to the right of $y = Y$,

$$Z(Y, T) = \mathbb{P}(y(T) > Y | y(0) = 0). \quad (3)$$

We also need to introduce $H(Y, T)$ the logarithm of this probability, our observable of interest here. It also equals

$$Z(Y, T) = e^{H(Y, T)} = \int_Y^{+\infty} dy q_\eta(y, T), \quad (4)$$

with $q_\eta(y, 0) = \delta(y)$. Note that $H(Y, T) \in [-\infty, 0]$ since $Z = Z(Y, T) \in [0, 1]$. $Z(Y, T)$ is itself a random variable that fluctuates depending on the realization of $\eta(y, \tau)$, which from now on is a standard white noise in space and time. We consider the diffusive scaling so that Y, T are large, with $Y = \xi\sqrt{T}$, where $\xi = \mathcal{O}(1)$ is fixed and plays the role of the asymmetry parameter. We are interested in the tails of the PDF of $Z = Z(Y, T)$, equivalently of $H = H(Y, T)$, which take the large deviation forms for $T \gg 1$,

$$\mathcal{P}(Z) \sim e^{-\sqrt{T}\Phi(Z)}, \quad \mathcal{P}(H) \sim e^{-\sqrt{T}\Phi(H)}, \quad (5)$$

where $\Phi(H) = \hat{\Phi}(Z = e^H)$ is the rate function which we want to compute, together with its (implicit) dependence in ξ .

We perform a change of variable $y = x\sqrt{T}$, $\tau = tT$, and $\sqrt{T}q_\eta(y, \tau) = Q_{\tilde{\eta}}(x, t)$ so that Eq. (2) becomes

$$\partial_t Q_{\tilde{\eta}} = \partial_x^2 Q_{\tilde{\eta}}(x, t) - T^{-1/4} \partial_x (\sqrt{2}\tilde{\eta}(x, t) Q_{\tilde{\eta}}(x, t)), \quad (6)$$

where $\tilde{\eta}$ is a standard white noise and $Z(Y, T) = \int_\xi^{+\infty} dx Q_{\tilde{\eta}}(x, 1)$. To obtain $\Phi(H)$ in Eq. (5) we will first calculate the rate function $\Psi(z)$ which is the cumulant generating

function with Laplace parameter z ,

$$\overline{\exp(-z\sqrt{T}Z(Y, T))} \sim \exp(-\sqrt{T}\Psi(z)). \quad (7)$$

Since Z is a random variable taking values in $[0, 1]$, $\Psi(z)$ is defined for any real value of the Laplace parameter z , with $\Psi'(z) \in [0, 1]$; see Appendix D. Using Eq. (5) one can compute the expectation value in the left-hand side (l.h.s.) of Eq. (7) for $T \gg 1$ via a saddle-point method and obtain the relation

$$\Psi(z) = \min_{H \leq 0} [\Phi(H) + ze^H] = \min_{Z \in [0, 1]} [\hat{\Phi}(Z) + zZ], \quad (8)$$

which shows that $\Psi(z)$ and $\Phi(H)$ are Legendre transforms [37]. The minimum in Eq. (8) is attained at $H = H(z)$ which is a solution of $\Phi'(H) = -ze^H$. As will be explained subsequently, a remarkable feature of the present problem is that for $\xi > \sqrt{8}$ this equation has more than one solution, which leads to different possible branches for $\Psi(z)$. In that case, we will call the ‘‘optimal’’ $\Psi(z)$ the function defined from Eq. (8) [and Eq. (7)], i.e., as a global minimum, which will thus exhibit a *first-order transition*, with a jump in $\Psi'(z)$. Our strategy will be to compute all branches of $\Psi(z)$, which allow us to reconstruct $\Phi(H)$ and $\hat{\Phi}(Z)$. As we will see below, both $\Phi(H)$ and $\hat{\Phi}(Z)$ are smooth functions. However, they can develop nonconvex parts leading to a first-order transition in $\Psi(z)$, as in other large deviation problems [44].

C. Outline

The outline of the paper is as follows. We start by showing that the problem is described by the interpolating system in Sec. II. In Sec. III we solve the interpolating system using the inverse scattering method for mixed-time boundary conditions. Section IV is devoted to the results as applied to the present problem in MFT. In Sec. IV A we give the main branch of $\Psi(z)$ and in Sec. IV B we show that there are other branches, we obtain them as well as $\Phi(H)$. In Sec. IV C we discuss the first-order transition in $\Psi(z)$ and in Sec. IV D the structure in terms of solitons. In Sec. V we study the large ξ limit and show that it matches the known results from WNT for the KPZ equation at short time. In Sec. VI we sketch an asymptotic analysis of a Fredholm determinant formula. In Sec. VII A we apply our results to the problem of the extremal diffusion. Finally, in Sec. VII B we discuss other models such as the SEP. The derivations in the main text have been streamlined, and all the details are contained the Appendices.

II. INTERPOLATING SYSTEM

To compute $\Psi(z)$ we note that, as in Ref. [10], the l.h.s. of Eq. (7) can be represented as a path integral

$$\int \mathcal{D}QDP e^{-\sqrt{T}(S[P, Q] + z \int_\xi^{+\infty} dx Q(x, 1))}, \quad (9)$$

where the associated dynamical action is

$$S[P, Q] = \int_0^1 dt \int_{\mathbb{R}} dx [P(\partial_t - \partial_x^2)Q - Q^2(\partial_x P)^2], \quad (10)$$

and $P\sqrt{T}$ is the response field. In the large T limit the path integral in Eq. (9) is controlled by its saddle point.

Taking the functional derivatives w.r.t. $\{P, Q\}$, introducing the field $R(x, t) = \partial_x P(x, t)$, and performing a Galilean transformation $x \rightarrow x - \xi t$ to bring ξ back to zero (see details in Appendix A), we arrive at the system of coupled equations

$$\begin{aligned} \partial_t Q &= \partial_x^2 Q + 2\beta \partial_x(Q^2 R) + 2gQ^2 R, \\ -\partial_t R &= \partial_x^2 R - 2\beta \partial_x(QR^2) + 2gQR^2, \end{aligned} \quad (11)$$

with $\beta = -1$ [38] and $g = -\beta\xi/2$ and with the mixed-time boundary conditions

$$Q(x, t=0) = \delta(x), \quad R(x, t=1) = \Lambda\delta(x), \quad (12)$$

with $\beta\Lambda = ze^{-\frac{\xi^2}{4}}$ [39]. Once this system is solved, the value of $\Psi(z)$ is obtained from the saddle point via (see Appendix A)

$$\Psi'(z) = \int_0^{+\infty} dx Q(x, 1) e^{-\frac{1}{2}x\xi - \frac{\xi^2}{4}} \quad (13)$$

and $\Psi(0) = 0$, where $Q(x, 1)$ is the z -dependent solution of the above system. This system interpolates between (i) the $\{P, Q\}$ system for $\beta = 0$ (with P called R here), i.e., the cousin of the NLS equation [12,13] which controls the WNT of the KPZ equation [10,11], and (ii) the cousin of the DNLS equation [14] for $g = 0$, which controls the MFT for this model for $\xi = 0$ [40]. Thus, as $\xi = \frac{Y}{\sqrt{T}}$ is increased, g increases and in the limit of large ξ , which corresponds to atypical directions, one recovers the large deviations associated to the KPZ equation (see below). Remarkably, this interpolating system is again integrable [41]. We will thus extend the inverse scattering analysis of our previous work [10,11] on the $\{P, Q\}$ system. Note in passing that the functions $Q(x, t)$ and $R(x, t)$ are not even for $\beta \neq 0$ but as in the $\{P, Q\}$ system they still enjoy the symmetry

$$R(x, t) = \Lambda Q(-x, 1-t). \quad (14)$$

III. INVERSE SCATTERING SOLUTION OF THE INTERPOLATING SYSTEM

We now solve the problem using the inverse scattering method. It is a simple generalization of our previous works [10,11] so we will sketch it. The Lax pair of linear differential equation reads $\partial_x \vec{v} = U_1 \vec{v}$, $\partial_t \vec{v} = U_2 \vec{v}$, where $\vec{v} = (v_1, v_2)^T$ is a two component vector (depending on x, t, k), where

$$U_1 = \begin{pmatrix} -\frac{ik}{2} & -(g + i\beta k)R(x, t) \\ Q(x, t) & \frac{ik}{2} \end{pmatrix}, \quad U_2 = \begin{pmatrix} \mathbf{A} & \mathbf{B} \\ \mathbf{C} & -\mathbf{A} \end{pmatrix}, \quad (15)$$

with $\mathbf{A} = \frac{k^2}{2} - (g + i\beta k)QR$, $\mathbf{B} = -(g + i\beta k)((ik - \partial_x)R + 2\beta QR^2)$, $\mathbf{C} = (\partial_x + ik)Q + 2\beta Q^2 R$. One can check that the compatibility condition $\partial_t U_1 - \partial_x U_2 + [U_1, U_2] = 0$ recovers (11). Let $\vec{v} = e^{k^2 t/2} \phi$ with $\phi = (\phi_1, \phi_2)^T$ and $\vec{v} = e^{-k^2 t/2} \bar{\phi}$ be two independent solutions of the linear problem such that at $x \rightarrow -\infty$, $\phi \simeq (e^{-ikx/2}, 0)^T$ and $\bar{\phi} \simeq (0, -e^{ikx/2})^T$. Assuming from now on that $\{Q, R\}$ vanish at infinity, the $x \rightarrow +\infty$ behavior of these solutions defines scattering amplitudes

$$\phi_{x \rightarrow +\infty} \simeq \begin{pmatrix} a(k, t) e^{-\frac{ikx}{2}} \\ b(k, t) e^{\frac{ikx}{2}} \end{pmatrix}, \quad \bar{\phi}_{x \rightarrow +\infty} \simeq \begin{pmatrix} \tilde{b}(k, t) e^{-\frac{ikx}{2}} \\ -\tilde{a}(k, t) e^{\frac{ikx}{2}} \end{pmatrix}. \quad (16)$$

Plugging this form into the ∂_t equation of the Lax pair at $x \rightarrow +\infty$, one finds a very simple time dependence, $a(k, t) = a(k)$ and $b(k, t) = b(k)e^{-k^2 t}$, $\tilde{a}(k, t) = \tilde{a}(k)$ and $\tilde{b}(k, t) = \tilde{b}(k)e^{k^2 t}$. Another normalization relation is obtained from the Wronskian of the two solutions, $a(k)\tilde{a}(k) + b(k)\tilde{b}(k) = 1$.

Integrating the ∂_x equation of the Lax pair successively for $\bar{\phi}$ and ϕ at $t = 0$ and at $t = 1$, using Eq. (12), allows us to obtain (see details in Appendix B)

$$\tilde{b}(k) = (g + i\beta k)\Lambda e^{-k^2}, \quad b(k) = 1, \quad (17)$$

and

$$\begin{aligned} a(k) &= 1 - (g + i\beta k)\Lambda Q_-(k), \\ \tilde{a}(k) &= 1 - (g + i\beta k)\Lambda Q_+(k), \end{aligned} \quad (18)$$

where we have defined the half-Fourier transforms

$$Q_{\pm}(k) = \int_{\mathbb{R}^{\pm}} dx Q(x, 1) e^{-ikx}, \quad (19)$$

where \mathbb{R}^{\pm} refers to the positive axis \mathbb{R}^+ or the negative axis \mathbb{R}^- , respectively. From the normalization relation one also obtains

$$a(k)\tilde{a}(k) = 1 - b(k)\tilde{b}(k) = 1 - (g + i\beta k)\Lambda e^{-k^2}, \quad (20)$$

which $Q_{\pm}(k)$ must satisfy. For $\beta = 0$ this equation was first obtained by us in Ref. [10] and used recently in Ref. [42]. As noted there, it is akin to the Fourier transform of the Wiener-Hopf formulas obtained in Ref. [35, Eqs. (S65) and (S66)]. Our Eq. (20) is thus the natural extension to arbitrary g, β .

Taking these relations in the large k limit we obtain that $Q(x, 1)$ has a jump at $x = 0$, with some relation between the right and left values $Q(0^{\pm}, 1)$. We now follow similar manipulations as in the recent work [40], the details are given in Appendix C. As $k \rightarrow \infty$ one has

$$Q_{\pm}(k) \simeq \pm \frac{1}{ik} Q(0^{\pm}, 1), \quad (21)$$

$$a(k) \simeq 1 + \beta\Lambda Q(0^-, 1), \quad (22)$$

$$\tilde{a}(k) \simeq 1 - \beta\Lambda Q(0^+, 1). \quad (23)$$

Equation (20) at $k \rightarrow \infty$ thus implies a first relation,

$$[1 - \beta\Lambda Q(0^+, 1)][1 + \beta\Lambda Q(0^-, 1)] = 1. \quad (24)$$

The complete solution of Eq. (20) is given by (see Appendix C)

$$\begin{aligned} a(k) &= (1 + \beta\Lambda Q(0^-, 1))e^{\Phi_+(k)}, \\ \tilde{a}(k) &= (1 - \beta\Lambda Q(0^+, 1))e^{\Phi_-(k)}, \end{aligned} \quad (25)$$

where

$$\begin{aligned} \Phi_{\pm}(k) &= \pm \int_{\mathbb{R}} \frac{dq}{2i\pi} \frac{\ln(1 - (g + i\beta q)\Lambda e^{-q^2})}{q - k \mp i0^+} \\ &= \pm \int_{\mathbb{R}} \frac{dq}{2i\pi} \frac{\ln(1 - (g + i\beta q)\Lambda e^{-q^2})}{q - k} \\ &\quad + \frac{1}{2} \ln(1 - (g + i\beta k)\Lambda e^{-k^2}). \end{aligned} \quad (26)$$

The first expression for $\Phi_{\pm}(k)$ is valid for k in the complex upper/lower half plane including the real line, while the

second is valid for real k only. In the limit $\beta \rightarrow 0$ one has $Q(0^+, 1) = Q(0^-, 1)$ and one recovers the same formula as first obtained in Ref. [10]. In the limit $g \rightarrow 0$ one recovers the recent result in Ref. [40].

We still need to determine the two unknown constants $Q(0^\pm, 1)$ which are related by Eq. (24). Combining Eqs. (18) and (25) we obtain the relation

$$(g + i\beta k)\Lambda Q_\mp(k) = 1 - (1 \pm \beta\Lambda Q(0^\mp, 1))e^{\Phi_\pm(k)}, \quad (27)$$

which is valid for $\Im(k) \in \mathbb{R}^\pm$. Taken at $k = \frac{ig}{\beta} = -i\frac{\xi}{2}$ one obtains

$$1 \pm \beta\Lambda Q(0^\mp, 1) = e^{-\Phi_\pm(ig/\beta)}, \quad (28)$$

where, for $g/\beta \neq 0$,

$$\Phi_\pm(ig/\beta) = \pm\beta \int_{\mathbb{R}} \frac{dq \ln(1 - (g + i\beta q)\Lambda e^{-q^2})}{2\pi(g + i\beta q)} \quad (29)$$

are opposite real numbers, so that Eq. (28) is compatible with Eq. (24). As discussed below and in Appendix C, Eqs. (26) and (29) are valid only for $\Lambda g < 1$.

IV. SPECIALIZATION OF THE SOLUTION TO THE MFT PROBLEM

A. Rate function $\Psi(z)$: main branch

We now compute $\Psi(z)$ from Eq. (13) and replace $\beta = -1$, $g = -\beta\frac{\xi}{2}$ and $\beta\Lambda = ze^{-\xi^2/4}$. We note that the right-hand side (r.h.s.) of Eq. (13) is equal to

$$\Psi'(z) = Q_+\left(k = -i\frac{\xi}{2}\right)e^{-\frac{\xi^2}{4}} = 1 - Q_-\left(k = -i\frac{\xi}{2}\right)e^{-\frac{\xi^2}{4}}, \quad (30)$$

where the second equality comes from the conservation of probability [see Eq. (A13)]. These quantities $[Q_\pm(k = -i\frac{\xi}{2})]$ can be obtained by taking derivatives. Taking a derivative w.r.t. k of Eq. (27) at $k = \frac{ig}{\beta} = -i\frac{\xi}{2}$ and using Eq. (28) one obtains (see details in Appendix E)

$$z\Psi'(z) = \int_{\mathbb{R}} \frac{dq \ln\left(1 - z\left(iq - \frac{\xi}{2}\right)e^{-q^2 - \frac{\xi^2}{4}}\right)}{2\pi\left(iq - \frac{\xi}{2}\right)^2} + z\Theta(-\xi), \quad (31)$$

where here and below we use the convention that $\Theta(0) = 1/2$ and the principal part is needed only for $\xi = 0$. Integrating over z one obtains

$$\Psi(z) = -\int_{\mathbb{R}} \frac{dq \operatorname{Li}_2\left(z\left(iq - \frac{\xi}{2}\right)e^{-q^2 - \frac{\xi^2}{4}}\right)}{2\pi\left(iq - \frac{\xi}{2}\right)^2} + z\Theta(-\xi), \quad (32)$$

where the last term guarantees analyticity of $\Psi(z)$ in ξ . Denoting here $\Psi_\xi(z)$ to indicate the dependence in ξ and performing the change $q \rightarrow -q$ in the integrand we see that it obeys the symmetry

$$\Psi_{-\xi}(z) = \Psi_\xi(-z) + z, \quad (33)$$

which is expected from the definition (7), since upon the symmetry $y \rightarrow -y$ in Eqs. (2) and (4), the PDF of $Z(Y, T)$ must be the same as the PDF of $1 - Z(-Y, T)$, see Appendix D.

For $\xi = 0$ one can check (see Appendix H5) that Eq. (32) is consistent with the result in Ref. [40].

Expanding Eq. (32) in series of z one predicts the cumulants of the probability $Z = Z(Y, T)$ in Eq. (3). The first one is the typical value $\bar{Z} = Z_{\text{typ}}(\xi) = e^{H_{\text{typ}}(\xi)}$ (i.e., in a typical random field η),

$$\begin{aligned} Z_{\text{typ}}(\xi) &= \Psi'(0) = -\int_{\mathbb{R}} \frac{dq}{2\pi} \frac{e^{-q^2 - \frac{\xi^2}{4}}}{iq - \frac{\xi}{2}} + \Theta(-\xi) \\ &= \frac{1}{2} \operatorname{Erfc}\left(\frac{\xi}{2}\right) = \int_{\xi}^{+\infty} \frac{dx}{\sqrt{4\pi}} e^{-\frac{x^2}{4}}, \end{aligned} \quad (34)$$

as expected since the mean (and typical) behavior is standard diffusion. The second cumulant is predicted as $\bar{Z}(Y, T)^2 \simeq -T^{-1/2}\Psi''(0) = \frac{1}{4\sqrt{2\pi T}}e^{-\frac{\xi^2}{2}}$, as confirmed by a direct weak-noise expansion, see Appendix H6 (and Appendix H7 for the cumulants of $H = \ln Z$).

B. Branch cuts, branches of $\Psi(z)$, and the rate function $\Phi(H)$

We will determine in this section the rate function $\Phi(H)$ for $\xi \geq 0$ [for $\xi < 0$ we rely on the symmetry (33)]. From our expression for $\Psi(z)$ *a priori* one can now determine the rate function for the PDFs in Eq. (5) by inverting the Legendre transform (8), which gives the parametric representation

$$\Phi(H) = \Psi(z) - ze^H, \quad \Psi'(z) = e^H, \quad (35)$$

and in terms of Z ,

$$\hat{\Phi}(Z) = \Psi(z) - zZ, \quad Z = \Psi'(z). \quad (36)$$

As mentioned in the Introduction, the parametric representation (36) can lead to different branches, i.e., a multivaluation of $\Psi(z)$. The "optimal" $\Psi(z)$, i.e., solution of the Legendre transform (8), is defined as the minimum over the different branches.

The origin of these different branches can be traced to the ambiguity which remains for $\Psi(z)$ since we have not specified the determination of the logarithm in Eq. (31). The functions $\ln(1 - x)$, and $\operatorname{Li}_2(x)$ [which appeared in Eq. (32)], admit a branch cut for $x > 1$. There are thus branch cuts in the complex plane for q , which is the integration variable in Eq. (31), and for some values of $\{z, \xi\}$ one of these branch cuts may cross the integration axis, see figures in Appendix G (see also Appendix F for a recall of the case of the KPZ equation). These branch cuts originate from the values of q such that the argument of the logarithm in Eq. (31) vanishes. Parameterizing the integration variable as $q = ip$, we then have to find the solutions (i.e., the zeros) of the following equation

$$e^{-p^2 + \frac{\xi^2}{4}} + z\left(p + \frac{\xi}{2}\right) = 0. \quad (37)$$

For $z > z_c$ where $z_c = -\frac{2}{\xi}e^{\xi^2/4} \leq 0$, there is never a branch cut crossing the real axis, see Appendix G, hence Eqs. (31) and (32) are valid in this regime and determine what we call the *main branch* (as detailed in Appendix E).

For $z < z_c$ all real solutions of Eq. (37) for p are negative and as consequence one branch cut crosses the real axis, see Appendix G. It is then necessary to obtain the analytical

TABLE I. Determination of the jump function $\Delta(z)$ in the different phases in the case $\xi \geq 0$. One has $z_c = -\frac{2}{\xi}e^{\xi^2/4} \leq 0$ and the points $z = z_{c1}$ and $z = z_{c2}$ are turning points which depend on ξ . In the interval $z \in [z_{c1}, z_{c2}]$, the function $\Delta(z)$ is multivalued (i.e., it has several branches) due to these turning points. The definition of Δ_ℓ is given in Eq. (39).

ξ	$0 \leq \xi \leq \xi_1$	$\xi_1 \leq \xi \leq \xi_2$ $z_{c1} < z_{c2} < z_c$	$\xi_2 \leq \xi$ $z_{c1} < z_c < z_{c2}$
$\Delta(z) =$	$\begin{cases} 0, & z_c < z \\ \Delta_1(z), & z < z_c \end{cases}$	$\begin{cases} 0, & z_c < z \\ \Delta_1(z), & z_{c1} < z < z_c \\ \Delta_2(z), & z_{c1} < z < z_{c2} \\ \Delta_3(z), & z < z_{c2} \end{cases}$	$\begin{cases} 0, & z_c < z \\ \Delta_1(z), & z_{c1} < z < z_c \\ \Delta_2(z), & z_{c1} < z < z_c \\ \Delta_2(z) - \Delta_1(z), & z_c < z < z_{c2} \\ \Delta_3(z) - \Delta_1(z), & z_c < z < z_{c2} \\ \Delta_3(z), & z < z_c \end{cases}$

continuation of Eqs. (31) and (32) to any z by deforming the contour of integration for q to avoid this branch cut. In the easiest case this is possible in the complex plane, and in other cases one needs to consider the Riemann sheets, which leads to more branches and multivaluation. The analysis is involved and detailed in Appendix G. Here we summarize the main results. The general formula for $\Psi(z)$ takes the form

$$\Psi(z) = \Psi_0(z) + \Delta(z), \tag{38}$$

where $\Psi_0(z)$ is the same integral as in Eq. (32) [43], and $\Delta(z)$ is the jump contribution from the branch cut, which is discussed below. The convention $\Delta(z) = 0$ defines the main branch of $\Psi(z)$. The other branches and the form of $\Delta(z)$ as a function of ξ and z are shown in Table I.

To understand Table I one needs to first discuss the behavior of the real zeros of Eq. (37) which are the relevant ones to determine $\Psi(z)$. For $z_c \leq z \leq 0$, there is always one positive zero to Eq. (37) denoted $p_1 = p_1(z, \xi)$. For $z < z_c$, the zeros of Eq. (37) are all negative and their number is:

- (1) for $0 < \xi < \xi_1 = \sqrt{8}$, there is one zero $p_1(z, \xi)$;
- (2) for $\xi_1 < \xi$ and $z \in [z_{c1}, z_{c2}[$ there are three zeros $p_1(z, \xi) > p_2(z, \xi) > p_3(z, \xi)$. The zeros degenerate, i.e., $p_1 = p_2$ for $z = z_{c1}$ and $p_2 = p_3$ for $z = z_{c2}$ which define z_{c1}, z_{c2} . For $z > z_{c2}$, there is only one zero $p_1(z, \xi)$. For $z < z_{c1}$, there is only one zero $p_3(z, \xi)$.

Note that $z_{c1} < z_{c2} < 0$, with $z_{c1} = z_{c2}$ at $\xi = \xi_1$, and their explicit expression and dependence on ξ is given in the Appendix in Eq. (H2).

To come back to $\Psi(z)$ we now define a jump function for $\ell = \{1, 2, 3\}$ as

$$\Delta_\ell(z) = - \int_z^{z_c} \frac{dz'}{z'} \frac{4p_\ell(z', \xi)}{\xi(2p_\ell(z', \xi) + \xi)}, \tag{39}$$

see Eqs. (G14) and (G17) in the Appendix for more explicit formula. Our result, as we now discuss, is that the jump $\Delta(z)$ in Eq. (38) is always a linear combination of the $\Delta_\ell(z)$.

Remarkably, the behavior of $\Psi(z)$ exhibits three ‘‘phases’’ depending on the value of ξ with respect to the two critical values $\xi_1 = \sqrt{8}$ and $\xi_2 \simeq 3.13$, Eq. (H1) in the Appendix; see Table I. The function $\Delta(z)$ is multivalued (i.e., it has several branches) for $\xi > \xi_1$ and $z \in [z_{c1}, z_{c2}]$. Using the corresponding expressions for $\Psi(z) = \Psi_0(z) + \Delta(z)$ one can compute $\Psi'(z)$ for each branch, which is shown in Fig. 1(a). Using the parametric system (35) one obtains the relation between z and H , which reads $Z = e^H = \Psi'(z)$ and is shown in Fig. 1(b). Note that $z(H)$ is single-valued but $H(z)$ may not be. One also

obtains the rate function $\Phi(H)$, plotted in Fig. 1(c) and $\hat{\Phi}(Z)$, plotted in Fig. 1(d). We now comment on these plots.

We start with $\xi < \xi_1$. In that case, see Fig. 1(a), the function $\Psi'(z)$ is nicely decreasing from $\Psi'(-\infty) = 1$ to $\Psi'(+\infty) = 0$ and it leads to a function $H(z)$ which is single-valued and monotonous. In Table I, the appearance of $\Delta_1(z)$ below z_c is due to the fact that the zero p_1 becomes negative and the branch cut of the logarithm in Eq. (31) crosses the real axis.

For $\xi > \xi_1$ the function $\Psi'(z)$ is multivalued in the interval $z \in [z_{c1}, z_{c2}]$, as can be seen in Fig. 1(a). Outside of $z \in [z_{c1}, z_{c2}]$, $\Psi'(z)$ is monotonously decreasing and it still has the correct limits $\Psi'(-\infty) = 1$ to $\Psi'(+\infty) = 0$. As a consequence of the multivaluation of $\Psi'(z)$, the corresponding function $z(H)$, shown in Fig. 1(b), is not monotonous anymore, which implies that H as a function of $z \in [z_{c1}, z_{c2}]$ has three branches, $H_j(z)$, $j = 1, 2, 3$. These correspond to the three extrema of $\Phi(H) + ze^H$, and among these extrema only one is the absolute minimum. In Table I, the appearance of $\Delta_2(z)$ and $\Delta_3(z)$ arise from the fact that (i) at the turning point $z = z_{c1}$ we stop following the first zero p_1 and start following p_2 instead, (ii) at the turning point $z = z_{c2}$ we stop following the second zero p_2 and start following p_3 instead. The turning points are located where the consecutive zeros $p_i(z, \xi)$ coalesce.

For $\xi \geq \xi_2$, the ordering between z_c and z_{c2} changes. Hence, to follow the second zero p_2 until its coalescence with p_3 , one needs to cross $z = z_c$ where the branch cut of the logarithm in Eq. (31) crosses again the real axis, requiring to take into account the jump $\Delta_1(z)$ again.

C. Multivaluation and first-order transition

To interpret the S-shape form of $\Psi'(z)$ shown with all its branches in Fig. 1(a), we recall that the optimal $\Psi'(z) = \langle Z \rangle_z$ is the expectation value of the random variable Z under the z -dependent tilted measure

$$\mathcal{P}(Z)e^{-\sqrt{T}zZ} \sim e^{-\sqrt{T}(\hat{\Phi}(Z)+zZ)}. \tag{40}$$

The key point is that for $\xi > \xi_1$ the function $\hat{\Phi}(Z)$ has a concave part; see Fig. 1(d). As a consequence, for $z \in [z_{c1}, z_{c2}]$ the tilted measure (40) develops three extrema at $Z_j(z) = e^{H_j(z)}$, solutions of $\hat{\Phi}'(Z) = -z$. They lead to the three branches of $\Psi'(z) = Z_j(z)$. Equivalently, there are three extremal values $H_j(z)$ in Eq. (8) solutions of Eq. (35). The ‘‘optimal’’ $\Psi(z)$ is

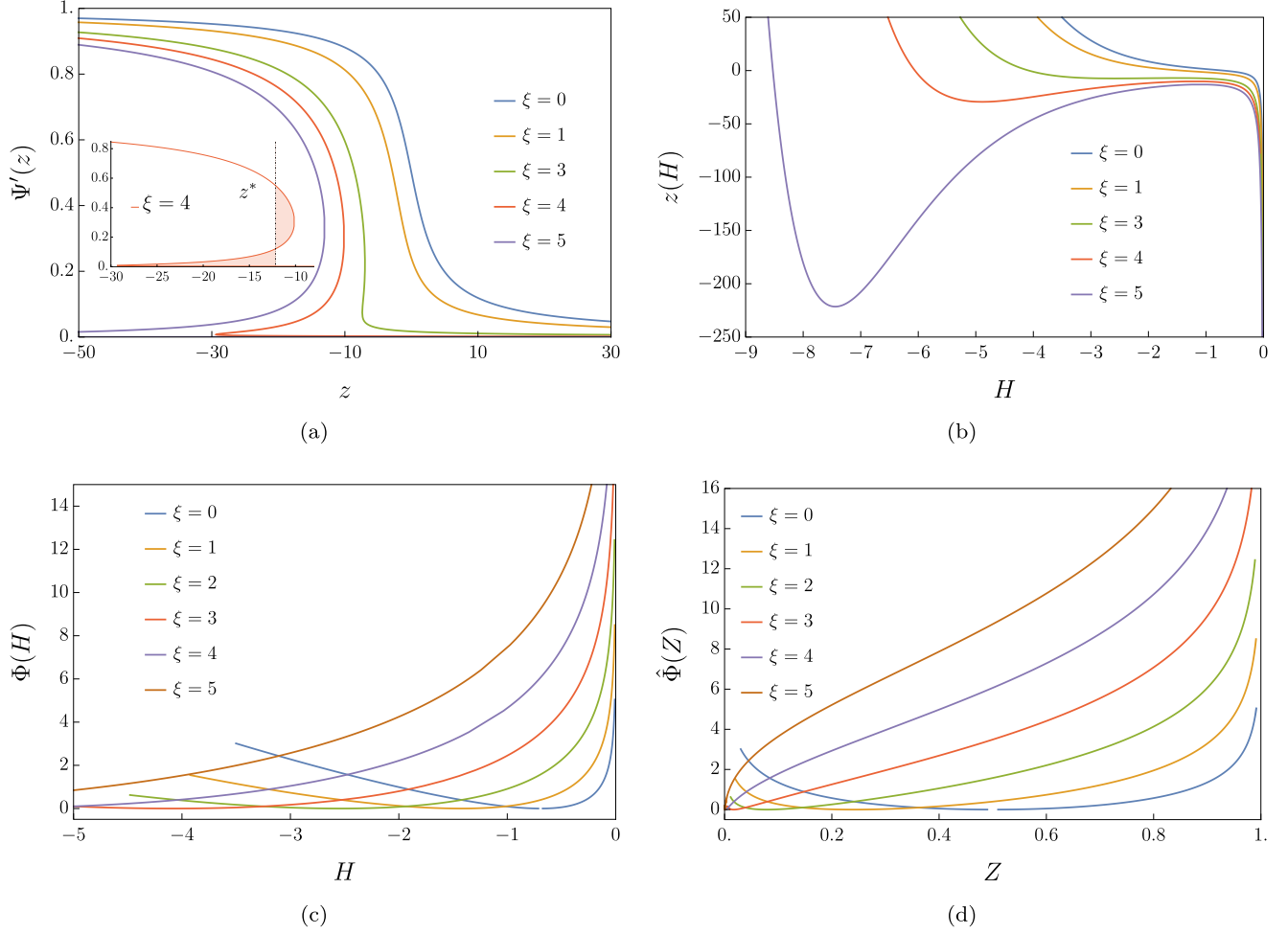


FIG. 1. For $\xi = (0, 1, 2, 3, 4, 5)$ we plot the following. (Top left (a)) The derivative rate function $\Psi'(z)$ from Table I as a function of z , with $\Psi'(+\infty) = 0$ and $\Psi'(-\infty) = 1$ (all the branches are shown). For $\xi > \xi_1$ and $z \in [z_{c1}, z_{c2}]$ the function is multivalued (see text). (Inset) First-order transition: at $z = z^*$ such that the areas of the two shaded regions become equal the value of (the optimal) $\Psi'(z)$ jumps from one branch to the other, shown for $\xi = 4$. (Top right (b)) The function $z = z(H)$ from the Legendre transform (35). The reciprocal function $H(z)$ is multivalued for $\xi > \xi_1$ and $z \in [z_{c1}, z_{c2}]$. (Bottom left (c)) The large deviation rate function $\Phi(H)$ versus H , obtained using the parametric representation (35) and Table I. As ξ increases, the location H_{typ} of the minimum at $\Phi(H_{\text{typ}}) = 0$ is shifted toward negative values. (Bottom right (d)) The rate function $\hat{\Phi}(Z)$ versus Z . For $\xi = 0$, it is symmetric around $Z = 0.5$ and one recovers the result of Ref. [40] (in general, the symmetry is $Z(\xi) \leftrightarrow 1 - Z(-\xi)$). For large values $\xi > \xi_1$, $\hat{\Phi}(Z)$ develops a concave part which is responsible for the first-order phase transition.

determined by the minimum in Eq. (35); hence, it is given by

$$\Psi(z) = \min_{j=1,2,3} [\hat{\Phi}(Z_j) + zZ_j], \quad (41)$$

and the optimal j switches from $j = 1$ to $j = 3$ at $z = z^*(\xi)$, where z^* is the solution of (see Appendix H)

$$\Delta_1(z^*) = \Delta_3(z^*). \quad (42)$$

It is also the point given by an equal area law on the curve $\Psi'(z)$, as in standard magnetization versus field curve for a first-order phase transition; see Fig. 1(a) (inset). The points $Z = \{Z_1, Z_3\}$ are “stable,” whereas $Z = Z_2$ is “unstable.” The optimal rate function $\Psi(z)$ thus exhibits a first-order transition. This type of transition occurs in other large deviation problems [44].

D. Solitons

Let us discuss the significance of the multiple branches in terms of the nature of the solutions of the interpolating system (11). For any value of ξ , the logarithm in the integrand of Φ_{\pm} in Eq. (26) has branch cuts for q in the complex plane. Equivalently, the product $a(k)\tilde{a}(k)$ in Eq. (20) vanishes for some complex $k = k_s = ip_c$ where p_c are generic complex solutions of Eq. (37), indicating the spontaneous generation of a soliton [12]. This means that additional solutions with a solitonic component are possible, as was the case for the WNT of the KPZ equation [10,11]. For that problem, by obtaining the exact solution of the $\{P, Q\}$ system for any space-time point, we were able to show that the multivaluation of $\Psi(z)$ was equivalent to the coexistence of two solutions (in that case with and without a soliton) for the same mixed-time boundary conditions. Here, for $\xi > \sqrt{8}$ the multivaluation of

$\Psi(z)$ similarly indicates the coexistence of three solutions for $\Delta g \in [z_{c2}/z_c, z_{c1}/z_c]$ (a ξ -dependent interval), at least two of them being solitonic. Each of these solutions give rise to a different value $Z_j(z)$, i.e., of the value of the right hand side of Eq. (13). The precise nature and interactions of these solitons will be investigated in a subsequent work [45].

V. LARGE ξ LIMIT AND CONVERGENCE TO KPZ.

We now consider the limit where the tracer particle is located extremely far, i.e., $\xi \rightarrow +\infty$. In that limit we can approximate in Eq. (32) $iq - \frac{\xi}{2} \simeq -\frac{\xi}{2}$ and define $\tilde{z} = z \frac{\xi}{2} e^{-\frac{\xi^2}{4}} = -z/z_c$ to obtain

$$\Psi_0(z) \simeq -\int_{\mathbb{R}} \frac{dq}{2\pi} \frac{\text{Li}_2(-z \frac{\xi}{2} e^{-q^2 - \frac{\xi^2}{4}})}{(\frac{\xi}{2})^2} = \frac{4}{\xi^2} \Psi_{\text{KPZ}}(\tilde{z}), \quad (43)$$

where

$$\Psi_{\text{KPZ}}(\tilde{z}) = -\frac{1}{\sqrt{4\pi}} \text{Li}_{5/2}(-\tilde{z}) \quad (44)$$

is the main branch of the large-deviation rate function for the height field $h_{\text{KPZ}}(0, T_{\text{KPZ}})$ of the KPZ equation with droplet initial condition. This rate function was obtained in Ref. [46] from a Fredholm determinant formula and in Ref. [10] from the exact solution of the WNT, i.e., of the $\{P, Q\}$ system. It admits a second branch denoted $\Psi_{\text{KPZ}}(\tilde{z}) + \Delta_{\text{KPZ}}(\tilde{z})$, which is also recovered; see below.

Hence, at the level of the large deviations, the MFT in the regime $Y \sim \sqrt{T}$ recovers, in the large $\xi = \frac{Y}{\sqrt{T}}$ limit, the result of the WNT for the KPZ equation valid for small KPZ time $T_{\text{KPZ}} \ll 1$. Comparing [10,46] and the present result (43) shows that the correspondence between the MFT time T and the KPZ time T_{KPZ} reads (see Appendix I7)

$$T_{\text{KPZ}} = \frac{Y^4}{16T^3} = \frac{\xi^4}{16T}. \quad (45)$$

This can be compared with Ref. [20] where it was shown, in the different scaling regime $Y \sim T^{3/4}$, i.e., $T_{\text{KPZ}} = \mathcal{O}(1)$, that in law $Z(Y, T) \simeq \frac{Y}{2T} e^{-\frac{Y^2}{4T}} e^{h_{\text{KPZ}}(0, T_{\text{KPZ}})}$, with the same T_{KPZ} as in Eq. (45) (see Appendix I7 for details). Since $\tilde{z} = z \frac{\xi}{2} e^{-\frac{\xi^2}{4}}$, the two results match perfectly, showing that no intermediate regime exists between the diffusive scaling $Y \sim \sqrt{T}$ and the of the finite-time KPZ equation scaling $Y \sim T^{3/4}$ (note that the large-time Tracy-Widom KPZ class universality is seen only for $Y \gg T^{3/4}$).

Finally, as detailed in Appendices I1 and I7, we obtain the convergence at large $\xi \gg 1$ of the rate function for the logarithm $H = \ln Z$, to the rate function of the reduced KPZ height H_{KPZ}

$$\Phi(H) \simeq \frac{4}{\xi^2} \Phi_{\text{KPZ}}(H_{\text{KPZ}}), \quad (46)$$

with the correspondence $H = -\frac{\xi^2}{4} - \ln(\frac{\xi}{2}) + H_{\text{KPZ}}$ and Φ_{KPZ} is the rate function for the KPZ equation, see details and definitions in I7.

We now discuss what happens to the other branches of $\Psi(z)$ at large ξ . We show how the second branch of the KPZ rate function and the value of its jump, Δ_{KPZ} , is recovered in the

limit. Recovering this second branch, which exists for $-1 \leq \tilde{z} < 0$, is necessary for Eq. (46) to hold for all $H_{\text{KPZ}} \in \mathbb{R}$. To this aim, we first define the rescaled critical values of z as

$$\tilde{z}_c = -\frac{z_c}{z_c}, \quad \tilde{z}_{c1} = -\frac{z_{c1}}{z_c}, \quad \tilde{z}_{c2} = -\frac{z_{c2}}{z_c}, \quad (47)$$

and take their large ξ limit which reads

$$\tilde{z}_c = -1, \quad \tilde{z}_{c1} \simeq -1, \quad \tilde{z}_{c2} \simeq 0. \quad (48)$$

From the last column of Table I we now see that, in that limit:

(1) the branches $\Delta_1(z)$ and $\Delta_2(z)$ disappear due to the coalescence of z_c and z_{c1} ,

(2) the next branch recovers the second branch of the KPZ limit, i.e.,

$$\Delta_2(z) - \Delta_1(z) \rightarrow \frac{4}{\xi^2} \Delta_{\text{KPZ}}(\tilde{z}) = \frac{16}{3\xi^2} \ln\left(\frac{-1}{\tilde{z}}\right)^{\frac{3}{2}}, \quad (49)$$

which can be explicitly checked (I1).

(3) When \tilde{z} approaches \tilde{z}_{c2} , we obtain in the large ξ limit that the corresponding value of H_{KPZ} goes to $+\infty$, hence the branches $\Delta_3(z) - \Delta_1(z)$ and $\Delta_3(z)$ disappear at infinity, see Fig. 7 in Appendix I. This corresponds to events where $Z = \mathcal{O}(1)$ which become irrelevant in that limit [47].

VI. FREDHOLM DETERMINANT FORMULA

We can now compare our result (32) obtained using the inverse scattering method, to a formula obtained by completely different methods, for a model of sticky Brownian motions [19]. That model, which allows for a rigorous formulation, is believed (up to mathematical subtleties) to be equivalent to the one considered here. The original formula of Ref. [19] is valid for any time T and any Y , and here we obtain its limit in the large deviation diffusive scaling regime. Applied to our model this formula reads

$$\overline{e^{-uZ(Y,T)}} = \det(I - K_u), \quad (50)$$

where the kernel K_u was derived in Ref. [19, Theorem 1.11] and is recalled in Eq. (J4).

We scale $u = \sqrt{T}z$ with $z = \mathcal{O}(1)$ in Eq. (50) so that the l.h.s. of Eq. (50) can be identified to the l.h.s. of Eq. (7). We perform asymptotic analysis on the kernel K_u and extract the large T large deviation rate function $\Psi(z)$ by using the first cumulant method introduced in Refs. [48–50]. The manipulations, sketched in Appendix J, are quite heuristic, but allow us to recover nicely the algebraic form of formula (32). It remains open how to make it more mathematically rigorous.

VII. APPLICATIONS

A. Extremal diffusions

Consider the rightmost of N independent particles in the same random field, of position $Y_N(T) = \max_{i=1, \dots, N} Y_i(T)$. Without random field and for $N \gg 1$, $Y_N(T)$ has a deterministic part $\simeq 2\sqrt{T \ln N}$ plus a ‘‘thermal’’ fluctuation part $\simeq G\sqrt{\frac{T}{\ln N}}$, G being a Gumbel random variable. With the random field, for $\ln N \sim T \gg 1$, there is also a $\mathcal{O}(1)$ sample-to-sample fluctuation part, with a Tracy-Widom distribution

[15,22]. In the more accessible regime $\ln N \sim \sqrt{T} \gg 1$, as shown in Refs. [16,20] this fluctuating term is distributed as $h(0, T_{\text{KPZ}})/\sqrt{\ln N}$, the droplet solution of the KPZ equation. These phenomena go beyond the Gaussian nature of Einstein's diffusion. They allow for a detectable fingerprint of the random medium. Recently, these two regimes have been observed numerically [51]. The present results allow us to study yet another regime, $\ln N \ll \sqrt{T}$, where diffusive scaling holds and the scaled position $y_N(T) = \frac{Y_N(T)}{\sqrt{T}}$ of the maximum converges to

$$y_N(T) \simeq 2\sqrt{\ln N} + \frac{G - c_N + \delta H}{\sqrt{\ln N}}, \quad (51)$$

where for typical environments $\delta H = \mathcal{O}(T^{-1/4})$ is an Edwards-Wilkinson random variable with a computable variance, see Appendix K, and for rare environments $\delta H = H - H_{\text{typ}}(\xi) = \mathcal{O}(1)$ with the rate function (5) computed here and $\xi = 2\sqrt{\ln N}$. We also find that in the regime $N \sim \sqrt{T}$ the disorder average CDF takes the large deviation form $\mathbb{P}(y_N(T) < \xi) \sim e^{-\sqrt{T}\Sigma_\xi(n)}$, with $n = \frac{N}{\sqrt{T}} = \mathcal{O}(1)$ fixed, and $\Sigma_\xi(n)$ a rate function explicitly obtained in Appendix K.

B. Extension to the SEP

Our results are relevant within the class of MFT models with quadratic noise variance $\sigma(\varrho)$. These models enjoy a mapping to the $\{R, Q\}$ DNLS system (A7); see Appendix L. Recently, the exact solution of the MFT of the SEP was investigated in Ref. [42] using the well-known gauge transformation of Wadati and Sogo [65, Eq. (4.5)], to map the $\{R, Q\}$ DNLS system to the $\{P, Q\}$ NLS system. The remarkable result of Ref. [42] is that under this gauge transformation, the annealed initial condition of the SEP is mapped onto the initial condition solved by us in Ref. [10] (with different coupling constant [52]). The natural extension of Ref. [42] would be to study the statistics of a tracer at arbitrary position in an MFT model with quadratic variance and annealed initial condition. The inverse scattering method we have pursued in this work provides the right tools to answer this question.

VIII. CONCLUSION

We have elucidated here in great detail the crossover upon adding an asymmetry, between the MFT for diffusive systems

and the WNT of the KPZ equation. We have focused on the example of the diffusion of a tracer in a time-dependent random medium in an atypical direction and a ‘‘droplet’’-type initial condition. We have obtained the large-deviation functions in the context of classical integrability using simple, standard and versatile inverse scattering methods. For this model it was based on the integrable crossover between the DNLS and NLS equations. Obtaining the complete solution of this interpolating system (11) beyond the large-deviation observable requires further efforts involving the use of Fredholm determinants similarly to what we have achieved in Refs. [10,11] for the complete solution of the WNT. This is one open question that we leave to subsequent works [45], together with other outstanding questions, such as investigating the MFT-KPZ crossover for more general models, or within the present model, to study Eq. (2) for other initial conditions, in particular those identified in Ref. [16] to converge in atypical directions to solutions of the KPZ equation for flat and stationary geometries [11].

Note added. After completion, the paper in Ref. [53] appeared, where the results of Ref. [11] are proved rigorously.

ACKNOWLEDGMENTS

We thank G. Barraquand for discussions and collaborations on closely related topics, as well as for a careful reading of the manuscript. A.K. acknowledges support from ERC under Consolidator Grant No. 771536 (NEMO) and P.L.D. acknowledges support from the ANR Grant No. ANR-17-CE30-0027-01 RaMaTraF. This article is based upon work supported by the National Science Foundation under Grant No. DMS-1928930 while the two authors participated in a program hosted by the Mathematical Sciences Research Institute in Berkeley, California. P.L.D. also acknowledges hospitality from LPTMS-Orsay.

APPENDIX A: DERIVATION OF THE INTERPOLATING SYSTEM

Let us detail the steps performed in the text to obtain $\Psi(z)$ defined from the expectation value in Eq. (7) via the saddle-point method. Introducing the standard dynamical path integral representation, one has (where overlines represent averages w.r.t. the random field $\tilde{\eta}$)

$$\overline{e^{-z\sqrt{T}Z(Y,T)}} = \overline{e^{-z\sqrt{T} \int_{\xi}^{+\infty} dx Q_{\tilde{\eta}}(x,t=1)}} \quad (A1)$$

$$= \overline{\iint \mathcal{D}\tilde{Q}\mathcal{D}\tilde{P} e^{-\int_0^1 dt \int_{\mathbb{R}} dx [\sqrt{T}\tilde{P}(\partial_t \tilde{Q} - \partial_x^2 \tilde{Q} - \partial_x \sqrt{2\tilde{\eta}}(x,t)\tilde{Q})] - z\sqrt{T} \int_{\xi}^{+\infty} dx \tilde{Q}(x,t=1)}}} \quad (A2)$$

$$= \iint \mathcal{D}\tilde{Q}\mathcal{D}\tilde{P} e^{-\sqrt{T}(S[\tilde{P}, \tilde{Q}] + z \int_0^1 dt \delta(t-1) \int_{\xi}^{+\infty} dx \tilde{Q}(x,t))}, \quad (A3)$$

where the equation of motion (6) has been expressed using the response field $\tilde{P}\sqrt{T}$, and the associated dynamical action is

$$S[\tilde{P}, \tilde{Q}] = \int_0^1 dt \int_{\mathbb{R}} dx [\tilde{P}(\partial_t - \partial_x^2)\tilde{Q} - \tilde{Q}^2(\partial_x \tilde{P})^2]. \quad (A4)$$

For $T \rightarrow +\infty$ one can use the saddle-point method. Here we denote the fields and their saddle-point values in the original frame as $\{\tilde{P}, \tilde{Q}\}$ to distinguish them from the Galilean transformed fields $\{P, Q\}$ introduced below. Taking the functional derivative w.r.t. $\{\tilde{P}, \tilde{Q}\}$ we obtain

$$\partial_t \tilde{Q} = \partial_x^2 \tilde{Q} + 2\beta \partial_x (\tilde{Q}^2 (\partial_x \tilde{P})), \quad (\text{A5})$$

$$-\partial_t \tilde{P} = \partial_x^2 \tilde{P} - 2\beta \tilde{Q} (\partial_x \tilde{P})^2 - z \delta(t-1) \Theta(x-\xi), \quad (\text{A6})$$

with $\beta = -1$. We will keep β as a parameter but for the application to obtain $\Psi(z)$ it is understood that it is set to $\beta = -1$. Initially the upper boundary in time is $t = +\infty$ but since \tilde{P} vanishes for $t > 1$, we can equivalently restrict the equations for $t \in [0, 1]$ and interpret the last term in the second equation (which must be integrated backward in time) as a boundary condition $P(x, t=1) = -z \Theta(x-\xi)$ for $\tilde{P}(x, t)$, so it drops from the equation. To make the two equations more symmetric let us now introduce the derivative field $\tilde{R}(x, t) = \partial_x \tilde{P}(x, t)$, leading to

$$\begin{aligned} \partial_t \tilde{Q} &= \partial_x^2 \tilde{Q} + 2\beta \partial_x (\tilde{Q}^2 \tilde{R}), \\ -\partial_t \tilde{R} &= \partial_x^2 \tilde{R} - 2\beta \partial_x (\tilde{Q} \tilde{R}^2), \end{aligned} \quad (\text{A7})$$

with the boundary conditions

$$\begin{aligned} \tilde{Q}(x, t=0) &= \delta(x), \\ \tilde{R}(x, t=1) &= \Lambda_0 \delta(x-\xi), \quad \Lambda_0 = -z. \end{aligned} \quad (\text{A8})$$

This system is the cousin of the DNLS equation (identical to it upon the change $t \rightarrow it$).

Now we perform a Galilean transformation $x \rightarrow x - \xi t$ to bring back ξ to zero. Anticipating a bit, let us introduce the interpolating system introduced in the text in Eq. (11), which we recall here

$$\begin{aligned} \partial_t Q &= \partial_x^2 Q + 2\beta \partial_x (Q^2 R) + 2g Q^2 R, \\ -\partial_t R &= \partial_x^2 R - 2\beta \partial_x (Q R^2) + 2g Q R^2, \end{aligned} \quad (\text{A9})$$

and notice that if \tilde{Q}, \tilde{R} satisfies this system with couplings (β, g) , then

$$\begin{aligned} Q(x, t) &= \tilde{Q}(x - vt, t) e^{-\frac{1}{2}xv + \frac{v^2}{4}t}, \\ R(x, t) &= \tilde{R}(x - vt, t) e^{\frac{1}{2}xv - \frac{v^2}{4}t} \end{aligned} \quad (\text{A10})$$

also satisfies the same system with couplings $(\beta, g + \beta \frac{v}{2})$. Thus, consider \tilde{Q}, \tilde{R} which satisfy the above DNLS system (A7) with boundary conditions $\tilde{Q}(x, 0) = Q_0(x)$ and $\tilde{R}(x, 1) = \Lambda_0 \delta(x-\xi)$. We will choose $v = -\xi$ so that

$$\begin{aligned} Q(x, t) &= \tilde{Q}(x + \xi t, t) e^{\frac{1}{2}x\xi + \frac{\xi^2}{4}t}, \\ R(x, t) &= \tilde{R}(x + \xi t, t) e^{-\frac{1}{2}x\xi - \frac{\xi^2}{4}t} \end{aligned} \quad (\text{A11})$$

satisfies the interpolating system (A9) with couplings $(\beta, -\beta \frac{\xi}{2})$ and boundary conditions

$$Q(x, 0) = \tilde{Q}_0(x) e^{\frac{1}{2}x\xi}, \quad R(x, 1) = \Lambda_0 \delta(x) e^{-\frac{\xi^2}{4}}, \quad (\text{A12})$$

which for $\tilde{Q}_0(x) = \delta(x)$ gives the result (12) in the text, where we called $\Lambda = \Lambda_0 e^{-\frac{\xi^2}{4}}$.

1. Symmetries

Note that the DNLS equation (A7) is invariant by $x \rightarrow -x$ and $R \rightarrow -R$. The interpolating system $\{R, Q\}$ (A9) is invariant by $x \rightarrow -x, R \rightarrow -R$ and $g \rightarrow -g$.

2. Conserved quantities

Note that the system (A7) admits a series of conserved (i.e., time independent) quantities, the simplest one being $\int_{\mathbb{R}} dx \tilde{Q}(x, t) = 1$ [here its value is fixed to unity by the initial condition (A8)]. This conservation law originates from the conservation of probability in the Fokker-Planck equation, $\frac{d}{dt} \int dt q_\eta(x, t) = 0$. Upon a Galilean transformation it becomes

$$\int_{\mathbb{R}} dx Q(x, t) e^{-x\frac{\xi}{2} - \frac{\xi^2}{4}t} = 1. \quad (\text{A13})$$

Note that \tilde{R} also satisfies the conservation law $\int_{\mathbb{R}} dx \tilde{R}(x, t) = \Lambda$ and after a Galilean transformation $\int_{\mathbb{R}} dx R(x, t) e^{x\frac{\xi}{2} + \frac{\xi^2}{4}t} = \Lambda_0 = \Lambda e^{\xi^2/4}$. One can check that this is consistent with the symmetry (14).

3. Coupling constant

If one compares with Ref. [10] the true coupling constant of the $\{P, Q\}$ (i.e., here $\{R, Q\}$) system used there (called g there) is $\hat{g} = \Lambda g$. Since $\beta \Lambda = z e^{-\xi^2/4}$ and $g = -\beta \frac{\xi}{2}$, this gives $\hat{g} = -z \frac{\xi}{2} e^{-\xi^2/4}$. The special point z_c discussed in the text thus corresponds to $\hat{g} = 1$, as for the case of the WNT of the KPZ equation.

4. The rate function $\Psi(z)$ from the saddle point

The value of $\Psi(z)$ defined in Eq. (7) is then obtained from the saddle-point value in Eq. (A3). One has

$$\Psi(z) = \left[S[\tilde{P}, \tilde{Q}] + z \int_{\xi}^{+\infty} dx \tilde{Q}(x, 1) \right] \Big|_{\text{sp}}, \quad (\text{A14})$$

where \tilde{P}, \tilde{Q} must be replaced by the z dependent solutions of the system (A7) with boundary conditions (A8). Taking a derivative w.r.t. z and using the saddle-point conditions, only the explicit derivation w.r.t. z remains, and one obtains the formula (13) given in the text

$$\Psi'(z) = \int_{\xi}^{+\infty} dx \tilde{Q}(x, 1) = \int_0^{+\infty} dx Q(x, 1) e^{-\frac{1}{2}x\xi - \frac{\xi^2}{4}}, \quad (\text{A15})$$

where $Q(x, 1)$ is the z -dependent solution of the interpolating system (A9) with boundary conditions (12). Since by definition $\Psi(0) = 0$ this equation is sufficient to obtain $\Psi(z)$ if the r.h.s. is known as a function of z .

APPENDIX B: DIRECT SCATTERING SOLUTION FOR THE INTERPOLATING SYSTEM

In this section we derive formulas (17) and (18) for the scattering amplitudes $\{a(k), \tilde{a}(k), b(k), \tilde{b}(k)\}$ given in the text.

1. Equation for $\bar{\phi}$ at $t = 1$

This equation allows us to obtain the relations involving $\bar{a}(k)$ and $\bar{b}(k)$. We call $\bar{\phi}_{1,2}(x, t)$ the two components of $\bar{\phi}$ (the dependence in k is implicit). Let us recall that at $x \rightarrow -\infty$, $\bar{\phi} \simeq (0, -e^{ikx/2})^\top$. The first equation of the Lax pair $\partial_x \bar{v} = U_1 \bar{v}$ with $\bar{v} = e^{-k^2 t/2} \bar{\phi}$ reads in components at $t = 1$, from Eq. (15) and using that $R(x, 1) = \Lambda \delta(x)$,

$$\begin{aligned} \partial_x (e^{i\frac{k}{2}x} \bar{\phi}_1) &= -(g + i\beta k) \Lambda \delta(x) \bar{\phi}_2 e^{i\frac{k}{2}x}, \\ \partial_x (e^{-i\frac{k}{2}x} \bar{\phi}_2) &= Q(x, 1) \bar{\phi}_1 e^{-i\frac{k}{2}x}. \end{aligned} \quad (\text{B1})$$

$$\begin{aligned} e^{-i\frac{k}{2}x} \bar{\phi}_2(x, 1) &= \bar{\phi}_2(0, 1) + \bar{b}(k, 1) \int_0^x dx' Q(x', 1) e^{-ikx'}, \quad x > 0, \\ \bar{\phi}_2(x, 1) &= -e^{i\frac{k}{2}x}, \quad x < 0, \end{aligned} \quad (\text{B4})$$

where in the second equation we have used that $\bar{\phi}_2(x, 1) \simeq -e^{i\frac{k}{2}x}$ for $x \rightarrow -\infty$. Assuming continuity of $\bar{\phi}_2(x, 1)$ at $x = 0$, this leads to $\bar{\phi}_2(0, 1) = -1$ and to

$$\bar{b}(k, t = 1) = (g + i\beta k) \Lambda \Rightarrow \bar{b}(k) = (g + i\beta k) \Lambda e^{-k^2}, \quad (\text{B5})$$

since we recall that $\bar{b}(k, t) = \bar{b}(k) e^{k^2 t}$. Taking the $x \rightarrow +\infty$ limit of Eq. (B4) and using the asymptotics (16) we also obtain the relation

$$\bar{a}(k, 1) = \bar{a}(k) = 1 - (g + i\beta k) \Lambda \int_0^{+\infty} dx' Q(x', 1) e^{-ikx'}. \quad (\text{B6})$$

2. Equation for ϕ at $t = 0$

This equation allows us to obtain the relations involving $a(k)$ and $b(k)$. We call $\phi_{1,2}(x, t)$ the two components of ϕ (the dependence in k is implicit). Let us recall that at $x \rightarrow -\infty$,

$$\begin{aligned} e^{i\frac{k}{2}x} \phi_1(x, 0) &= \phi_1(0, 0) - (g + i\beta k) b(k, 0) \int_0^x dx' R(x', 0) e^{ikx'}, \quad x > 0, \\ \phi_1(x, 0) &= e^{-i\frac{k}{2}x}, \quad x < 0, \end{aligned} \quad (\text{B10})$$

where in the second equation we have used that $\phi_1(x, 0) \simeq e^{i\frac{k}{2}x}$ for $x \rightarrow -\infty$. Assuming continuity of $\phi_1(x, 0)$ at $x = 0$, this leads to $\phi_1(0, 0) = 1$ and to

$$b(k, t = 0) = b(k) = 1. \quad (\text{B11})$$

Taking the $x \rightarrow +\infty$ limit of Eq. (B10) and using the asymptotics (16) we also obtain the relation

$$a(k, 0) = a(k) = 1 - (g + i\beta k) \int_0^{+\infty} dx' R(x', 0) e^{ikx'}. \quad (\text{B12})$$

At this stage we can use the symmetry (14) and obtain

$$a(k) = 1 - (g + i\beta k) \Lambda \int_{-\infty}^0 dx' Q(x', 1) e^{-ikx'}, \quad (\text{B13})$$

Let us integrate the first equation from $x = -\infty$ to x . Since $\bar{\phi}_1$ vanishes at $x = -\infty$, it gives

$$\bar{\phi}_1(x, 1) = -(g + i\beta k) \Lambda e^{-i\frac{k}{2}x} \Theta(x) \bar{\phi}_2(0, 1). \quad (\text{B2})$$

Taking the limit $x \rightarrow +\infty$, we thus obtain

$$\bar{b}(k, t = 1) = -(g + i\beta k) \Lambda \bar{\phi}_2(0, 1). \quad (\text{B3})$$

To determine $\bar{\phi}_2(0, 1)$ we can integrate the second equation in Eq. (B1), which gives, using Eqs. (B2) and (B3),

$\phi \simeq (e^{-ikx/2}, 0)^\top$. The first equation of the Lax pair $\partial_x \bar{v} = U_1 \bar{v}$ with $\bar{v} = e^{k^2 t/2} \phi$ reads in components at $t = 0$, from Eq. (15) and using that $Q(x, 1) = \delta(x)$,

$$\begin{aligned} \partial_x (e^{i\frac{k}{2}x} \phi_1) &= -(g + i\beta k) R(x, 0) \phi_2 e^{i\frac{k}{2}x}, \\ \partial_x (e^{-i\frac{k}{2}x} \phi_2) &= \delta(x) \phi_1 e^{-i\frac{k}{2}x}. \end{aligned} \quad (\text{B7})$$

Integrating the second equation of Eq. (B7) from $x = -\infty$ to x . Since ϕ_2 vanishes at $x = -\infty$, it gives

$$\phi_2(x, 0) = e^{i\frac{k}{2}x} \Theta(x) \phi_1(0, 0). \quad (\text{B8})$$

Taking the limit $x \rightarrow +\infty$, we thus obtain

$$b(k, t = 0) = \phi_1(0, 0). \quad (\text{B9})$$

To determine $\phi_1(0, 0)$ we can integrate the first equation in Eq. (B7), which gives, using Eqs. (B8) and (B9),

which completes the derivation of the Eqs. (18) and (17) in text. Alternatively one may derive Eq. (B13) without using the symmetry (14) by considering the equation for ϕ at $t = 1$. We now present that derivation.

3. Equation for ϕ at $t = 1$

This equation allows us to obtain $a(k)$ in Eq. (B13). Let us recall that at $x \rightarrow -\infty$, $\phi \simeq (e^{-ikx/2}, 0)^\top$. The first equation of the Lax pair, $\partial_x \bar{v} = U_1 \bar{v}$ with $\bar{v} = e^{k^2 t/2} \phi$ as given in the text now reads, in components and at $t = 1$, using that $R(x, 1) = \Lambda \delta(x)$,

$$\begin{aligned} \partial_x (e^{i\frac{k}{2}x} \phi_1) &= -(g + i\beta k) \Lambda \delta(x) \phi_2 e^{i\frac{k}{2}x}, \\ \partial_x (e^{-i\frac{k}{2}x} \phi_2) &= Q(x, 1) \phi_1 e^{-i\frac{k}{2}x}. \end{aligned} \quad (\text{B14})$$

Integrating these two equations, and using the asymptotics (16) at $x \rightarrow +\infty$ we obtain

$$\begin{aligned}\phi_1(x, 1) &= e^{-i\frac{k}{2}x}[\Theta(-x) + a(k)\Theta(x)], \\ a(k) - 1 &= -(g + i\beta k)\Lambda\phi_2(0, 1),\end{aligned}\quad (\text{B15})$$

$$\phi_2(x, 1) = e^{i\frac{k}{2}x} \int_{-\infty}^x dx' Q(x', 1) e^{-ikx'} [\Theta(-x') + a(k)\Theta(x')],$$

where we used that $a(k, t) = a(k)$; see the main text. Setting $x = 0$ in the second equation we obtain the relation displayed in the text

$$\begin{aligned}\phi_2(0, 1) &= \int_{-\infty}^0 dx' Q(x', 1) e^{-ikx'}, \\ a(k) &= 1 - (g + i\beta k)\Lambda \int_{-\infty}^0 dx' Q(x', 1) e^{-ikx'}.\end{aligned}\quad (\text{B16})$$

APPENDIX C: DETAILS OF THE CALCULATION OF THE SCATTERING AMPLITUDES

So far the scattering amplitudes $\{a, \tilde{a}\}$ have been expressed as half-Fourier transforms in Eqs. (B6) and (B16). To determine them more explicitly, one wants to solve Eq. (20), namely the normalization relation of the scattering amplitudes, which read here

$$a(k)\tilde{a}(k) = 1 - (g + i\beta k)\Lambda e^{-k^2}, \quad (\text{C1})$$

where $a(k)$ and $\tilde{a}(k)$ satisfy Eq. (18), which we recall reads

$$\begin{aligned}a(k) &= 1 - (g + i\beta k)\Lambda Q_-(k), \\ \tilde{a}(k) &= 1 - (g + i\beta k)\Lambda Q_+(k),\end{aligned}\quad (\text{C2})$$

$$Q_{\pm}(k) = \int_{\mathbb{R}^{\pm}} dx Q(x, 1) e^{-ikx}.$$

Clearly for k complex, $Q_+(k)$, hence $\tilde{a}(k)$, is analytic in the lower half-plane, and $Q_-(k)$, hence $a(k)$, is analytic in the upper half-plane. Now we define the parametrization

$$a(k) = a(\infty)e^{\Phi_+(k)}, \quad a(\infty) = 1 + \beta\Lambda Q(0^-, 1), \quad (\text{C3})$$

$$\tilde{a}(k) = \tilde{a}(\infty)e^{\Phi_-(k)}, \quad \tilde{a}(\infty) = 1 - \beta\Lambda Q(0^+, 1), \quad (\text{C4})$$

where $a(\infty)$ and $\tilde{a}(\infty)$ were obtained in Eq. (21), so that $\Phi_{\pm}(k) \rightarrow 0$ as $k \rightarrow \pm\infty$. Using Eq. (24), i.e., $a(\infty)\tilde{a}(\infty) = 1$, one can thus rewrite Eq. (C1) for real k as

$$1 - (g + i\beta k)\Lambda e^{-k^2} = e^{\Phi_+(k)} e^{\Phi_-(k)}, \quad (\text{C5})$$

where $e^{\Phi_{\pm}(k)}$ are analytic, respectively, in the upper-half plane (UHP)/lower-half plane (LHP). This is a typical Riemann-Hilbert [54–56] or Wiener-Hopf problem. In some domain, taking the logarithm of this equation, it can be written as

$$\ln(1 - (g + i\beta k)\Lambda e^{-k^2}) = \Phi_+(k) + \Phi_-(k) + 2i\pi n(k) \quad (\text{C6})$$

for some integer-valued function $n(k)$. One can check that for $\hat{g} = \Lambda g < 1$ the l.h.s. of Eq. (C6) is analytic in a strip around the real axis in k (see Appendix G) and decays fast at infinity along the real axis. In this strip $n(k) = 0$, and for $\hat{g} = \Lambda g < 1$ the multivaluation occurs only outside this strip. As

in Ref. [40], one can use the well-known Sokhotskiy-Plemelj formula

$$\int_{\mathbb{R}} \frac{dq}{2i\pi} \frac{f(q)}{q - k \pm i0^+} = \mp \int_{\mathbb{R}} \frac{dq}{2i\pi} \frac{f(q)}{q - k} \mp \frac{1}{2} f(k), \quad (\text{C7})$$

which leads to the decomposition of a general function $f(k)$,

$$f(k) = \int_{\mathbb{R}} \frac{dk'}{2i\pi} \frac{f(k')}{k' - k - i0^+} - \int_{\mathbb{R}} \frac{dk'}{2i\pi} \frac{f(k')}{k' - k + i0^+} \quad (\text{C8})$$

in parts which are analytic in the UHP and LHP, respectively. This implies that

$$\Phi_{\pm}(k) = \pm \int_{\mathbb{R}} \frac{dq}{2i\pi} \frac{\ln(1 - (g + i\beta q)\Lambda e^{-q^2})}{q - k \mp i0^+}. \quad (\text{C9})$$

The formula for $\Phi_+(k)$ is valid only in the UHP and the one for $\Phi_-(k)$ is valid only in the LHP (at least in a strip around the real axis). This recovers Eq. (26) in the text.

1. Validity

The results above are valid for $\Lambda g < 1$. For their continuation beyond that domain see Appendix G below.

2. Recovering the case $\beta = 0$

If we set $\beta = 0$ in the interpolating system (11), then we obtain the $\{P, Q\}$ system extensively discussed in Refs. [10,11]. Let us show that one then recovers the solution obtained in our previous work [10]. There, we studied a more general initial condition $Q(x, t = 0) = Q_0(x)$, and to identify we must set $g \rightarrow g\Lambda$ (since there $R(x, t = 1) = \delta(x)$ while here $R(x, t = 1) = \Lambda\delta(x)$ while there Λ is set to unity). Taking this into account there we obtained $\tilde{b}(k) = ge^{-k^2}$ which agrees with Eq. (17), and

$$\begin{aligned}a(k) &= \sqrt{1 - gb(k)\Lambda e^{-k^2}} e^{-i\varphi(k)}, \\ \varphi(k) &= \int_{\mathbb{R}} \frac{dq}{2\pi} \frac{1}{q - k} \ln(1 - gb(q)\Lambda e^{-q^2}),\end{aligned}\quad (\text{C10})$$

together with $\tilde{a}(k) = a(-k)$ for real k , and $\varphi(-k) = -\varphi(k)$. It is easy to see that it agrees with Eq. (C9) for $\beta = 0$ using Eq. (C7) with $f(k) = \ln(1 - gb(k)\Lambda e^{-k^2})$, that is, in that case for $k \in \mathbb{R}$,

$$\Phi_{\pm}(k) = -i\varphi(\pm k) + \frac{1}{2} \ln(1 - gb(k)\Lambda e^{-k^2}). \quad (\text{C11})$$

Of course here we restricted to the special case of the droplet initial condition $Q_0(x) = \delta(x)$, where $b(k) = 1$ as found in Ref. [10] and recovered here in Eq. (17).

3. General initial condition for $\beta \neq 0$

Extending the previous discussion we see that the solution of the interpolating system for a more general initial condition $Q(x, 0) = Q_0(x)$ reads

$$\Phi_{\pm}(k) = \pm \int_{\mathbb{R}} \frac{dq}{2i\pi} \frac{\ln(1 - (g + i\beta q)\Lambda b(q)e^{-q^2})}{q - k \mp i0^+}, \quad (\text{C12})$$

where there is a map between $Q_0(x)$ and $b(q)$ which can be obtained by solving the scattering problem.

APPENDIX D: BOUNDS AND SYMMETRIES FOR $\Psi(z)$

We give here some properties of the function $\Psi(z)$. Since we start from its definition (7) we are dealing here with what we call in the text the “optimal” $\Psi(z)$, also given by the minimization (8). From its definition (7) the expansion of $\Psi(z)$ in powers of z around $z = 0$ gives the cumulants of $Z = Z(Y, T)$,

$$\Psi(z) = -\frac{1}{\sqrt{T}} \ln \exp(-z\sqrt{T}Z) = -\sum_{p \geq 1} \frac{(-z)^p}{p!} T^{\frac{p-1}{2}} \overline{Z^p}^c, \tag{D1}$$

hence the leading behavior of each cumulant at large time is given by

$$\overline{Z^p}^c \simeq (-1)^{p+1} T^{\frac{1-p}{2}} \Psi^{(p)}(0), \tag{D2}$$

However, taking derivatives of $\Psi(z)$ w.r.t. z for any z lead to

$$\begin{aligned} \Psi'(z) &= \langle Z \rangle_z, \quad \Psi''(z) = -\sqrt{T} \langle Z^2 \rangle_z^c, \\ \langle \mathcal{O} \rangle_z &= \frac{\overline{\mathcal{O} \exp(-z\sqrt{T}Z)}}{\overline{\exp(-z\sqrt{T}Z)}}, \end{aligned} \tag{D3}$$

where the expectation values are w.r.t. the tilted measure also defined in the text. Since the random variable Z obeys $0 < Z < 1$ it implies

$$0 < \Psi'(z) < 1, \quad \Psi''(z) < 0. \tag{D4}$$

The function $\Psi(z)$ must thus be concave. Note that some of the branches obtained in the text are not concave hence they do not appear in the optimal $\Psi(z)$. In such cases there is instead a jump of $\Psi'(z)$ from one branch to another one, for $z = z^*$. As discussed in the text, at this point the tilted measure has two degenerate maxima hence the fluctuations are anomalously large, $\sqrt{T} \langle Z^2 \rangle_{z=z^*}^c = +\infty$.

Let us now make the dependence in ξ apparent and denote $Z_\xi = Z(Y, T)$. By definition one has

$$Z_\xi = \int_{\xi}^{+\infty} dy q_\eta(y, T), \quad 1 - Z_{-\xi} = \int_{-\infty}^{-\xi} dy q_\eta(y, T), \tag{D5}$$

where $0 < Z_\xi < 1$. Equation (2) is invariant by $y \rightarrow -y$ and $\eta(y, \tau) \rightarrow -\eta(-y, -\tau)$, which leaves the PDF of the noise invariant, hence Z_ξ and $1 - Z_{-\xi}$ have the same PDF. This observation inserted into Eq. (7) gives

$$\begin{aligned} \overline{\exp(-z\sqrt{T}Z_\xi)} &\sim \overline{\exp(-\sqrt{T}\Psi_\xi(z))} \\ &= \overline{\exp(-z\sqrt{T}(1 - Z_{-\xi}))} \\ &= \overline{\exp(-\sqrt{T}(z + \Psi_{-\xi}(-z)))}, \end{aligned} \tag{D6}$$

hence it implies the symmetry given in the text,

$$\Psi_{-\xi}(z) = \Psi_\xi(-z) + z. \tag{D7}$$

1. Remark

To measure Z_ξ and $-Z_{-\xi}$ one can use the DNLS equation with boundary condition $P(x, 1) = \Theta(x - \xi)$, i.e., $R(x, 1) = \delta(x - \xi)$ for the first, and $P(x, 1) = \Theta(-x - \xi)$,

i.e., $R(x, 1) = -\delta(-x - \xi)$ for the second. Using the symmetry $x \rightarrow -x$ and $R \rightarrow -R$ one arrives at the same conclusion.

APPENDIX E: DERIVATION OF THE RATE FUNCTION $\Psi(z)$ —MAIN BRANCH

Let us give some more details on how Eq. (32) in the text is obtained. Taking a derivative w.r.t. k of Eq. (27) at $k = \frac{ig}{\beta}$ and using Eq. (28) one obtains

$$i\beta \Lambda Q_{\mp} \left(\frac{ig}{\beta} \right) = -\Phi'_{\pm} \left(\frac{ig}{\beta} \right). \tag{E1}$$

Let us verify that this is consistent with the second equality in Eq. (30) (which comes from the conservation of probability). For that let us first recall that [from Eq. (C6) with $n(k) = 0$]

$$\ln(1 - (g + i\beta k)\Lambda e^{-k^2}) = \Phi_+(k) + \Phi_-(k), \tag{E2}$$

where $\Phi_{\pm}(k)$ are given in Eq. (C9) for k in the complex upper/lower half planes.

Taken at $k = \frac{ig}{\beta}$ it again shows that $\Phi_{\pm}(\frac{ig}{\beta})$ are opposite quantities. Taking a derivative w.r.t. k at $k = \frac{ig}{\beta} = -i\frac{\xi}{2}$ one obtains

$$-i\beta \Lambda e^{\xi^2/4} = \Phi'_+ \left(\frac{ig}{\beta} \right) + \Phi'_- \left(\frac{ig}{\beta} \right), \tag{E3}$$

which, from Eq. (E1), is exactly equivalent to the second equality in Eq. (30).

One must be careful in computing $\Phi'_{\pm}(k)$ for $k = \frac{ig}{\beta} = -i\xi/2$ since the formula (26) given in the text and above in Eq. (C9) for $\Phi_{\pm}(k)$ are valid only for k in the UHP/LHP, respectively. There are thus two cases:

(1) If $g/\beta > 0$, i.e., $\xi < 0$, then we can use Eq. (26) for Φ_+ for $\Im(k) \geq 0$ and one obtains

$$\Phi'_+ \left(\frac{ig}{\beta} \right) = \int_{\mathbb{R}} \frac{dq}{2i\pi} \frac{\ln(1 - (g + i\beta q)\Lambda e^{-q^2})}{(q - \frac{ig}{\beta})^2}, \tag{E4}$$

while, using Eq. (E3) one has

$$\begin{aligned} \Phi'_- \left(\frac{ig}{\beta} \right) &= - \int_{\mathbb{R}} \frac{dq}{2i\pi} \frac{\ln(1 - (g + i\beta q)\Lambda e^{-q^2})}{(q - \frac{ig}{\beta})^2} \\ &\quad - i\beta \Lambda e^{\xi^2/4} \Theta(-\xi). \end{aligned} \tag{E5}$$

(2) If $g/\beta < 0$, i.e., $\xi > 0$, then we can use Eq. (26) for Φ_- for $\Im(k) \leq 0$ and one obtains

$$\Phi'_- \left(\frac{ig}{\beta} \right) = - \int_{\mathbb{R}} \frac{dq}{2i\pi} \frac{\ln(1 - (g + i\beta q)\Lambda e^{-q^2})}{(q - \frac{ig}{\beta})^2}, \tag{E6}$$

while, using Eq. (E3) one has

$$\begin{aligned} \Phi'_+ \left(\frac{ig}{\beta} \right) &= \int_{\mathbb{R}} \frac{dq}{2i\pi} \frac{\ln(1 - (g + i\beta q)\Lambda e^{-q^2})}{(q - \frac{ig}{\beta})^2} \\ &\quad - i\beta \Lambda e^{\xi^2/4} \Theta(\xi). \end{aligned} \tag{E7}$$

Putting the two cases together, we obtain from the equality (E1)

$$\begin{aligned}
 i\beta\Lambda Q_{\mp}\left(\frac{ig}{\beta}\right) &= -\Phi'_{\pm}\left(\frac{ig}{\beta}\right) \\
 &= \mp \int_{\mathbb{R}} \frac{dq}{2i\pi} \frac{\ln(1 - (g + i\beta q)\Lambda e^{-q^2})}{(q - \frac{ig}{\beta})^2} \\
 &\quad + i\beta\Lambda e^{\xi^2/4} \Theta(\pm\xi), \tag{E8}
 \end{aligned}$$

a result which remains true for $g = \xi = 0$ provided the integrals are then interpreted as principal values and that we use the convention $\Theta(0) = 1/2$.

Now using Eq. (30) and inserting $\beta = -1$, $g = -\beta \frac{\xi}{2}$, and $\beta\Lambda = ze^{-\xi^2/4}$ we obtain the result (31) in the text, from which Eq. (32) is obtained upon integration over z .

1. Remark on the Heaviside function

The appearance of the term $\Theta(\pm\xi)$ in Eq. (E8) can also be seen as follows. Let us expand Eq. (26) in series of Λ

$$\Phi'_{\pm}(k) = \mp \sum_{n \geq 1} \frac{(i\beta\Lambda)^n}{n} \int_{\mathbb{R}} \frac{dq}{2i\pi} \frac{(q - \frac{ig}{\beta})^n e^{-nq^2}}{(q - k \mp i0^+)^2}. \tag{E9}$$

Taking $k = \frac{ig}{\beta}$ we can neglect the term $\pm i0^+$ except for $n = 1$. The term $n = 1$ is

$$\begin{aligned}
 \mp (i\beta\Lambda) \int_{\mathbb{R}} \frac{dq}{2i\pi} \frac{e^{-q^2}}{q + \frac{i\xi}{2} \mp i0^+} \\
 = \mp (i\beta\Lambda) \int_{\mathbb{R}} \frac{dq}{2i\pi} \frac{e^{-q^2}}{q + \frac{i\xi}{2}} - i\beta\Lambda e^{\xi^2/4} \Theta(\pm\xi). \tag{E10}
 \end{aligned}$$

2. Recovering the typical probability

Similarly the expansion of $z\Psi'(z)$ in powers of z contains a term with a pole at $q = -i\xi/2$ only for $n = 1$. As shown in the text, this term recovers the typical probability $\bar{Z} = Z_{\text{typ}}$. In deriving Eq. (34) we have used the identity, for real a ,

$$\int_{\mathbb{R}} \frac{dq}{2\pi} \frac{1}{iq + a} e^{-q^2} = \frac{1}{2} e^{a^2} (\text{Erfc}(a) - 2\Theta(-a)). \tag{E11}$$

3. Range of validity

As discussed in the text the formula for $\Psi(z)$ presented in this section is what we call the ‘‘main branch’’ valid only for $z/z_c < 1$ with $z_c = -\frac{2}{\xi} e^{\xi^2/4}$. As a result it only allows us to determine $\Phi(H)$ for $H < H_c$. To obtain the full solution to the problem we need to consider analytical continuations, to which we now turn.

APPENDIX F: ANALYTIC CONTINUATION IN THE CASE OF THE WNT FOR THE KPZ EQUATION

Before discussing the intricacies of the analytic continuations for the present problem, we recall here how it works in the case of the WNT for the KPZ equation. It is necessary to do so since we show below that at large ξ the results for KPZ equation are recovered. We present further details than given in Ref. [10] as they will be very useful below. Indeed

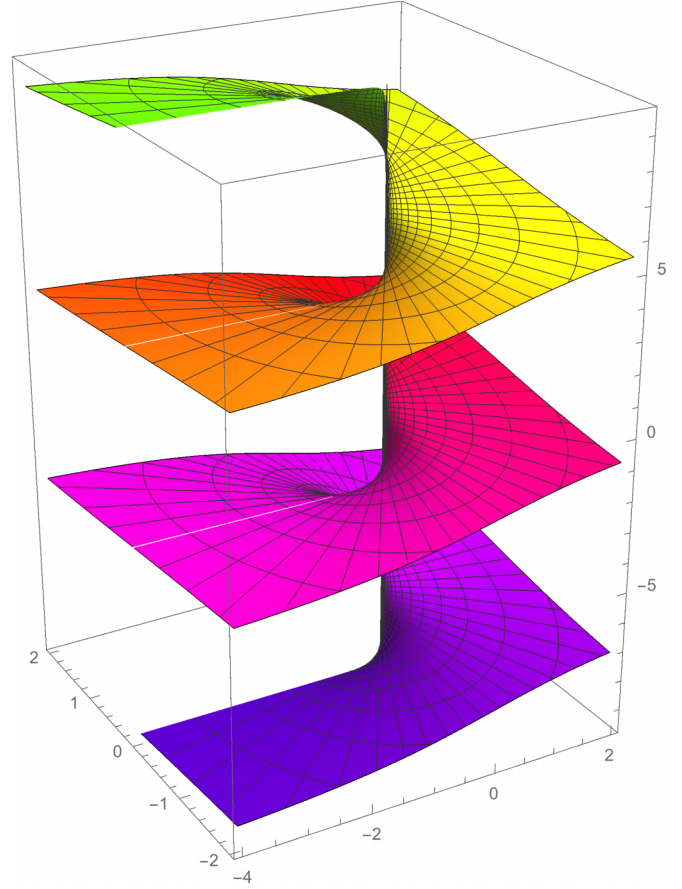


FIG. 2. Plot of the Riemann surface of the logarithm $z \mapsto \ln z$. This surface is composed of different sheets continuously connected in a staircase manner.

the situation in the present paper is already quite similar to the one for the KPZ equation where $\Psi_{\text{KPZ}}(\tilde{z})$ admits a second branch for $-1 \leq \tilde{z} < 0$.

For the KPZ equation one first obtains for $\tilde{z} \in [0, +\infty)$

$$\Psi_{\text{KPZ}}(\tilde{z}) = \Psi_{\text{KPZ},0}(\tilde{z}) := -\frac{1}{\sqrt{4\pi}} \text{Li}_{5/2}(-\tilde{z}), \tag{F1}$$

which can be continued for $\tilde{z} \in [-1, +\infty)$. The polylogarithm function $\text{Li}_{5/2}(-\tilde{z})$ is analytic in the complex \tilde{z} plane except on a branch cut for $\tilde{z} \in (-\infty, -1]$. Across this branch cut it has a jump, which leads to

$$\begin{aligned}
 \Psi_{\text{KPZ},0}(\tilde{z} + i0^+) - \Psi_{\text{KPZ},0}(\tilde{z} - i0^+) &= \Delta_{\text{KPZ}}(\tilde{z}), \\
 \Delta_{\text{KPZ}}(\tilde{z}) &= \frac{4}{3} i (\ln(-\tilde{z}))^{3/2} \tag{F2}
 \end{aligned}$$

for $z \in (-\infty, -1]$.

1. Analogy with the logarithm

This situation is analogous to the study of the logarithm which admits different determination in the complex plane. Indeed, along the negative real axis, the logarithm has a jump of value $2i\pi$. A better understanding of the logarithm is done by considering its domain of definition not in the complex plane but rather on a Riemann surface, see Fig. 2, where it does not have any jump. In the case of the logarithm, the

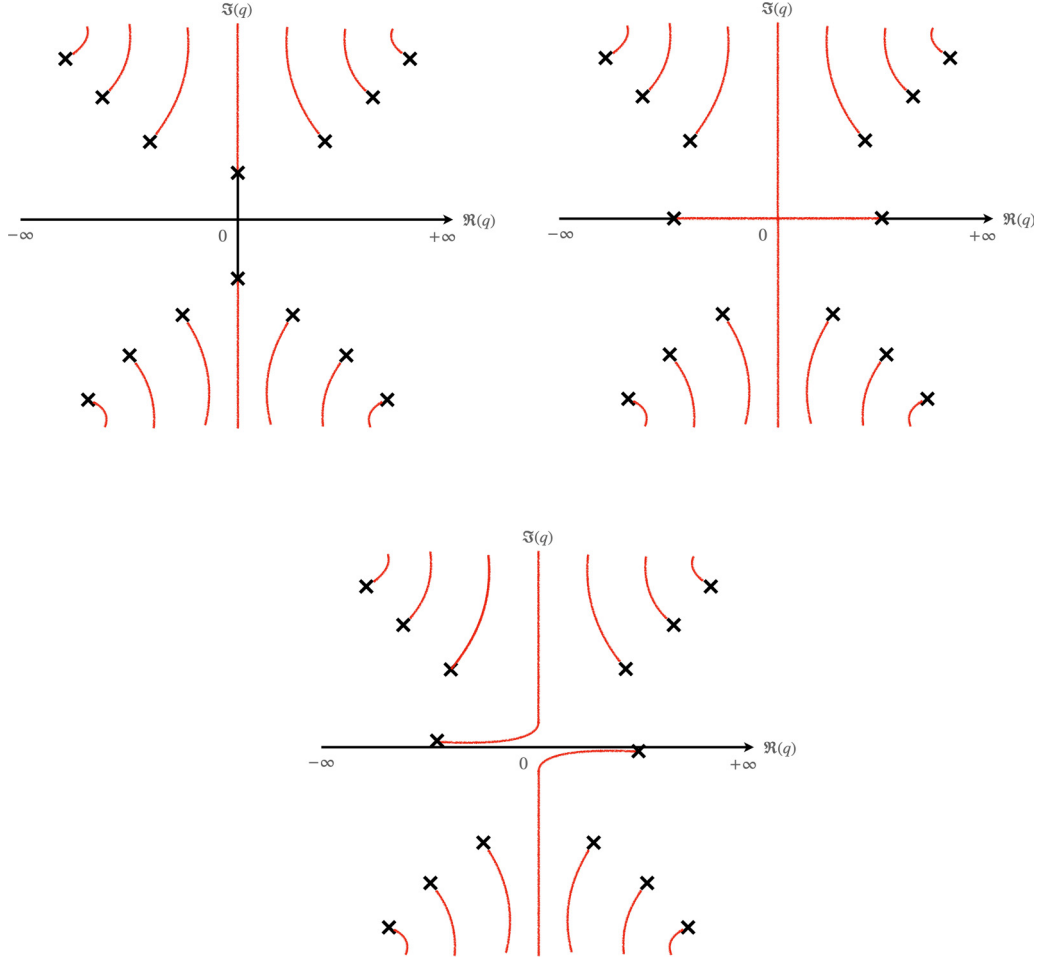


FIG. 3. Schematic plot of the argument of the logarithm in Eq. (F5) in the complex q plane for various values of \tilde{z} . (Top left) $\tilde{z} \leq -1$, $\tilde{z} \in \mathbb{R}$. (Top right) $\tilde{z} \leq -1$, $\tilde{z} \in \mathbb{R}$. (Bottom) $\Re(\tilde{z}) < -1$, $\Im(\tilde{z}) = 0^+$. The black crosses correspond to the locations where the argument $A_{\text{KPZ}}(q)$ is zero and the red curves correspond to the branch cuts of $\ln A_{\text{KPZ}}(q)$.

Riemann surface is composed of different sheets joined by winding around the origin and the correct definition of the logarithm on the n th sheet is $\ln z + 2i\pi n$ where $\ln z$ is the principal determination or main branch.

Pursuing the construction of $\Psi_{\text{KPZ}}(\tilde{z})$ on a Riemann surface rather than on the complex plane, we extend continuously the definition $\Psi_{\text{KPZ},0}(\tilde{z})$ to the first Riemann sheet along the branch cut as follows:

$$\Psi_{\text{KPZ}}(\tilde{z}) = \begin{cases} \Psi_{\text{KPZ},0}(\tilde{z}), & \Im(\tilde{z}) > 0, \\ \Psi_{\text{KPZ},0}(\tilde{z}) + \Delta_{\text{KPZ}}(\tilde{z}), & \Im(\tilde{z}) < 0. \end{cases} \quad (\text{F3})$$

On the real axis it is multivalued, i.e., there is a first branch for $\Psi_{\text{KPZ}}(\tilde{z})$ given by the first line, and a second branch given by the second line. One can now continue these two branches for $\tilde{z} \in]-1, 0]$ and one finds that the second branch is

$$\Psi_{\text{KPZ},0}(\tilde{z}) + \Delta_{\text{KPZ}}(\tilde{z}) = -\frac{1}{\sqrt{4\pi}} \text{Li}_{5/2}(-\tilde{z}) + \frac{4}{3} (-\ln(-\tilde{z}))^{3/2} \quad (\text{F4})$$

for $\tilde{z} \in]-1, 0]$.

2. Another route to find the analytic continuation

One can arrive at the same result from the integral representation. Indeed, for $\tilde{z} \in]-1, +\infty[$ one has

$$\begin{aligned} \tilde{z} \Psi'_{\text{KPZ}}(\tilde{z}) &= \int_{\mathbb{R}} \frac{dq}{2\pi} \ln(1 + \tilde{z} e^{-q^2}) = \tilde{z} \Psi'_{0,\text{KPZ}}(\tilde{z}) \\ &= -\frac{1}{\sqrt{4\pi}} \text{Li}_{3/2}(-\tilde{z}). \end{aligned} \quad (\text{F5})$$

Let us plot the argument of the logarithm $A_{\text{KPZ}}(q) = 1 + \tilde{z} e^{-q^2}$ in the complex q plane. This is shown schematically in Fig. 3. For $\tilde{z} > -1$ no branch cut crosses the real axis (integration axis). When \tilde{z} reaches -1 the two symmetric branch cuts along the imaginary axis join. For $\tilde{z} < -1$ they form a “cross” [see Fig. 3 (top right)] with ends located at $q = \pm\sqrt{\ln(-1/\tilde{z})}$. It is impossible to integrate over the real axis without crossing them. However, suppose now we consider $\tilde{z} \rightarrow \tilde{z} \pm i\epsilon$. We can see that the two branch cuts then avoid each other, and it is possible to deform slightly the integration contour to avoid crossing them [see Fig. 3 (bottom)]. This is consistent with the function $\text{Li}_{3/2}(-\tilde{z})$ being analytic away from the negative real axis for \tilde{z} .

Now one can see that the additional contribution $\Delta_{\text{KPZ}}(\tilde{z})$ comes for $\tilde{z} < -1$ from the jump across the horizontal part of

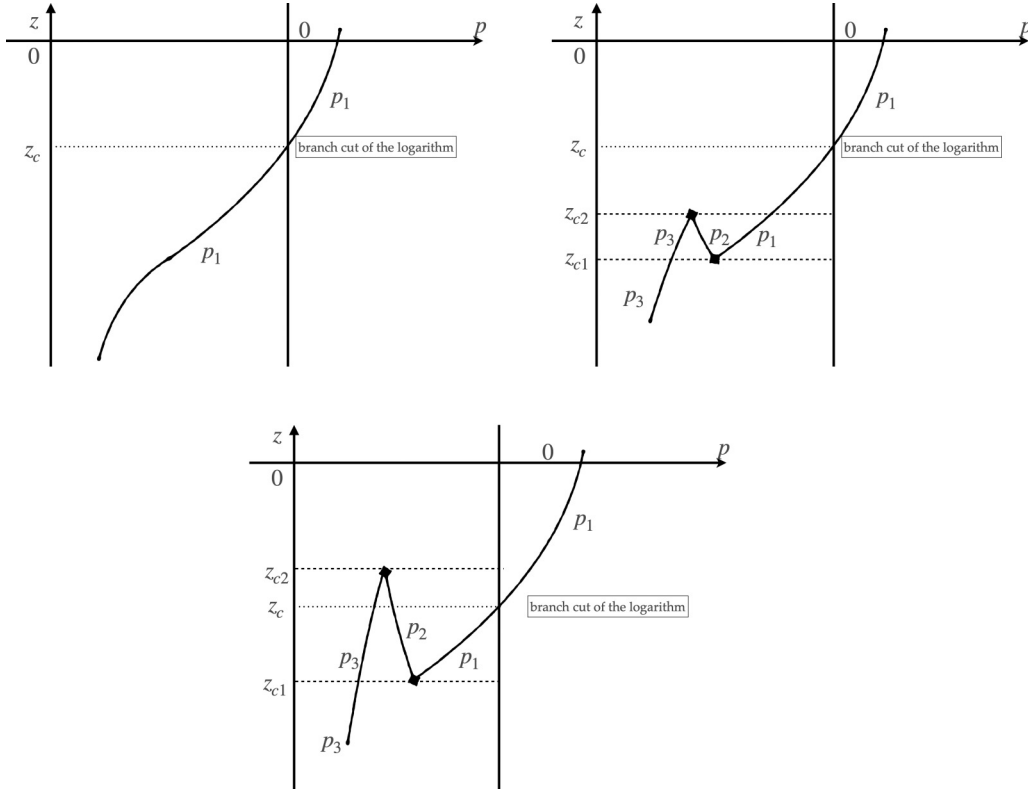


FIG. 4. Schematic behavior of the zeros p_i of the equation $f_{z,\xi}(p_i) = 0$ as a function of $z < 0$ for $\xi > 0$. (Top left) The case $\xi < \xi_1 = \sqrt{8}$ in which case there is a single zero, which changes sign at $z = z_c$. (Top right) The case $\xi_1 < \xi < \xi_2$ in which case there are three zeros $p_1 > p_2 > p_3$ in the interval $z \in (z_{c1}, z_{c2})$ and $z_{c2} < z_c$. (Bottom) The case $\xi > \xi_2$, same but now $z_{c2} > z_c$. The zeros p_2, p_3 coalesce and annihilate at $z = z_{c2}$ and p_2, p_3 at $z = z_{c1}$. The points z_{c1} and z_{c2} also serve as turning points in the definition of the function $\Psi(z)$.

the “cross” [see Fig. 3 (bottom)] and is precisely

$$\tilde{z}\Delta'_{\text{KPZ}}(\tilde{z}) = 2i\pi \int_{-\sqrt{-\ln(-1/\tilde{z})}}^{\sqrt{-\ln(-1/\tilde{z})}} \frac{dq}{2\pi} = 2i[\ln(-\tilde{z})]^{1/2}, \quad (\text{F6})$$

while its continuation for $\tilde{z} > -1$ —which enters the second branch—can be obtained as an integral around the complementary of the branch cut in Fig. 3 (top left),

$$\tilde{z}\Delta'_{\text{KPZ}}(\tilde{z}) = 2i\pi \int_{-i\sqrt{\ln(-1/\tilde{z})}}^{i\sqrt{\ln(-1/\tilde{z})}} \frac{dq}{2\pi} = -2[-\ln(-\tilde{z})]^{1/2}, \quad (\text{F7})$$

consistent with the previous argument. These considerations will be useful for the next subsection.

APPENDIX G: ANALYTIC CONTINUATION AND ADDITIONAL BRANCHES OF THE RATE FUNCTION $\Psi(z)$

1. Preliminaries: Solutions of Eq. (37) in the text

As mentioned in the text, and for the discussion below about the branch cuts in the integration in the formulas (31) and (32) for $z\Psi'(z)$ and $\Psi(z)$, it is important to study the argument of the logarithm in Eq. (31), which we denote $A(q)$

$$A(q) := 1 - z \left(iq - \frac{\xi}{2} \right) e^{-q^2 - \frac{\xi^2}{4}} \quad (\text{G1})$$

and in particular to find the points where it vanishes, i.e., the zeros, solutions of $A(q) = 0$. There are many such zeros but

it turns out, see below, that the zeros on the imaginary axis are the ones which play an important role. Setting $q = ip$, it is equivalent to study $A(ip)$ or the function $f_{z,\xi}(p)$ defined as

$$f_{z,\xi}(p) = e^{-p^2 + \frac{\xi^2}{4}} A(ip) = e^{-p^2 + \frac{\xi^2}{4}} + z \left(p + \frac{\xi}{2} \right) \quad (\text{G2})$$

and finding its real zeros, $f_{z,\xi}(p) = 0$, which is Eq. (37) in the text.

We will consider $\xi > 0$ (the case $\xi < 0$ can be studied from the symmetry $(\xi, z) \rightarrow (-\xi, -z)$). Consider also $z < 0$ (see $z > 0$ below). Since $f_{z,\xi}(p) \rightarrow \mp\infty$ as $p \rightarrow \pm\infty$ it has at least one real zero, but in some cases can have three. When there are three zeros we will denote them $p_1 > p_2 > p_3$ in decreasing order. They are functions of (z, ξ) , i.e., $p_i = p_i(z, \xi)$.

The evolution of the zeros when $z < 0$ is varied is shown in Fig. 4. There are three cases depending in the values of ξ which we now describe. In all three cases the largest zero p_1 vanishes for the value of $z = z_c = z_c(\xi) = -\frac{2e^{\frac{\xi^2}{4}}}{\xi} < 0$. One finds that

(1) for $0 < \xi < \xi_1 = \sqrt{8}$, and for all $z < 0$, there is only one zero, $p_1 = p_1(z, \xi)$; see Fig. 4 (top left).

(2) for $\xi > \xi_1$ there is an interval of values of z , $z \in [z_{c1}, z_{c2}]$, where there are three zeros. To find this interval one

looks for double zeros $f_{z,\xi}(p) = f'_{z,\xi}(p) = 0$, i.e.,

$$e^{-p^2 + \frac{\xi^2}{4}} = -z \left(p + \frac{\xi}{2} \right) = \frac{z}{2p}. \quad (\text{G3})$$

For a given ξ one can solve these conditions for the couple (z, p) . One finds that there are no real solutions for $\xi < \sqrt{8}$ but that there are two solutions (z_{c1}, p_{c1}) and (z_{c2}, p_{c2}) for $\xi > \xi_1 = \sqrt{8}$. These read, with $z_{c1} < z_{c2}$,

$$\begin{aligned} z_{c1} &= z_{c1}(\xi) = -\frac{1}{2} e^{\frac{1}{8}[\xi(\xi + \sqrt{\xi^2 - 8}) + 4]} (\xi - \sqrt{\xi^2 - 8}), \\ p_{c1} &= -\frac{1}{4} (\xi - \sqrt{\xi^2 - 8}), \end{aligned} \quad (\text{G4})$$

$$\begin{aligned} z_{c2} &= z_{c2}(\xi) = -\frac{1}{2} e^{\frac{1}{8}[\xi(\xi - \sqrt{\xi^2 - 8}) + 4]} (\xi + \sqrt{\xi^2 - 8}), \\ p_{c2} &= -\frac{1}{4} (\xi + \sqrt{\xi^2 - 8}). \end{aligned} \quad (\text{G5})$$

For any $\xi > \xi_1$, and as can be seen in Fig. 4, the two smallest zeros annihilate at $z = z_{c2}$ where their values are $p_2 = p_3 = p_{c2}$ and the two largest zeros annihilate at $z = z_{c1}$ where their values are $p_1 = p_2 = p_{c1}$. Note that at $\xi = \sqrt{8}$ the interval is a single point and one has $z_{c1} = z_{c2} = -\sqrt{2}e^{3/2}$ and $p_{c1} = p_{c2} = -1/\sqrt{2}$.

(3) It will turn out to be important below to distinguish the cases where $z_{c2} < z_c$ and $z_{c2} > z_c$; see Fig. 4. Let us determine the value of ξ , denoted $\xi = \xi_2$, at which $z_c(\xi) = z_{c2}(\xi)$. Inserting $z = z_c(\xi) = -\frac{2e^{\frac{\xi^2}{4}}}{\xi}$ into Eq. (G3) one gets two equations,

$$\xi p e^{-p^2} = -1, \quad p^2 + \frac{p\xi}{2} = -\frac{1}{2}, \quad (\text{G6})$$

where here p should be set to $p = p_{c2}(\xi)$ given in Eq. (G5). Combining we obtain a closed equation for $p\xi/2$, i.e.,

$$\frac{p\xi}{2} e^{\frac{p\xi}{2}} = -\frac{1}{2} e^{-1/2} \Rightarrow \frac{\xi p_{c2}(\xi)}{2} = W_{-1} \left(-\frac{1}{2\sqrt{e}} \right), \quad (\text{G7})$$

which using $p_{c2}(\xi)$ from Eq. (G5) and solving for ξ finally leads to $\xi = \xi_2$, with

$$\xi_2 = -2 \sqrt{\frac{2}{-2W_{-1}(-\frac{1}{2\sqrt{e}}) - 1}} W_{-1} \left(-\frac{1}{2\sqrt{e}} \right) \simeq 3.13395. \quad (\text{G8})$$

Note that we have discarded the other solution $\xi p_{c2}(\xi) = -1$ of Eq. (G7) which does not provide a solution for ξ_2 . Hence, we finally find that for $\xi < \xi_2$ one has $z_{c2} < z_c$ and for $\xi > \xi_2$ one has $z_c < z_{c2}$; see Fig. 4. This will be important below.

2. Continuation and branches of $\Psi(z)$ for $0 < \xi < \xi_1$

We now study the analytical continuations and various branches of $\Psi(z)$. Let us first recall the expressions of $\Psi(z)$ and $\Psi'(z)$ obtained in the text in Eqs. (31) and (32) for $\xi > 0$,

$$\begin{aligned} z\Psi'(z) &= \int_{\mathbb{R}} \frac{dq}{2\pi} \frac{\ln \left(1 - z(iq - \frac{\xi}{2}) e^{-q^2 - \frac{\xi^2}{4}} \right)}{(iq - \frac{\xi}{2})^2}, \\ \Psi(z) &= -\int_{\mathbb{R}} \frac{dq}{2\pi} \frac{\text{Li}_2 \left(z(iq - \frac{\xi}{2}) e^{-q^2 - \frac{\xi^2}{4}} \right)}{(iq - \frac{\xi}{2})^2}. \end{aligned} \quad (\text{G9})$$

The argument of the logarithm and polylogarithm is $A(q)$ defined in Eq. (G1). The integrand has branch cuts in the complex plane for q when $A(q) \in \mathbb{R}^-$, i.e., is real negative. In the previous subsection we found some of the zeros (those on the imaginary axis) from which the branch cuts originate. There are additional ones, and the full picture for all $\xi > 0$ is shown schematically in Fig. 5 where the zeros of $A(q)$ are represented by crosses and the branch cuts by red lines.

Here we examine the simplest case $\xi < \xi_1 = \sqrt{8}$. Then one finds that for $z_c < z < 0$ (top left in Fig. 5) no branch cut crosses the real axis. This corresponds to the regime with a single positive zero $p = p_1$ to Eq. (37). In that regime the formula in Eq. (G9) are valid. This is the *main branch*.

For $z \leq z_c(\xi) = -\frac{2e^{\frac{\xi^2}{4}}}{\xi}$ the single zero $p = p_1$ becomes negative hence the branch cut along the positive imaginary axis intersects the real axis at $q = 0$. This is represented in Fig. 5 (top right). In the case however, i.e., for $0 < \xi < \xi_1$, it is always possible (i.e., for any $z \leq z_c$) to deform the integration contour of q away from the real axis to pass below the branch cut (as represented in Fig. 5). We call this new contour C . This provides a natural analytical continuation to all real z . This leads to

$$\begin{aligned} z\Psi'(z) &= \int_C \frac{dq}{2\pi} \frac{\ln \left(1 - z(iq - \frac{\xi}{2}) e^{-q^2 - \frac{\xi^2}{4}} \right)}{(iq - \frac{\xi}{2})^2} \\ &= z\Psi'_0(z) + z\Delta'_1(z), \end{aligned} \quad (\text{G10})$$

$$z\Psi'_0(z) = \int_{\mathbb{R}} \frac{dq}{2\pi} \frac{\ln \left(1 - z(iq - \frac{\xi}{2}) e^{-q^2 - \frac{\xi^2}{4}} \right)}{(iq - \frac{\xi}{2})^2}.$$

In the second line we have split the integral into an integral over the real axis which passes right through the branch cut, and a contribution denoted $z\Delta'_1(z)$ which represents the contribution of a contour around the branch cut (taking into account the $2i\pi$ discontinuity of the logarithm), which reads

$$z\Delta'_1(z) = \int_0^{p_1} \frac{dp}{(p + \xi/2)^2} = \frac{4p_1}{\xi(2p_1 + \xi)}, \quad (\text{G11})$$

with $p_1 = p_1(z, \xi)$. The first piece, $z\Psi'_0(z)$ is by definition the integral over \mathbb{R} computed “naively,” that is with a jump of the integrand when the argument of the logarithm crosses the negative real axis (which occurs for $q = 0$) and in such a way that the invariance under the change of variable $iq \rightarrow -iq$ ensures that the result is real (in other words one can, e.g., replace $\int_{\mathbb{R}} = 2\Re \int_{\mathbb{R}^-}$) and not worry about the branch cut.

We can repeat the same procedure for the formula for $\Psi(z)$ itself in Eq. (G9), the branch cut of the Li_2 function being identical to the one of the logarithm with however a different value of the jump,

$$\text{Li}_2(t + i0^+) - \text{Li}_2(t - i0^+) = -2i\pi \ln t. \quad (\text{G12})$$

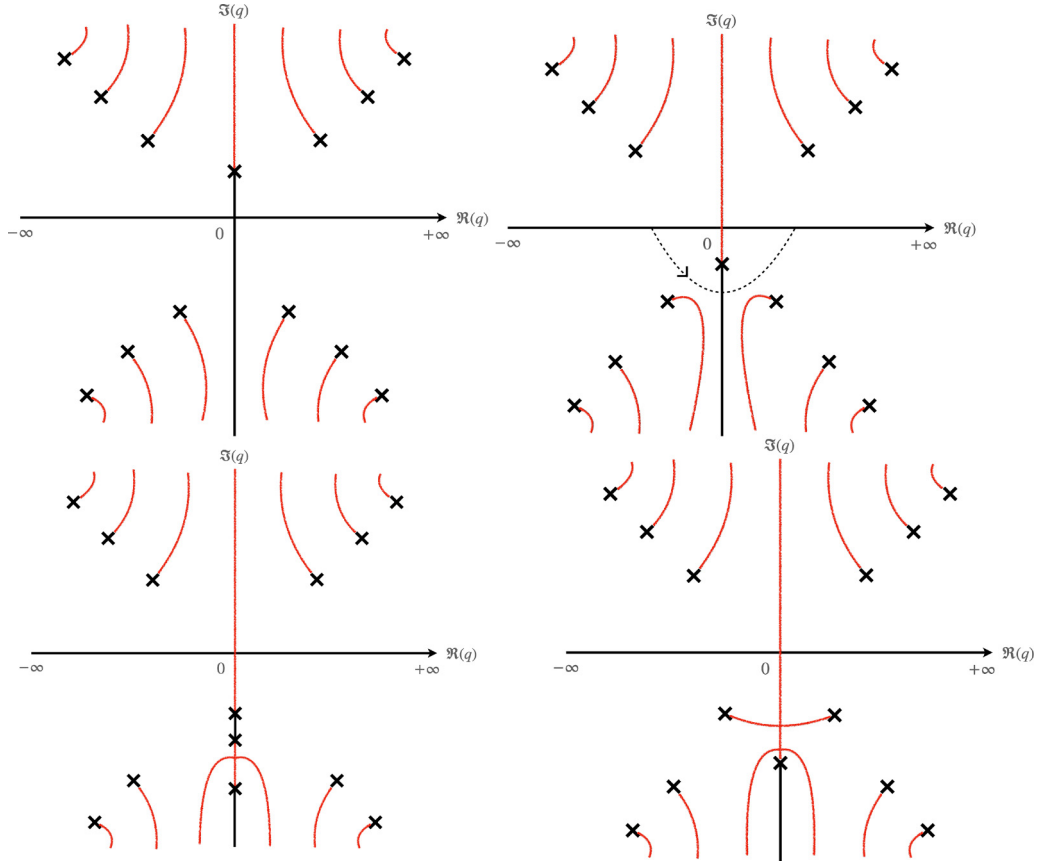


FIG. 5. Schematic plots of the argument of the logarithm $A(q)$ given in Eq. (G1) as a function of q in the complex plane for $\xi > 0$ and $z < 0$. The crosses indicate the positions of the zeros of $A(q)$ and the red lines are the branch cuts. (Top left) $z_c < z < 0$ for all $\xi > 0$. No branch cut crosses the real axis. (Top right) $z < z_c$ for $0 < \xi < \xi_1 = \sqrt{8}$, and $z_{c2} < z < z_c$ for $\xi_1 < \xi < \xi_2$. In that case one branch cut crosses the real axis. The integration contour in q in Eq. (G9) can be deformed (dotted lines) to avoid the branch cut. (Bottom left) $z_{c1} < z < z_{c2}$ for $\xi_1 < \xi$. It is still possible to avoid the branch cut. (Bottom right) $\xi > \xi_1$ and $z < z_{c1}$. In that case the branch cuts have met and form a cross, and there is no way to deform the integration contour to avoid them.

One obtains

$$\begin{aligned} \Psi(z) &= - \int_C \frac{dq}{2\pi} \frac{\text{Li}_2(z(iq - \frac{\xi}{2})e^{-q^2 - \frac{\xi^2}{4}})}{(iq - \frac{\xi}{2})^2} \\ &= \Psi_0(z) + \Delta_1(z), \end{aligned} \tag{G13}$$

$$\Psi_0(z) = - \int_{\mathbb{R}} \frac{dq}{2\pi} \frac{\text{Li}_2(z(iq - \frac{\xi}{2})e^{-q^2 - \frac{\xi^2}{4}})}{(iq - \frac{\xi}{2})^2},$$

with

$$\Delta_1(z) = - \int_0^{p_1} \frac{dp}{(p + \xi/2)^2} \ln \left(-z \left(p + \frac{\xi}{2} \right) e^{p^2 - \frac{\xi^2}{4}} \right) \tag{G14}$$

$$\begin{aligned} &= \hat{\Delta}(p_1(z, \xi)), \\ \hat{\Delta}(p) &= \frac{1}{\xi} \left[-(\xi^2 + 2)(\ln(\xi) - \ln(\xi + 2p)) \right. \\ &\quad \left. + 2p(p - \xi) - \frac{4p}{\xi + 2p} \right], \end{aligned} \tag{G15}$$

where we have defined a new function $\hat{\Delta}(p)$ which will be useful below. To obtain this expression for $\Delta_1(z)$ one can

either compute the contribution of the branch cut, as done above, or integrate the expression (G11) over z . In the latter case one uses the following differential relation for $p_1 = p_1(z)$,

$$\frac{dp_1}{dz} = - \frac{1}{z} \frac{p_1 + \frac{\xi}{2}}{1 + 2p_1(p_1 + \frac{\xi}{2})}, \tag{G16}$$

and write

$$\begin{aligned} \Delta_1(z) &= - \int_z^{z_c} \frac{dz'}{z'} \frac{4p_1(z')}{\xi(2p_1(z') + \xi)} \\ &= \int_0^{p_1} dp \frac{2p}{\xi} \frac{1 + 2p(p + \frac{\xi}{2})}{(p + \frac{\xi}{2})^2}, \end{aligned} \tag{G17}$$

which also yields (G14), showing that the two methods agree.

The above formula are those used for the plots of $\Psi'(z)$ in the main text for $0 < \xi < \xi_1$. We have checked numerically that for large negative $z \rightarrow -\infty$, $\Psi'(z) \rightarrow 1$ since $p_1 \rightarrow -\frac{\xi}{2} - \frac{1}{z} + o(1/z)$. This gives confidence that this is the correct solution.

3. Remark

We call $\Psi(z) = \Psi_0(z) + \Delta_1(z)$ for $z < z_c$ a new branch different from the main branch, although in a sense they are the same branch by some choice of integration contour. The important point here is the identification of the jump function $\Delta_1(z)$ which, as we will see now, plays an important role to determine the several other branches for $\xi > \xi_1$.

4. Remark

The structure of branch cuts in the complex plane discussed here for $\xi > 0$ is already present for $\xi = 0$, although in that case $z_c = -\infty$ (for $\xi \rightarrow 0^+$) so no analytic continuation is needed. There is some interpretation of the corresponding zeros of $a(k)$ and $\tilde{a}(k)$ in terms of additional solitonic solutions of the DNLS equation, as discussed in the main text. For $z > z_c$ these are presumably irrelevant for the large deviations.

5. Continuation and branches of $\Psi(z)$ for $\xi > \xi_1$

Let us consider now the case $\xi > \xi_1 = \sqrt{8}$. First, for $z_c(\xi) < z < 0$ it is still true that no branch cut crosses the real axis. This is because the largest zero p_1 is strictly positive hence the branch cut $q \in [ip_1, +i\infty[$ does not cross the real axis. Thus, the formula in Eq. (G9) are valid, and this is again the *main branch*.

Next, as discussed in a previous subsection, see Fig. 4, there is an interval of values of z , $z \in]z_{c1}, z_{c2}[$, where there are three real zeros $p_1 > p_2 > p_3$ to the equation $A(ip) = 0$. Then there are two sub-cases, for $\xi_1 < \xi < \xi_2$ one has $z_{c2} < z_c$, while for $\xi_2 < \xi$ one has $z_c < z_{c2}$.

In terms of branch cuts, as one can see in Fig. 5, one finds that for $z < z_c$ the branch cut $q \in [ip_1, +i\infty[$ crosses the real axis. However, as long as $z > z_{c1}$ there is a way to deform the contour of integration avoid this branch cut. For $z < z_{c1}$ something nasty happens, the upper and lower branch cuts meet and form a cross see Fig. 5 (bottom right). The same happened for the KPZ equation, as discussed in the previous section. In that case, it is not possible anymore to deform the integration contour to avoid these branch cuts. We can now use the ‘‘jump’’ function $\Delta_1(z)$ obtained in the previous section to propose the proper analytical continuations and the ensuing new branches.

When z reaches z_{c1} the zeros p_1 and p_2 annihilate (corresponding to the merging of the upper and lower branch cuts) and for $z < z_{c1}$ the only remaining zero is p_3 . Thus, one would like to write

$$\Psi(z) = \Psi_0(z) + \Delta_3(z), \quad \Delta_3(z) = \hat{\Delta}(p_3(z)), \quad (\text{G18})$$

where $\hat{\Delta}(p)$ was defined in Eq. (G15). This branch appears indeed in the Table I. However, since $\Delta_3(z_{c1}) \neq \Delta_1(z_{c1})$ it is not a continuous extension of $\Psi_0(z) + \Delta_1(z)$. This means that there are other branches that will allow a continuous extension. As we now discuss, they will be constructed by first decreasing z from $+\infty$ down to a turning point, increasing it up to a second turning point, and finally decreasing it again down to $-\infty$.

We will thus consider the point $z = z_{c1}$ as the first turning point and start to follow the second zero $p_2 = p_2(z)$. One then

proposes the continuous extension defined for $z \in]z_{c1}, z_{c2}[$,

$$\Psi(z) = \Psi_0(z) + \Delta_2(z), \quad \Delta_2(z) = \hat{\Delta}(p_2(z)). \quad (\text{G19})$$

It is a new branch and since $\Psi_0(z) + \Delta_1(z)$ also exists in the same interval $z \in]z_{c1}, z_{c2}[$ the function $\Psi(z)$ is multivalued in that interval.

When z reaches z_{c2} the zeros $p_2 = p_2(z)$ and $p_3 = p_3(z)$ annihilate [corresponding to the disappearance of the lower branch-cut as seen in Fig. 5 (top right)]. We then again consider $z = z_{c2}$ as a second turning point and start following the third zero p_3 . The candidate for the next continuous extension is therefore

$$\Psi(z) = \Psi_0(z) + \Delta_3(z), \quad \Delta_3(z) = \hat{\Delta}(p_3(z)), \quad (\text{G20})$$

which is precisely the one in Eq. (G18).

This procedure is sufficient for $\xi_1 < \xi < \xi_2$ and leads the third column in the Table I. Using the two turning points one thus obtains a continuous extension, which is multivalued in the interval $]z_{c1}, z_{c2}[$.

In the case $\xi > \xi_2$ this however is insufficient. Indeed, there is a last feature of the branch cuts to take into account. When z increases from z_{c1} to z_{c2} and then decreases from z_{c2} to $-\infty$ it can cross the value $z = z_c$ depending whether z_c is in the interval $]z_{c1}, z_{c2}[$. This is the case when $\xi > \xi_2$. When z crosses the value z_c , the branch point ip_1 crosses the real axis, either descending from the upper half plane or ascending from the lower half plane. We have observed for the first branch that crossing z_c from above, i.e., $z = z_c + 0^+ \rightarrow z_c + 0^-$ implies that the function Ψ_0 is modified as

$$\Psi_0 \rightarrow \Psi_0 + \Delta_1. \quad (\text{G21})$$

Conversely, crossing z_c from below, i.e., $z = z_c + 0^- \rightarrow z_c + 0^+$ implies that the function Ψ_0 should be modified as

$$\Psi_0 \rightarrow \Psi_0 - \Delta_1. \quad (\text{G22})$$

To obtain the complete solution for $\xi > \xi_2$ one then needs to take into account the coalescence of the zeros p_1, p_2, p_3 shown in Fig. 4 and also the different crossing of $z = z_c$ independently. This leads to the fourth column of Table I.

6. Remark

In all these formula $\Psi_0(z)$ denotes the integral (G13) along the real axis which may or may not have a jump in the integrand depending on whether $z < z_c$ or $z > z_c$.

APPENDIX H: SUMMARY OF THE RESULTS: DETERMINATION OF $\Phi(H)$

In this Appendix we summarize the exact results for the large-deviation rate function $\Phi(H)$ of the diffusion in time-dependent random medium for arbitrary position of the tracer $\xi > 0$. The rate function $\hat{\Phi}(Z)$ defined in the text is simply obtained as $\hat{\Phi}(Z) = \Phi(\ln Z)$.

TABLE II. Case $\xi = 0$.

Interval of H	Interval of z	$H =$	$\Phi(H) =$
$H \in \mathbb{R}^-$	$z \in \mathbb{R}$	$\ln \Psi'_0(z)$	$\Psi_0(z) - z\Psi'_0(z)$

1. Exact expressions for all rate functions and critical values

a. Critical values of ξ

There are two critical values of the position of tracer denoted ξ_1 and ξ_2 . Their value is given as

$$\begin{aligned} \xi_1 &= \sqrt{8} \simeq 2.82843, \\ \xi_2 &= -2\sqrt{\frac{2}{-2W_{-1}\left(-\frac{1}{2\sqrt{e}}\right) - 1}}W_{-1}\left(-\frac{1}{2\sqrt{e}}\right) \simeq 3.13395, \end{aligned} \tag{H1}$$

where W_{-1} is the second real branch of the Lambert function [57].

(1) For $\xi \geq \xi_1$ there can be three real zeros to Eq. (37) depending on z , whereas for $\xi \leq \xi_1$ there is only one real zero.

(2) The value ξ_2 is determined as the solution of $z_c(\xi) = z_{c2}(\xi)$. For $\xi \geq \xi_2$, we have the ordering $z_{c1} < z_c < z_{c2}$.

b. Critical values of z

There are three critical values of the parameter z denoted z_c , z_{c1} and z_{c2} . Their dependence on the tracer position ξ is given as

$$\begin{aligned} z_c(\xi) &= -\frac{2e^{\frac{\xi^2}{4}}}{\xi}, \\ z_{c1}(\xi) &= -\frac{1}{2}e^{\frac{1}{8}[\xi(\xi + \sqrt{\xi^2 - 8}) + 4]}(\xi - \sqrt{\xi^2 - 8}), \\ z_{c2}(\xi) &= -\frac{1}{2}e^{\frac{1}{8}[\xi(\xi - \sqrt{\xi^2 - 8}) + 4]}(\xi + \sqrt{\xi^2 - 8}). \end{aligned} \tag{H2}$$

(1) The quantities z_{c1} , z_{c2} are real only for $\xi > \xi_1$. They are determined by the value of p where the function $f_{z,\xi}$ has two degenerate zeros, i.e., $f_{z,\xi}(p) = f'_{z,\xi}(p) = 0$.

(2) For $z < z_c$, the largest real zero of $f_{z,\xi}(p)$ is negative, whereas for $z > z_c$ it is positive.

c. Critical values of the zeros p

$$p_c = 0, \tag{H3}$$

$$p_{c1} = -\frac{1}{4}(\xi - \sqrt{\xi^2 - 8}), \tag{H4}$$

$$p_{c2} = -\frac{1}{4}(\xi + \sqrt{\xi^2 - 8}). \tag{H5}$$

2. The rate function $\Phi(H)$

We obtain the rate function $\Phi(H)$ parametrically. In practice, its numerical determination will be done by parts using all the different branches of $\Psi(z)$. Since $z(H)$ is single-valued, this procedure allows us to obtain $\Phi(H)$ in the whole range $]-\infty, 0]$. We provide in the following the representations which were used for the numerical plots.

a. $\xi = 0$

The rate function (see Table II) reads:

b. $0 < \xi \leq \xi_1$

Defining the critical height $H_c = \ln \Psi'_0(z_c)$, the rate function (see Table III) reads:

c. $\xi_1 < \xi \leq \xi_2$

Defining the three critical heights

$$\begin{aligned} H_c &= \ln \Psi'_0(z_c), \\ H_{c1} &= \ln(\Psi'_0(z_{c1}) + \Delta'_1(z_{c1})) = \ln(\Psi'_0(z_{c1}) + \Delta'_2(z_{c1})), \\ H_{c2} &= \ln(\Psi'_0(z_{c2}) + \Delta'_2(z_{c2})) = \ln(\Psi'_0(z_{c2}) + \Delta'_3(z_{c2})), \end{aligned} \tag{H6}$$

the rate function (see Table IV) reads:

It is important to note that the expressions for H and for $\Phi(H)$ as a function of z in the second and third line of the above table merge continuously at $H = H_{c1}$ around the turning point at $z = z_{c1}$. This can be seen from Eqs. (G11) and (G17) as the jumps $\Delta_j(z) = \hat{\Delta}(p_j(z))$, $j = 1, 2$ are the same function of the zeros $p_j(z)$, hence one has $\Delta_1(z_{c1}) = \Delta_2(z_{c1})$ as well as $\Delta'_1(z_{c1}) = \Delta'_2(z_{c1})$, since $p_1(z) = p_2(z)$ at $z = z_{c1}$. This implies that as z decreases from $+\infty$ down to the turning point z_{c1} and then increases again from z_{c1} , the function $H = H(z)$ smoothly increases, and $\Phi(H)$ is a smooth function of H around H_{c1} . These features can be seen in Fig. 1(b) in the text. The same holds for each turning point and is also valid for the table in the next section.

d. $\xi_2 < \xi$

Defining the five critical heights

$$\begin{aligned} H_c &= \ln \Psi'_0(z_c), \\ H_{c10} &= \ln(\Psi'_0(z_{c1}) + \Delta'_1(z_{c1})), \\ H_{c11} &= \ln(\Psi'_0(z_c) + \Delta'_2(z_c)), \\ H_{c20} &= \ln(\Psi'_0(z_{c2}) + \Delta'_2(z_{c2}) - \Delta'_1(z_{c2})), \\ H_{c21} &= \ln(\Psi'_0(z_c) + \Delta'_3(z_c)), \end{aligned} \tag{H7}$$

the rate function (see Table V) reads:

3. Optimal rate function $\Psi(z)$

As discussed in the text the ‘‘optimal’’ $\Psi(z)$ follows by definition the minimum of the different branches of $\Psi(z)$ that we have found. For $\xi < \xi_1$ there is no multivaluation of $\Psi(z)$, hence $\Psi(z)$ follows continuously the two branches $z > z_c$ and $z < z_c$. For $\xi > \xi_1$ there is multivaluation of $\Psi(z)$ for $z \in]z_{c1}, z_{c2}[$ leading to a discontinuity, i.e., a jump of $\Psi(z)$. The value of z for which $\Psi(z)$ jumps from a branch to the next [see inset of Fig. 1(a)] is given by z^* solution of

$$\Delta_1(z^*) = \Delta_3(z^*). \tag{H8}$$

This value is located between z_{c1} and z_{c2} . We provide in the two Tables VI the value of the optimal Legendre solution. Note that the jump in the value of Z is always $\Delta'_3(z^*) - \Delta'_1(z^*)$ (jumps between the two maxima of the tilted measure for Z as discussed in the text).

TABLE III. Case $0 < \xi \leq \xi_1$.

Interval of H	Interval of z	$H =$	$\Phi(H) =$
$H \leq H_c$	$z_c \leq z$	$\ln \Psi'_0(z)$	$\Psi_0(z) - z\Psi'_0(z)$
$0 > H > H_c$	$z_c > z$	$\ln(\Psi'_0(z) + \Delta'_1(z))$	$\Psi_0(z) + \Delta_1(z) - z(\Psi'_0(z) + \Delta'_1(z))$

4. Additional plots

In this Appendix we show the plot of $\Psi(z)$ versus z , as well as the plot of $\Phi(H(z))$ versus z , see Fig. 6.

5. Result for $\xi = 0$ and correspondence with Ref. [40]

We provide in this Appendix a correspondence between the variables and functions studied in this work and in the work [40] in the particular case $\xi = 0$. In that case $g = 0$. This is summarized in Table VII.

Consider the formulas (27) and (29) in Ref. [40]. Taken together they give

$$s(\lambda) - \lambda j(\lambda) = \int_{\mathbb{R}} \frac{dk}{8\pi k^2} \text{Li}_2(-\lambda^2 k^2 e^{-2k^2}),$$

$$\lambda j(\lambda) = \int_{\mathbb{R}} \frac{dk}{4\pi k^2} \ln(1 + \lambda^2 k^2 e^{-2k^2}). \quad (\text{H9})$$

From Table VII we should identify the first result as $\Psi(z) - z/2$ and the second as $z/2 - z\Psi'(z)$. Using the duplication formula for the dilogarithm

$$\text{Li}_2(z) + \text{Li}_2(-z) = \frac{1}{2}\text{Li}_2(z^2), \quad (\text{H10})$$

we indeed find agreement with our formulas (32) and (31) with $z = -\lambda$ and using $\Theta(\xi = 0) = 1/2$ as discussed in the text.

6. Cumulant expansion of Z and checks

From its definition (7) the function $\Psi(z)$ encodes the cumulant expansion

$$\Psi(z) = - \sum_{p \geq 1} \frac{(-z)^p}{p!} T^{\frac{p-1}{2}} \overline{Z(Y, T)^p}. \quad (\text{H11})$$

We will now check from perturbation theory that the lowest order matches our exact result. Since $Z(Y, T)$ is the cumulative probability (4), from Eq. (2) it satisfies the SDE

$$\partial_\tau Z(y, \tau) = \partial_y^2 Z(y, \tau) - \sqrt{2}\eta(y, \tau)\partial_y Z(y, \tau), \quad (\text{H12})$$

which we can call the derivative stochastic heat equation, with initial condition $Z(y, \tau = 0) = \Theta(-y)$. We rescale the space and time variables as $y = x\sqrt{T}$, $\tau = tT$. Here we will abuse notations and use the same letter to denote $Z(y, \tau) =$

$Z(x, t)$. The original variable is recovered at the end. The rescaling yields the dimensionless equation with small noise amplitude

$$\partial_t Z(x, t) = \partial_x^2 Z(x, t) - \sqrt{2}T^{-1/4}\eta(x, t)\partial_x Z(x, t), \quad (\text{H13})$$

with initial condition $Z(x, t = 0) = \Theta(-x)$. Denoting $G(x, t) = \frac{1}{\sqrt{4\pi t}}e^{-x^2/(4t)}$ the free Green's function, this can also be written as

$$Z(x, t) = Z_0(x, t) - \frac{\sqrt{2}}{T^{1/4}} \int_0^t du \int_{\mathbb{R}} dx' G(x - x', t - u) \times \eta(x', u)\partial_{x'} Z(x', u),$$

$$Z_0(x, t) = \int_{\mathbb{R}} dx' G(x - x', t)\Theta(-x'). \quad (\text{H14})$$

(1) For the first moment one recovers indeed

$$\overline{Z(Y, T)} = \overline{Z(x, 1)} = Z_0(x, 1) = \int_x^{+\infty} dy G(y, 1)$$

$$= \frac{1}{2}\text{Erfc}\left(\frac{x}{2}\right) = \Psi'(0). \quad (\text{H15})$$

(2) To lowest order in $T^{-1/2}$ one finds the second cumulant

$$\overline{Z(x, 1)^2}^c = 2T^{-1/2} \int_0^1 du \int_{\mathbb{R}} dx' G(x - x', 1 - u)^2 \times (\partial_{x'} Z_0(x', u))^2 + \mathcal{O}(T^{-1}). \quad (\text{H16})$$

Using that $\partial_{x'} Z_0(x', u) = -G(x', u)$ one finds the remarkably simple result

$$\overline{Z(Y, T)^2}^c = \overline{Z(\xi, 1)^2}^c = T^{-1/2} \frac{e^{-\frac{\xi^2}{2}}}{4\sqrt{2\pi}} + \mathcal{O}(T^{-1}). \quad (\text{H17})$$

However, one must have

$$-T^{1/2}\overline{Z(Y, T)^2}^c = \Psi''(0) = -\frac{1}{2} \int_{\mathbb{R}} \frac{dq}{2\pi} e^{-2q^2 - \frac{\xi^2}{2}}$$

$$= -\frac{1}{4\sqrt{2\pi}} e^{-\frac{\xi^2}{2}}, \quad (\text{H18})$$

since $\Psi''(0)$ is the coefficient of z^2 in $z\Psi'(z)$.

TABLE IV. Case $\xi_1 < \xi \leq \xi_2$.

Interval of H	Interval of z	$H =$	$\Phi(H) =$
$H \leq H_c$	$z_c \leq z$	$\ln \Psi'_0(z)$	$\Psi_0(z) - z\Psi'_0(z)$
$H_c < H \leq H_{c1}$	$z_{c1} \leq z < z_c$	$\ln(\Psi'_0(z) + \Delta'_1(z))$	$\Psi_0(z) + \Delta_1(z) - z(\Psi'_0(z) + \Delta'_1(z))$
$H_{c1} < H \leq H_{c2}$	$z_{c1} < z \leq z_{c2}$	$\ln(\Psi'_0(z) + \Delta'_2(z))$	$\Psi_0(z) + \Delta_2(z) - z(\Psi'_0(z) + \Delta'_2(z))$
$H_{c2} < H < 0$	$z_{c2} > z$	$\ln(\Psi'_0(z) + \Delta'_3(z))$	$\Psi_0(z) + \Delta_3(z) - z(\Psi'_0(z) + \Delta'_3(z))$

TABLE V. Case $\xi_2 < \xi$.

Interval of H	Interval of z	$H =$	$\Phi(H) =$
$H \leq H_c$	$z_c \leq z$	$\ln \Psi'_0(z)$	$\Psi_0(z) - z\Psi'_0(z)$
$H_c < H \leq H_{c10}$	$z_{c1} \leq z < z_c$	$\ln(\Psi'_0(z) + \Delta'_1(z))$	$\Psi_0(z) + \Delta_1(z) - z(\Psi'_0(z) + \Delta'_1(z))$
$H_{c10} < H \leq H_{c11}$	$z_{c1} < z \leq z_c$	$\ln(\Psi'_0(z) + \Delta'_2(z))$	$\Psi_0(z) + \Delta_2(z) - z(\Psi'_0(z) + \Delta'_2(z))$
$H_{c11} < H \leq H_{c20}$	$z_c < z \leq z_{c2}$	$\ln(\Psi'_0(z) + \Delta'_2(z) - \Delta'_1(z))$	$\Psi_0(z) + \Delta_2(z) - \Delta_1(z) - z(\Psi'_0(z) + \Delta'_2(z) - \Delta'_1(z))$
$H_{c20} < H \leq H_{c21}$	$z_c \leq z < z_{c2}$	$\ln(\Psi'_0(z) + \Delta'_3(z) - \Delta'_1(z))$	$\Psi_0(z) + \Delta_3(z) - \Delta_1(z) - z(\Psi'_0(z) + \Delta'_3(z) - \Delta'_1(z))$
$H_{c21} < H < 0$	$z_c > z$	$\ln(\Psi'_0(z) + \Delta'_3(z))$	$\Psi_0(z) + \Delta_3(z) - z(\Psi'_0(z) + \Delta'_3(z))$

This shows that our formula (32) for the large-deviation function $\Psi(z)$ yields correctly the two lowest cumulants, as stated in the text. These first two cumulants describe the typical fluctuations of $Z(Y, T)$ in the diffusive scaling regime, $Y \simeq \sqrt{T}$, a regime which was studied previously in the mathematical literature [59,60].

7. Cumulants of H

One can obtain the cumulants of H from the derivatives of the rate function $\Phi(H)$ (see, e.g., Ref. [58, Sec. 4.2.5 of the Supplemental Material]). Here they scale as $\overline{H^q} \sim T^{\frac{1-q}{2}}$. The typical value $H = H_{\text{typ}}$ is determined by $\Phi'(H_{\text{typ}}) = 0$, which leads $e^{H_{\text{typ}}} = \Psi'(0)$ (see previous subsection) and the second cumulant reads

$$\begin{aligned} \overline{H^2} &= \frac{T^{-\frac{1}{2}}}{\Phi''(H_{\text{typ}})} = -T^{-\frac{1}{2}} \frac{\Psi''(0)}{\Psi'(0)^2} = C_2(\xi) T^{-\frac{1}{2}}, \\ C_2(\xi) &= \frac{1}{\sqrt{2\pi}} e^{-\frac{\xi^2}{2}} \left(\text{Erfc}\left(\frac{\xi}{2}\right) \right)^{-2}. \end{aligned} \quad (\text{H19})$$

Indeed, one can relate the derivatives $\Phi^{(q)}(H_{\text{typ}})$ to those of $\Psi(z)$ around $z = 0$ by differentiating the relations $\Psi'(z) = e^H$ and $\Phi(H) = -ze^H$. One obtains $\Phi''(H) - \Phi'(H) = -\frac{dz}{dH} e^H = -\frac{e^{2H}}{\Psi''(z)}$. Taken at $z = 0$ and $H = H_{\text{typ}}$ they lead to Eq. (H19). One has the asymptotics at small and large ξ ,

$$\begin{aligned} C_2(\xi) &= \frac{1}{\sqrt{2\pi}} + \frac{\sqrt{2}}{\pi} \xi + \mathcal{O}(\xi^2), \\ C_2(\xi) &= \sqrt{\frac{\pi}{2}} \left(\frac{\xi^2}{4} + 1 \right) + \mathcal{O}\left(\frac{1}{\xi^2}\right). \end{aligned} \quad (\text{H20})$$

TABLE VI. (Left) Case $\xi_1 < \xi \leq \xi_2$. In the inversion of the Legendre-Fenchel transform, Z jumps from $\Psi'_0(z^*) + \Delta'_1(z^*)$ to $\Psi'_0(z^*) + \Delta'_3(z^*)$. (Right) Case $\xi_2 < \xi$ (assuming $z_c < z^*$). In the inversion of the Legendre-Fenchel transform, Z jumps from $\Psi'_0(z^*)$ to $\Psi'_0(z^*) + \Delta'_3(z^*) - \Delta'_1(z^*)$. Note that $z_c > z^*$ would lead to a jump between the second branch and the last branch with the same jump criterion (H8).

Interval of z	“Optimal” $\Psi(z) =$	Interval of z	“Optimal” $\Psi(z) =$
$z_c \leq z$	$\Psi_0(z)$	$z^* \leq z$	$\Psi_0(z)$
$z^* \leq z < z_c$	$\Psi_0(z) + \Delta_1(z)$	$z_c \leq z < z^*$	$\Psi_0(z) + \Delta_3(z) - \Delta_1(z)$
$z^* > z$	$\Psi_0(z) + \Delta_3(z)$	$z_c > z$	$\Psi_0(z) + \Delta_3(z)$

APPENDIX I: CONVERGENCE TO THE LARGE DEVIATIONS OF THE KARDAR-PARISI-ZHANG EQUATION

1. Large ξ limit: Matching MFT at large time $T \gg 1$ to WNT at small time $T_{\text{KPZ}} \ll 1$

We ought to understand in this Appendix the behavior of our solution in the large ξ limit. In this regime, one first needs to rescale the variable z as

$$\tilde{z} = z \frac{\xi}{2} e^{-\frac{\xi^2}{4}} = -\frac{z}{z_c}. \quad (\text{I1})$$

2. Values of the main branch of the large-deviation function $\Psi_0(z)$

Recalling the definition of $\Psi_0(z)$ in Eq. (32) for $\xi > 0$, approximating $iq - \frac{\xi}{2} \sim -\frac{\xi}{2}$ and using the series expansion of the dilogarithm $\text{Li}_2(y) = \sum_{n>0} y^n/n^2$, we obtain that

$$\begin{aligned} \Psi_0(z) &\simeq -\frac{1}{\left(\frac{\xi}{2}\right)^2} \sum_{n=1}^{+\infty} \frac{(-\tilde{z})^n}{n^2} \int_{\mathbb{R}} \frac{dq}{2\pi} e^{-nq^2} \\ &\simeq \frac{4}{\xi^2} \Psi_{\text{KPZ},0}(\tilde{z}). \end{aligned} \quad (\text{I2})$$

To go from the first line to the second one, we performed the Gaussian integral and used the identity

$$\Psi_{\text{KPZ},0}(\tilde{z}) = -\frac{1}{\sqrt{4\pi}} \text{Li}_{5/2}(-\tilde{z}). \quad (\text{I3})$$

3. Critical values of z

In the same way, we rescale the critical values of z as follows:

$$\tilde{z}_c = -\frac{z_c}{z_c}, \quad \tilde{z}_{c1} = -\frac{z_{c1}}{z_c}, \quad \tilde{z}_{c2} = -\frac{z_{c2}}{z_c}, \quad (\text{I4})$$

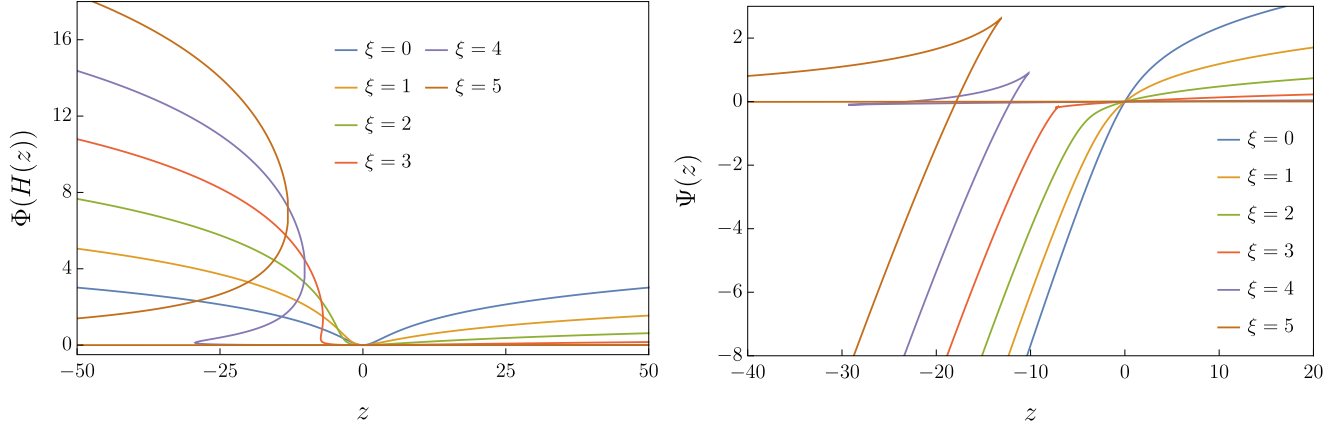


FIG. 6. Plots for various values of $\xi = 0, 1, 2, 3, 4, 5$. (Left) Large deviation rate function $\Phi(H(z))$ as a function of z using the definition (35). The function is symmetric for $\xi = 0$ and becomes asymmetric for nonzero values of ξ . It satisfies the symmetry $\Phi(H(z))|_{-\xi} = \Phi(H(-z))|_{\xi}$. (Right) Large deviation rate function $\Psi(z)$. The minimum branch of $\Psi(z)$ defines the “optimal” solution to the Legendre inversion of Eq. (8). For large negative values of z , the function becomes almost linear, i.e., $\Psi(z) \simeq z$.

and we take the $\xi \gg 1$ limit to obtain the limiting values

$$\begin{aligned} \bar{z}_c &= -1, & \bar{z}_{c1} &= -1 + \mathcal{O}\left(\frac{1}{\xi^2}\right), \\ \bar{z}_{c2} &= e^{1-\frac{\xi^2}{4}} \left[1 - \frac{\xi^2}{2} + \mathcal{O}\left(\frac{1}{\xi^2}\right) \right]. \end{aligned} \quad (15)$$

4. Values of the zeros p_1, p_2, p_3

Equation (37) determining the position of the branch cut reads with this variable

$$e^{-p^2} + \bar{z} \left(1 + \frac{2p}{\xi} \right) = 0. \quad (16)$$

At the first order at large ξ , the zeros of this equation read

$$\begin{aligned} p_1 &\simeq \sqrt{\ln\left(\frac{\bar{z}_c}{z}\right)} = \sqrt{-\ln(-\bar{z})}, \\ p_2 &\simeq -\sqrt{\ln\left(\frac{\bar{z}_c}{z}\right)} = -\sqrt{-\ln(-\bar{z})}, \\ p_3 &\simeq -\frac{\xi}{2} - \frac{1}{z} = -\frac{\xi}{2} - \frac{\xi}{2\bar{z}} e^{-\xi^2/4}. \end{aligned} \quad (17)$$

To study only real zeros imposes that $\bar{z} \in [-1, 0]$.

TABLE VII. Correspondence between the variables of this work and Ref. [40] for $\xi = 0$.

Present work	Ref. [40]
$z = \beta\Lambda$	$-\lambda$
βR	v
Q	u
$Z = e^H = \Psi'(z)$	$j + \frac{1}{2}$
$\Phi(H) = \Psi(z) - ze^H = \Psi(z) - z\Psi'(z)$	$s(j)$
$-z = e^{-H} \Phi'(H)$	$\lambda = \frac{ds}{dj}$

5. Values of the derivative of the jump function

Recalling that the derivative of the jump function (39) reads

$$\bar{z} \partial_{\bar{z}} \Delta_\ell = \frac{4p_\ell}{\xi(2p_\ell + \xi)}. \quad (18)$$

It yields for the different zeros

$$\begin{aligned} \bar{z} \partial_{\bar{z}} \Delta_1 &\simeq_{\xi \rightarrow \infty} \frac{4}{\xi^2} \sqrt{-\ln(-\bar{z})}, \\ \bar{z} \partial_{\bar{z}} \Delta_2 &\simeq_{\xi \rightarrow \infty} -\frac{4}{\xi^2} \sqrt{-\ln(-\bar{z})}, \\ \bar{z} \partial_{\bar{z}} \Delta_3 &\simeq_{\xi \rightarrow \infty} z = \frac{2\bar{z}}{\xi} e^{\frac{\xi^2}{4}}. \end{aligned} \quad (19)$$

6. Discussion about which branches remain in the large ξ limit

Recalling the different branches of the large-deviation function $\Psi(z)$ in Table V, we now discuss how the different branches behave in the large ξ limit. Since we have $\bar{z}_c = \bar{z}_{c1}$, the branches

$$\begin{aligned} \Psi(z) &= \Psi_0(z) + \Delta_1(z), \\ \Psi(z) &= \Psi_0(z) + \Delta_2(z) \end{aligned} \quad (110)$$

disappear on the \bar{z} scale. We now explain that the next branch, i.e.,

$$\Psi(z) = \Psi_0(z) + \Delta_2(z) - \Delta_1(z), \quad (111)$$

is the only one, besides the main branch, to remain on the \bar{z} scale. Indeed, looking at the derivative

$$\begin{aligned} \bar{z} \partial_{\bar{z}} \Psi(z) &= \bar{z} \partial_{\bar{z}} \Psi_0(z) + \bar{z} \partial_{\bar{z}} \Delta_2(z) - \bar{z} \partial_{\bar{z}} \Delta_1(z) \\ &\simeq \frac{4}{\xi^2} [\bar{z} \partial_{\bar{z}} \Psi_{\text{KPZ},0}(\bar{z}) - 2\sqrt{-\ln(-\bar{z})}], \end{aligned} \quad (112)$$

which has a jump function part identical to Eq. (F7). Hence, that branch converges to the second branch of the KPZ rate function, i.e., to $\Psi_{\text{KPZ}}(\bar{z}) = \Psi_{\text{KPZ},0}(\bar{z}) + \Delta_{\text{KPZ}}(\bar{z})$, as claimed in the text.

Furthermore, as explained in the main text, the last two branches with $\Delta = \Delta_3 - \Delta_1$ and $\Delta = \Delta_3$ disappear in the

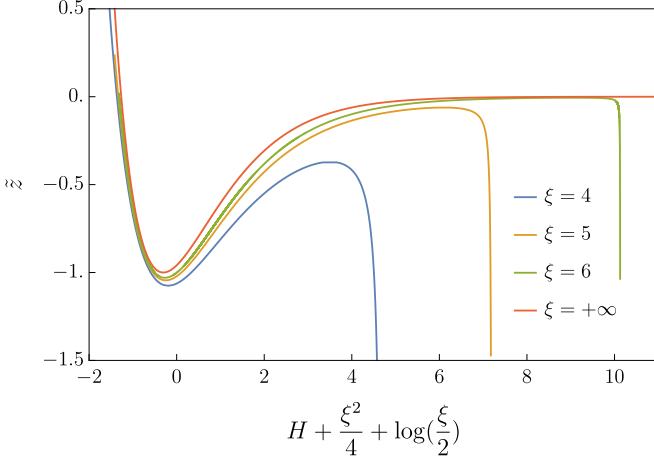


FIG. 7. Plot of $\tilde{z} = -z/z_c$ as a function of $H_{\text{KPZ}} = H + \frac{\xi^2}{4} + \ln(\frac{\xi}{2})$ for several values of $\xi = 4, 5, 6$ as compared with the asymptotic $\xi = \infty$ KPZ expression. All branches are represented. The convergence to KPZ is excellent. The last two branches in Table I correspond to the sharp decrease to $\tilde{z} \rightarrow -\infty$ and is pushed to $H_{\text{KPZ}} = +\infty$ as $\xi = +\infty$. It corresponds to events where $Z \approx 1$ which become irrelevant in that limit.

region $H \sim 0$ or equivalently $Z \sim 1$, which correspond to $H_{\text{KPZ}} \rightarrow +\infty$ see discussion below.

7. Matching to the regime $Y \sim T^{4/3}$

It was predicted in Refs. [16,18], and proved in Ref. [20], that the sample-to-sample fluctuations of the probability denoted here as $Z(Y, T) = e^{H(Y, T)}$ —defined in Eq. (3)—when seen in an atypical space time direction, are related to those of the random height field $h_{\text{KPZ}}(x, t) = h(x, t)$ solution of the KPZ equation

$$\partial_t h(x, t) = \partial_x^2 h(x, t) + (\partial_x h)^2 + \sqrt{2}\eta(x, t), \quad (\text{I13})$$

with droplet initial condition $e^{h(x,0)} = \delta(x)$, where η is a standard space-time white noise. The relation to the KPZ solution at finite time, $h_{\text{KPZ}}(0, t)$, holds when one scales $Y \sim T^{3/4}$. The scaling studied here $Y \sim T^{1/2}$ thus corresponds to short KPZ time, while the scaling $Y \sim T$ corresponds to the limit of infinite KPZ time, leading to the Tracy-Widom distribution [15].

Let us recall the result of Ref. [20, Sec. 3.2 Eq. (30)] established in the scaling regime $Y \sim T^{3/4}$ (we consider here $Y > 0$). Setting $y = 0$ and $t = 2T$ there (to account for the different units) it translates into the equality in law in the large T limit [for the diffusion (2)]

$$\ln \mathbb{P}[y(T) > \tilde{x}(2T)^{3/4}] + \frac{1}{2}\tilde{x}^2(2T)^{1/2} + \frac{1}{4} \ln(2T) - \ln \tilde{x} = h_{\text{KPZ}}\left(0, \frac{\tilde{x}^4}{2}\right), \quad (\text{I14})$$

where $\tilde{x} = \frac{Y}{(2T)^{3/4}}$. Hence, denoting

$$T_{\text{KPZ}} = \frac{Y^4}{16T^3} \quad (\text{I15})$$

we have the equalities in law

$$H(Y, T) = h_{\text{KPZ}}(0, T_{\text{KPZ}}) - \frac{Y^2}{4T} + \ln \frac{Y}{2T} \\ \Leftrightarrow Z(Y, T) = \frac{Y}{2T} e^{-\frac{Y^2}{4T}} e^{h_{\text{KPZ}}(0, T_{\text{KPZ}})}, \quad (\text{I16})$$

valid *a priori* in the regime $Y \sim T^{3/4}$. Let us now set $Y = \xi\sqrt{T}$, with $\xi > 0$. One gets

$$Z(Y, T) = \frac{\xi}{2\sqrt{T}} e^{-\frac{\xi^2}{4}} e^{h_{\text{KPZ}}(0, T_{\text{KPZ}})}, \quad T_{\text{KPZ}} = \frac{\xi^4}{16T}, \quad (\text{I17})$$

valid *a priori* in the regime $\xi \sim T^{1/4}$. We now show that it holds beyond that, i.e., in the large deviation regime where ξ is of order one but large, which is also the regime where the KPZ time is small, $T_{\text{KPZ}} \ll 1$. To compare with the known large deviation results for the KPZ equation at short time, it is useful to introduce

$$H_{\text{KPZ}} := h_{\text{KPZ}}(0, T_{\text{KPZ}}) + \ln(\sqrt{T_{\text{KPZ}}}). \quad (\text{I18})$$

These results read [46], given here in the form of [10, Eqs. (4) and (22)]

$$\overline{\exp(-\tilde{z}e^{h_{\text{KPZ}}(0, T_{\text{KPZ}})})} = \overline{\exp\left(-\frac{\tilde{z}}{\sqrt{T_{\text{KPZ}}}} e^{H_{\text{KPZ}}}\right)} \\ = \exp\left(-\frac{\Psi_{\text{KPZ}}(\tilde{z})}{\sqrt{T_{\text{KPZ}}}}\right), \quad (\text{I19})$$

where $\Psi_{\text{KPZ}}(\tilde{z}) = \Psi_{\text{KPZ},0}(\tilde{z}) = -\frac{1}{\sqrt{4\pi}} \text{Li}_{5/2}(-\tilde{z})$. While the l.h.s. exists *a priori* only for $\tilde{z} > 0$ this formula admits an analytic continuation, called the main branch, for $\tilde{z} \in [-1, +\infty]$. Already at this level we can match with the results of the present study. Indeed here we obtained for the main branch for $z > z_c$, see Eqs. (43) and (44) in the text

$$\overline{\exp(-z\sqrt{T}Z)} = \exp\left(-\sqrt{T} \frac{4}{\xi^2} \Psi_{\text{KPZ},0}(\tilde{z})\right), \quad \tilde{z} = z \frac{\xi}{2} e^{-\xi^2/4}, \quad (\text{I20})$$

which is in perfect agreement with Eq. (I19) using the relations in Eq. (I17). Hence, the large deviations in the regime $Y \sim T^{3/4}$ and the diffusive regime $Y \sim \sqrt{T}$ match smoothly.

As discussed in Refs. [10,46] one obtains the rate function for the KPZ equation, $\Phi_{\text{KPZ}}(H_{\text{KPZ}})$, upon Legendre inversion in the parametric form

$$\Phi_{\text{KPZ}}(H_{\text{KPZ}}) = \Psi_{\text{KPZ}}(\tilde{z}) - \tilde{z}e^{H_{\text{KPZ}}}, \quad e^{H_{\text{KPZ}}} = \Psi'_{\text{KPZ}}(\tilde{z}). \quad (\text{I21})$$

For the KPZ equation the main branch $\Psi_{\text{KPZ},0}(\tilde{z})$ allows us to obtain $\Phi_{\text{KPZ}}(H_{\text{KPZ}})$ only for $H_{\text{KPZ}} < H_{\text{KPZ},c} = \ln \frac{\zeta(3/2)}{4\pi}$ which corresponds to the field at which $\tilde{z} = \tilde{z}(H_{\text{KPZ}})$ solution of Eq. (I21) with $\Psi_{\text{KPZ}} \rightarrow \Psi_{\text{KPZ},0}$ reaches $\tilde{z} = -1$. For $H_{\text{KPZ}} > H_{\text{KPZ},c}$ one needs to use the second branch $\Psi_{\text{KPZ}} \rightarrow \Psi_{\text{KPZ},0} + \Delta_{\text{KPZ}}(\tilde{z})$ and $\tilde{z}(H_{\text{KPZ}})$ increases again from -1 to 0 as $H_{\text{KPZ}} \rightarrow +\infty$.

As we have shown in the previous subsection in the limit $\xi \rightarrow +\infty$ one obtains the convergence

$$\Psi(z) \rightarrow \frac{4}{\xi^2} \Psi_{\text{KPZ}}(\tilde{z}), \quad (\text{I22})$$

not just for the main branch, but for all the branches which survive in that limit. Thus, we expect the correspondence between the fields obtained upon Legendre transform

$$H(z) = \ln \left(\frac{d\Psi}{dz} \right) \underset{\xi \gg 1}{\simeq} \ln \left(\frac{4}{\xi^2} \frac{d\tilde{z}}{dz} \frac{d\Psi_{\text{KPZ}}}{d\tilde{z}} \right) \underset{\xi \gg 1}{\simeq} -\frac{\xi^2}{4} - \ln \left(\frac{\xi}{2} \right) + H_{\text{KPZ}}(\tilde{z}). \tag{I23}$$

The prediction is thus that using the results of the present work for $\xi \rightarrow +\infty$, one should have that $\tilde{z} = -z/z_c$ plotted versus $H_{\text{KPZ}} = H + \frac{\xi^2}{4} + \ln \frac{\xi}{2}$ reaches a limit curve identical to $\tilde{z}(H_{\text{KPZ}})$ for the KPZ equation. As one can see from Eq.(7) this is indeed the case.

Finally we can check that Eq. (I23) is indeed consistent with the correspondence discussed above from the matching to the $Y \sim T^{3/4}$ regime. Indeed, using Eqs. (I18) and (I17) one has

$$\begin{aligned} H_{\text{KPZ}}(\tilde{z}) &= h_{\text{KPZ}}(0, T_{\text{KPZ}}) + \ln(\sqrt{T_{\text{KPZ}}}) \\ &= h_{\text{KPZ}}(0, T_{\text{KPZ}}) - \ln(\sqrt{T}) + \ln(\xi^2/4) \\ &= H + \frac{\xi^2}{4} + \ln \frac{\xi}{2}, \end{aligned} \tag{I24}$$

which is identical to Eq. (I23).

In conclusion, inserting into the parametric representation of the Legendre transform one obtains for $\xi \gg 1$

$$\Phi(H) \simeq \frac{4}{\xi^2} \Phi_{\text{KPZ}}(H_{\text{KPZ}}), \quad H_{\text{KPZ}} = H + \frac{\xi^2}{4} + \ln \frac{\xi}{2}, \tag{I25}$$

as given in the text which means that one can identify the large deviations probabilities

$$\begin{aligned} \mathcal{P}(H) &\sim \exp(-\sqrt{T}\Phi(H)) \sim \exp\left(-\frac{\Phi(H_{\text{KPZ}})}{\sqrt{T_{\text{KPZ}}}}\right) \\ &\sim \mathcal{P}_{\text{KPZ}}(H_{\text{KPZ}}). \end{aligned} \tag{I26}$$

APPENDIX J: LARGE-TIME LIMIT OF THE FREDHOLM DETERMINANT RESULT FOR THE STICKY BROWNIAN MOTION

In this section we start from the formula of Ref. [19] and study the diffusive limit where T and Y are large with $\xi = Y/\sqrt{T}$ fixed. This leads to a conjectural form for $\Psi(z)$ which agrees with the one derived in the text using inverse scattering. The manipulations in this Appendix are quite heuristic but they have the merit to show that the algebraic structure which emerges from the Fredholm determinant is similar to the one derived in the text from first principles by the inverse scattering method. We hope that it will help to obtain in the future a more precise and rigorous derivation.

In Ref. [19] the quantity which corresponds to $Z(Y, T)$ was studied. It was denoted $K_{0,t}(0, [x, +\infty[)$ and called the kernel of the uniform Howitt-Warren flow [61]. The equivalence between the two objects, mathematically very subtle, was discussed in Ref. [19, Remark 2.4] (see also Refs. [62,63]). Note that the regime of typical fluctuations of $Z(Y, T)$ was studied in Ref. [59] (see also Ref. [60]) and it was shown to have Edwards-Wilkinson type of fluctuations with $T^{1/4}$ scaling.

Here, the quantity which we define as $Z(Y, T)$ obeys a backward Fokker-Planck equation. Indeed, from the definition

$$Z(Y, \tau) = \int_Y^{+\infty} dy q_\eta(y, \tau), \quad q_\eta(y, \tau) = -\partial_y Z(y, \tau), \tag{J1}$$

one easily obtains upon integrating Eq. (2)

$$\partial_\tau Z(Y, \tau) = \partial_Y^2 Z(Y, \tau) - \sqrt{2}\eta(Y, \tau)\partial_Y Z(Y, \tau), \tag{J2}$$

with initial condition $Z(Y, \tau = 0) = \Theta(-Y)$. This is equivalent to Ref. [19, Eq. (19)]. The correspondence of notations is that the space and time variables there must be replaced by $t \rightarrow 2T$ and $x = Y$. Note that in Ref. [19, Eq. (19)] the noise term is $-\sqrt{2}\eta(y, T) = \frac{\sqrt{2}}{\sqrt{\lambda}}\hat{\eta}(y, T)$ where $\hat{\eta}$ is standard space-time white noise. Hence, below λ is set to unity.

The identity proved in Ref. [19, Theorem 1.11] reads for u nonnegative

$$\mathbb{E}[e^{-uZ(Y, T)}] = \text{Det}(I - K_u)|_{\mathbb{L}^2(C)}, \tag{J3}$$

where C is a positively oriented circle with radius R and centered at R and

$$K_u(v, v') = \frac{1}{2i\pi} \int_{1/2+i\mathbb{R}} \frac{\pi}{\sin \pi s} u^s \frac{g(v)}{g(v+s)} \frac{ds}{s+v-v'}. \tag{J4}$$

The definition of $g(v)$ is

$$g(v) = \Gamma(v) e^{aY\psi_0(v)+bT\psi_1(v)}, \tag{J5}$$

where $\psi_{0,1}$ denote polygamma functions and $a = \lambda$ and $b = \lambda^2$. Here λ is set to unity.

We now use $\zeta = v + s$ as a variable, for which the integration contour can be chosen as $1/2 + 2R + i\mathbb{R}$ —see remark in Ref. [19, Proposition 2.3]—where we recall that C is the integration contour for v, v' . We factorize the kernel (J4) into the following form,

$$K_u(v, v') = \int_{1/2+2R+i\mathbb{R}} \frac{d\zeta}{2i\pi} A(v, \zeta) \tilde{A}(\zeta, v'), \tag{J6}$$

$$\begin{aligned} A(v, \zeta) &= \frac{\pi u^{\zeta-v}}{\sin(\pi(\zeta-v))} \frac{g(v)}{g(\zeta)}, \\ \tilde{A}(\zeta, v') &= \frac{1}{\zeta - v'}. \end{aligned} \tag{J7}$$

We now use the identity

$$\frac{\pi}{\sin(\pi s)} u^s = \int_{\mathbb{R}} dr \frac{u}{u + e^{-r}} e^{-sr}, \tag{J8}$$

which, inserted into Eq. (J7), allows us to factorize the kernel A as

$$\begin{aligned} A(v, \zeta) &= \int_{\mathbb{R}} dr \frac{u}{u + e^{-r}} e^{-(\zeta-v)r} \frac{g(v)}{g(\zeta)} \\ &= \int_{\mathbb{R}} dr \sigma(r) A_1(v, r) A_2(r, \zeta) \\ &= (A_1 \sigma A_2)(v, \zeta), \end{aligned} \tag{J9}$$

where the kernels A_1, A_2 and the function σ read

$$A_1(v, r) = g(v)e^{vr},$$

$$A_2(r, \zeta) = \frac{e^{-\zeta r}}{g(\zeta)},$$

$$\sigma(r) = \frac{u}{u + e^{-r}}. \tag{J10}$$

Hence, using Sylvester's identity

$$\begin{aligned} \text{Det}(I - K_u)|_{\mathbb{L}^2(C)} &= \text{Det}(I - A\tilde{A}) \\ &= \text{Det}(I - A_1\sigma A_2\tilde{A}) \\ &= \text{Det}(I - \sigma A_2\tilde{A}A_1)|_{\mathbb{L}^2(\mathbb{R})}. \end{aligned} \tag{J11}$$

This last Fredholm determinant has the typical structure for which the first cumulant method, developed in Refs. [48–50] to study the relevant asymptotics (here large T), applies. Defining a determinantal point process $\{a_\ell\}_{\ell \in \mathbb{N}}$ associated to the kernel $A_2\tilde{A}A_1$, the following identity holds,

$$\text{Det}(I - \sigma A_2\tilde{A}A_1) = \mathbb{E} \left[\prod_{\ell=1}^{\infty} (1 - \sigma(a_\ell)) \right] = \mathbb{E} \left[\prod_{\ell=1}^{\infty} e^{-\varphi(a_\ell)} \right], \tag{J12}$$

where $e^{-\varphi} = 1 - \sigma$. The first cumulant approximation asserts [48, Sec. 6] that as some parameter goes to infinity (here it will be T , see below), we expect the point process to self-average, i.e.,

$$\mathbb{E} \left[\prod_{\ell=1}^{\infty} e^{-\varphi(a_\ell)} \right] \sim e^{-\mathbb{E}[\varphi(a)]} = e^{-\text{Tr}(\varphi A_2\tilde{A}A_1)}. \tag{J13}$$

If the first cumulant method works, then we aim to have under the right scaling

$$\text{Det}(I - K_u)|_{\mathbb{L}^2(C)} \sim \exp[-\text{Tr}(\varphi A_2\tilde{A}A_1)]. \tag{J14}$$

The explicit expression of the kernel $A_2\tilde{A}A_1$ is obtained as

$$(A_2\tilde{A}A_1)(r, r') = \int_{1/2+2\mathbb{R}+i\mathbb{R}} \frac{d\zeta}{2i\pi} \int_C \frac{dv'}{2i\pi} \frac{g(v')}{g(\zeta)} \frac{1}{\zeta - v'} e^{r'v' - r\zeta}, \tag{J15}$$

taking into account that the measure on the variables v is $\frac{dv}{2i\pi}$. Using that

$$\varphi(r) = \ln(1 + ue^r) = -\text{Li}_1(-ue^r) \tag{J16}$$

to apply the first cumulant method we need to calculate the following quantity which only involves the diagonal part of the kernel $A_2\tilde{A}A_1$,

$$\begin{aligned} \text{Tr}(\varphi A_2\tilde{A}A_1) &= - \int_{\mathbb{R}} dr \int_{1/2+2\mathbb{R}+i\mathbb{R}} \frac{d\zeta}{2i\pi} \\ &\times \int_C \frac{dv'}{2i\pi} \text{Li}_1(-ue^r) \frac{g(v')}{g(\zeta)} \frac{1}{\zeta - v'} e^{r(v'-\zeta)}. \end{aligned} \tag{J17}$$

We recall that $\Re(\zeta - v') > 0$ by construction. We further proceed to an integration by part with respect to r to

obtain

$$\begin{aligned} \text{Tr}(\varphi A_2\tilde{A}A_1) &= - \int_{\mathbb{R}} dr \int_{1/2+2\mathbb{R}+i\mathbb{R}} \frac{d\zeta}{2i\pi} \\ &\times \int_C \frac{dv'}{2i\pi} \text{Li}_2(-ue^r) \frac{g(v')e^{rv'}}{g(\zeta)e^{r\zeta}}. \end{aligned} \tag{J18}$$

The boundary terms of the integration by part are zero since $e^{r(1+v'-\zeta)} \rightarrow 0$ for $r \rightarrow -\infty$ and the polylogarithms behave as $\text{Li}_s(e^r) \sim r^s$ at $r \rightarrow +\infty$.

At this stage we proceed to the large-time rescaling to the diffusive regime using the rescaled variables

$$\{Y = \xi\sqrt{T}, \quad v = w\sqrt{T}, \quad \zeta = \omega\sqrt{T}, \quad u = z\sqrt{T}\}. \tag{J19}$$

We then rewrite Eq. (J17) as

$$\begin{aligned} \text{Tr}(\varphi A_2\tilde{A}A_1) &= - \int_{\mathbb{R}} dr \text{Li}_2(-ue^r) I(r) \\ &= - \int_{\mathbb{R}} dr \text{Li}_2(-ze^r) I(r - \ln\sqrt{T}), \end{aligned} \tag{J20}$$

where we have shifted the variable r by $-\ln\sqrt{T}$ and defined

$$\begin{aligned} I(r - \ln\sqrt{T}) &= \int_{1/2+2\mathbb{R}+i\mathbb{R}} \frac{d\zeta}{2i\pi} \int_C \frac{dv'}{2i\pi} \frac{g(v')e^{(r-\ln(\sqrt{T}))v'}}{g(\zeta)e^{(r-\ln(\sqrt{T}))\zeta}} \\ &= \int_{1/2+2\mathbb{R}+i\mathbb{R}} \frac{d\zeta}{2i\pi} e^{-(\ln g(\zeta) + (r-\ln\sqrt{T})\zeta)} \\ &\times \int_C \frac{dv}{2i\pi} e^{(\ln g(v) + (r-\ln\sqrt{T})v)}. \end{aligned} \tag{J21}$$

The large-time expansion of the function $g(v)$ given in Eq. (J5) reads

$$\begin{aligned} \ln g(v) &= aY\psi_0(v) + bT\psi_1(v) + \ln \Gamma(v) \\ &= \sqrt{T}(\phi(w) + (w + a\xi) \ln \sqrt{T}) \\ &\quad + \chi(w) - \frac{1}{2} \ln(\sqrt{T}) + o(T), \end{aligned} \tag{J22}$$

where we defined

$$\begin{aligned} \phi(w) &= \frac{b}{w} - w + (w + a\xi) \ln(w), \\ \chi(w) &= \frac{b}{2w^2} - \frac{a\xi}{2w} + \frac{1}{2} \ln(2\pi w). \end{aligned} \tag{J23}$$

At this stage we will choose the radius of the circle C conveniently to be equal to $\mathbb{R} = T/Y$ so that its mapping under the large- T limit is a circle C' of radius $1/\xi$ centered at $1/\xi$ (we assume here and below that $\xi > 0$). Upon the change of variable (J19) in the large T limit, inserting Eq. (J22) into Eq. (J21) and noting that constant terms cancel from the two integrals we obtain

$$\begin{aligned} I(r - \ln\sqrt{T}) &\simeq T \int_{2/\xi+0^++i\mathbb{R}} \frac{d\omega}{2i\pi} e^{-\sqrt{T}(\phi(\omega)+r\omega)-\chi(\omega)} \\ &\times \int_{C'} \frac{dw}{2i\pi} e^{\sqrt{T}(\phi(w)+rw)+\chi(w)}. \end{aligned} \tag{J24}$$

In the large- T limit these integrals are dominated by saddle points. The saddle-point equation reads

$$\phi'(w) = -\frac{1}{w^2} + \frac{\xi}{w} + \ln(w) = -r \quad (\text{J25})$$

and the same for ω . Since w is on the circle C' we can parametrize it in the following way,

$$\frac{1}{w} = -iq + \frac{\xi}{2}, \quad q \in \mathbb{R}. \quad (\text{J26})$$

The saddle-point equation becomes

$$e^r = \left(-iq + \frac{\xi}{2}\right) e^{-q^2 - \frac{\xi^2}{4}}, \quad (\text{J27})$$

which is very reminiscent of Eq. (37). To make this saddle point easily attainable, one way is to deform the integration contour of r which is not \mathbb{R} anymore but the image of Eq. (J27) as q varies on the real axis, which we call γ . We will assume that this is possible. This is a closed curve for e^r , touching the real axis at values $e^r = 0$ and $e^r = \frac{\xi}{2} e^{-\frac{\xi^2}{4}}$. The solution of Eqs. (J26) and (J27) defines a function $w(r)$ so that the saddle-point evaluation of Eq. (J24) gives

$$I(r - \ln \sqrt{T}) \simeq -\frac{\sqrt{T}}{2i\pi} \frac{1}{\phi''(w(r))}, \quad (\text{J28})$$

where we have also assumed that the integration contour of ω could be deformed to be folded around C' . This ensures that the dominant exponential at the saddle-point cancel.

To summarize, the first cumulant (J20) of the Fredholm determinant reads in the large T -limit

$$\text{Tr}(\varphi A_2 \tilde{A} A_1) = \frac{\sqrt{T}}{2i\pi} \int_{\gamma} dr \text{Li}_2(-ze^r) \frac{1}{\phi''(w(r))}. \quad (\text{J29})$$

We will now perform the change of variable (J27). Using the saddle-point equation $\phi'(w(r)) = -r$ we obtain upon derivation the Jacobian of this change of variable

$$\begin{aligned} \phi''(w(r)) \frac{dw(r)}{dq} \frac{dq}{dr} &= -1, \\ \frac{1}{\phi''(w(r))} dr &= -i \frac{dq}{\left(iq - \frac{\xi}{2}\right)^2}. \end{aligned} \quad (\text{J30})$$

Inserting into Eq. (J29) we finally obtain

$$\Psi(z) = \frac{1}{\sqrt{T}} \text{Tr}(\varphi A_2 \tilde{A} A_1) = - \int_{\mathbb{R}} \frac{dq}{2\pi} \frac{\text{Li}_2\left(z\left(iq - \frac{\xi}{2}\right) e^{-q^2 - \frac{\xi^2}{4}}\right)}{\left(iq - \frac{\xi}{2}\right)^2}, \quad (\text{J31})$$

which is in agreement with Eq. (32) in the text.

APPENDIX K: EXTENSION TO THE EXTREMAL DIFFUSION BEYOND EINSTEIN'S DIFFUSION THEORY

In this section we study the position of the maximum of N walkers in the same random field (by sample below we mean one given environment, i.e., random field). Previous

works started with Refs. [15,22] which studied the β random walk and pointed out that for $N \gg 1$, and in the regime $\ln N \sim T$, the position of the maximum has sample to sample fluctuations given by the Tracy-Widom distribution. Another regime, $\ln N \sim \sqrt{T}$, was obtained in Refs. [16,20] where these fluctuations are described by the solution of the KPZ equation at finite time. Numerical simulations which confirm these regimes have been performed recently [51]. Extending these arguments, our present work allows us to study another regime, $\ln N \ll \sqrt{T}$, not studied previously.

Consider N independent particles in the same environment. One denotes $Y_N(T) = \max_i Y_i(T)$ with $i = 1, \dots, N$ and $Z_N(Y, T) = \mathbb{P}(Y_N(T) > Y)$. One has the exact relation

$$\begin{aligned} 1 - Z_N(Y, T) &= \mathbb{P}(Y_N(T) < Y) = \mathbb{P}(Y(T) < Y)^N \\ &= (1 - Z(Y, T))^N. \end{aligned} \quad (\text{K1})$$

We focus below on the diffusive scaling $Y \sim \sqrt{T}$ at large T , not considered previously in the discussion of the extremal diffusion. We will thus denote $y_N(T) = \frac{1}{\sqrt{T}} Y_N(T)$. There are several observables of interest.

1. Large deviations of the CDF of the maximum

The first observable is $Z_N = \mathbb{P}(y_N(T) > \xi)$, which is simply the analog of Z for the maximum position of N particles. One can ask, for any finite N , what are the large deviations of the PDF of Z_N for $T \gg 1$. From the above simple relation (K1) one finds for

$$\mathcal{P}(Z_N) \sim \exp(-\sqrt{T} \hat{\Phi}_{\xi}(1 - (1 - Z_N)^{1/N})), \quad (\text{K2})$$

where the rate function $\hat{\Phi}_{\xi}(Z)$ is the one obtained in the present work (for $N = 1$). Here and below we indicate explicitly the dependence in ξ of the rate functions.

2. Averaged CDF of the maximum

Another observable is the following average over the environment,

$$\begin{aligned} \overline{\mathbb{P}(y_N(T) < \xi)} &= \int_0^1 dZ e^{N \ln(1-Z)} \\ &\sim \int_0^1 dZ e^{N \ln(1-Z) - \sqrt{T} \hat{\Phi}_{\xi}(Z)}, \end{aligned} \quad (\text{K3})$$

where in the last equation we have substituted the large deviation form. Note that considering instead of the average moments of order q is equivalent to substitute $n \rightarrow nq$.

There are several regimes depending on N . If $N \ll \sqrt{T}$, then the second term dominates and implies that $Z \approx Z_{\text{typ}}(\xi)$ so that

$$\overline{\mathbb{P}(y_N(T) < \xi)} \simeq e^{N \ln(1 - Z_{\text{typ}}(\xi))}, \quad (\text{K4})$$

and the result is identical as the CDF of the maximum position for N particles in the absence of random field.

If $N = n\sqrt{T} \gg 1$ with $n = \mathcal{O}(1)$ fixed, then the two terms can balance each other and one finds that this observable takes

the large deviation form

$$\begin{aligned} \overline{\mathbb{P}(y_N(T) < \xi)} &\sim e^{-\sqrt{T}\Sigma_\xi(n)}, \\ \Sigma_\xi(n) &= \min_Z(\hat{\Phi}_\xi(Z) - n \ln(1 - Z)), \end{aligned} \quad (\text{K5})$$

with a rate function obtained from a non trivial variational formula. Here for a given ξ the value of Z which realizes the optimum is different from $Z_{\text{typ}}(\xi)$ and thus involves rare environments. Upon some simple manipulations, recalling that $Z = \Psi'(z)$ and $\hat{\Phi}'(Z) = -z$ we obtain $z = \frac{n}{1-Z}$ leading to the parametric representation

$$\Sigma_\xi(n) = \Psi_\xi(z) - z + n - n \ln\left(\frac{n}{z}\right), \quad z[1 - \Psi'_\xi(z)] = n. \quad (\text{K6})$$

Note that the approximation $N \ln(1 - Z) \simeq -NZ$ valid for $Z = \Psi'_\xi(z) \ll 1$ would instead lead to $z \simeq n$ and $\Sigma_\xi(n) \simeq \Psi_\xi(z)$. Although we leave this study to the future, it is quite likely that a phase transition similar to the one of $\Psi(z)$ for $\xi > \xi_1$ for and for some values of z should also occur here. For $n \rightarrow 0$ one has $n \simeq z[1 - \Psi'_\xi(0)] = z[1 - Z_{\text{typ}}(\xi)]$ and one recovers (K4). More precisely one has the expansion

$$\begin{aligned} \Sigma_\xi(n) &= -n \ln(1 - \Psi'_\xi(0)) + \frac{\Psi''_\xi(0)n^2}{2[1 - \Psi'_\xi(0)]^2} + \mathcal{O}(n^3), \\ \Psi'_\xi(0) &= Z_{\text{typ}}(\xi). \end{aligned} \quad (\text{K7})$$

3. Position of the maximum: Typical behavior

One can ask about the position of the maximum and its fluctuations. Let us introduce N i.i.d exponential random variables g_i of PDF $P(g) = e^{-g}\Theta(g)$, and call $G_N = \max_i g_i - \ln N$. At large N , $G_N \rightarrow G$ a Gumbel random variable with $\mathbb{P}(G < g) = e^{-e^{-g}}$. For any N one has $\mathbb{P}(G < g) = (1 - \frac{1}{N}e^{-g})^N$. In a given environment one can write

$$\begin{aligned} \mathbb{P}(Y_N(T) < Y) &= e^{N \ln(1 - Z(Y, T))} \\ &= \overline{\Theta(G_N + \ln N + H(Y, T) < 0)}^{G_N}. \end{aligned} \quad (\text{K8})$$

This formula is valid for any N and for large N one obtains the same formula with $G_N \rightarrow G$ by approximating $e^{N \ln(1 - Z)} \simeq e^{-NZ}$. Note that G_N and G in this formula are independent of $H(Y, T)$. As discussed below, the approximation $Z \ll 1$ is also realized for any N with large probability when $\xi = Y/\sqrt{T}$ is large. The random position of the maximum $Y_N(T)$, in a given environment is then given by

$$G_N + \ln N + H(Y, T) < 0 \Leftrightarrow Y_N(T) < Y \quad (\text{K9})$$

Note that $G_N + \ln N$ is a positive random variable. Since $Z(Y, T)$ and thus $H(Y, T)$ is a positive decreasing function of Y in any sample, one may argue [by taking a derivative w.r.t. Y in Eq. (K8)] that Eq. (K9) is equivalent to

$$G_N + \ln N + H(Y_N(T), T) = 0. \quad (\text{K10})$$

This formula generalizes Ref. [20, Eq. (50)] to any N .

Until now this is exact. Let us again consider the diffusive scaling regime $Y \sim \sqrt{T}$ at large T . In a typical environment, one has $H(Y, T) \simeq H_{\text{typ}}(\xi)$ where $\xi = Y/\sqrt{T}$ and $H_{\text{typ}}(\xi) = \ln(\int_\xi^{+\infty} \frac{e^{-x^2/4}}{\sqrt{4\pi}}) = \ln(\frac{1}{2}\text{Erfc}(\frac{\xi}{2})) =$

$-\frac{\xi^2}{4} - \ln(\sqrt{\pi}\xi) + \mathcal{O}(\xi^{-1})$. Note that $H_{\text{typ}}(\xi)$ varies from 0 for $\xi \rightarrow -\infty$ to $-\infty$ for $\xi \rightarrow +\infty$. Let us denote y_N^{typ} the scaled position of the maximum in a typical environment. At large T it reaches a finite limit in distribution such that

$$\begin{aligned} G_N + \ln N + H_{\text{typ}}(y_N^{\text{typ}}) &= 0 \\ \Leftrightarrow y_N^{\text{typ}} &= H_{\text{typ}}^{-1}(-G_N - \ln N), \end{aligned} \quad (\text{K11})$$

where $H_{\text{typ}}^{-1}(h) = \xi$ is the reciprocal function of $H_{\text{typ}}(\xi) = h$. This is correct for any N . The distribution of y_N^{typ} is exactly the same as the one for the maximum of N Brownian motions at time $t = 1$, performing each diffusion $dB_i(t)^2 = 2dt$, started at $B_i(0) = 0$ at $t = 0$, i.e., for the problem without the quenched random field. For $N \gg 1$, using the asymptotics of $H_{\text{typ}}(\xi)$ one finds the standard result

$$y_N^{\text{typ}} \simeq 2\sqrt{\ln N} + \frac{G - \frac{1}{2} \ln(4\pi \ln N)}{\sqrt{\ln N}} + \dots \quad (\text{K12})$$

We can now study the typical fluctuations from sample to sample. To lowest order one should take into account the typical fluctuations of $H(Y, T)$, which are $\delta H = \mathcal{O}(T^{1/4})$. The variance was obtained in Eq. (H19) as $\overline{H^2}^c = C_2(\xi)T^{-1/2}$, where the function $C_2(\xi)$ was given there. The position of the maximum is now determined by

$$G_N + \ln N + H_{\text{typ}}(y_N) + \sqrt{C_2(y_N)}T^{-1/4}\omega = 0, \quad (\text{K13})$$

where ω is a Gaussian random variable of unit variance. Inverting to leading order at large time we find (an equation valid for any N)

$$y_N = H_{\text{typ}}^{-1}(-G_N - \ln N - \sqrt{C_2(y_N^{\text{typ}})}T^{-1/4}\omega) + o(T^{-1/4}) \quad (\text{K14})$$

$$= y_N^{\text{typ}} - \frac{\sqrt{C_2(y_N^{\text{typ}})}}{H'_{\text{typ}}(y_N^{\text{typ}})}T^{-1/4}\omega + o(T^{-1/4}). \quad (\text{K15})$$

If $N \gg 1$, then one finds

$$\begin{aligned} y_N &= 2\sqrt{\ln N} + \frac{G - \frac{1}{2} \ln(4\pi \ln N) + \sqrt{C_2(y_N^{\text{typ}})}T^{-1/4}\omega}{\sqrt{\ln N}} \\ &\quad + \dots, \end{aligned} \quad (\text{K16})$$

where we recall that the ω term represents the sample-to-sample fluctuations and the Gumbel variable G the ‘‘thermal’’ fluctuations, the two random variables being uncorrelated.

We can compare this result with Ref. [20, Eqs. (57) and (58)] setting $D = 1$ and $r_0 = 2$ there, which were obtained when N and T are large with the parameter $g = \frac{\ln N}{\sqrt{T}}$ kept fixed. The KPZ time there is $T_{\text{KPZ}} = g^2 = \frac{(\ln N)^2}{T}$. This agrees perfectly with the KPZ time in the present work $T_{\text{KPZ}} = \xi^4/(16T)$ where $\xi \sim y_N \sim 2\sqrt{\ln N}$ from Eq. (K16). For the matching to Ref. [20, Eqs. (57) and (58)] to be perfect we need the variance of the KPZ height field at very short time (i.e., in the Edward-Wilkinson regime for droplet initial condition), which is given by [46]

$$\overline{h(0, T_{\text{KPZ}})^2}^c \simeq C_2^{\text{KPZ}}T_{\text{KPZ}}^{1/2}, \quad C_2^{\text{KPZ}} = \sqrt{\frac{2}{\pi}}. \quad (\text{K17})$$

One then easily checks that it exactly matches the amplitude of the fluctuating term $\sim \omega$ in Eq. (K16) using the large ξ behavior (H20), $C_2(\xi) \simeq \frac{\xi^2}{4} \sqrt{\frac{2}{\pi}}$.

To summarize, Eqs. (K14) and (K16) extend the results of Ref. [20] about “typical” extremal diffusion to the diffusive regime $Y \sim \sqrt{T}$. In that new regime $\ln N \ll \sqrt{T}$, i.e., $T \gg (\ln N)^2$ and the fluctuations are of the Edwards-Wilkinson type. If N is large, then $\ln N$ does not need to be very large. As $(\ln N)^2/T$ is increased there is a perfect match to the predictions of Ref. [20] in the regime $Y \sim T^{3/4}$ where the sample-to-sample fluctuations are governed by the finite-time KPZ equation.

4. Remark

The two independent random contributions in Eq. (K16) can be separated by considering simultaneously the “quantile” as done in numerical simulations [51], that is, instead of $y_N(T)$, $x_N(T) = \frac{X_N(T)}{\sqrt{T}}$ defined by $\int_{X_N(T)}^{+\infty} dy q_\eta(y, T) = \frac{1}{N}$ in a given sample, or in other words,

$$\ln H(X_N(T), T) = -\ln N, \quad Z(X_N(T), T) = \frac{1}{N}. \quad (\text{K18})$$

5. Position of the maximum: Large deviations

Finally, our results yield additional information about the large deviations of extremal diffusion, i.e., for rare environments such that $H - H_{\text{typ}} = \mathcal{O}(1)$. In that case, if one heuristically replaces in Eq. (K10), $H(Y_N(T), T) \rightarrow H_{\text{typ}}(y_N(T)) + (H - H_{\text{typ}}(y_N^{\text{typ}}))$, then one obtains

$$y_N \simeq H_{\text{typ}}^{-1}(-G_N - \ln N - (H - H_{\text{typ}})), \quad (\text{K19})$$

and for $N \gg 1$,

$$y_N \simeq 2\sqrt{\ln N} + \frac{G - \frac{1}{2} \ln(4\pi \ln N) + (H - H_{\text{typ}}(\xi))}{\sqrt{\ln N}} + \dots, \quad (\text{K20})$$

with $\xi = 2\sqrt{\ln N}$, for rare environments which occur with probability $\sim \exp(-\sqrt{T}\Phi_\xi(H))$. Since ξ is large, rewriting $H = -\frac{\xi^2}{4} - \ln \frac{\xi}{2} + H_{\text{KPZ}}$, this is equivalent to extend the estimate of Ref. [20] for the fluctuations of the position of the maximum to the large deviations regime of the KPZ equation (with rare environments occurring with probability $\sim \exp(-\frac{1}{\sqrt{T_{\text{KPZ}}}}\Phi_{\text{KPZ}}(H_{\text{KPZ}}))$ and with $T_{\text{KPZ}} = \frac{\xi^4}{16T} = \frac{(\ln N)^2}{T} \ll 1$).

APPENDIX L: EXTENSION TO GENERAL QUADRATIC MODELS IN THE MFT: DIFFUSION IN RANDOM MEDIUM AND THE SYMMETRIC SIMPLE EXCLUSION PROCESS

One definition of the MFT is as the Langevin equation of a diffusive gas with particle density $q(x, t)$ [64]

$$\partial_t q = \partial_x [D(q)\partial_x q - \sqrt{\sigma(q)}\xi(x, t)], \quad (\text{L1})$$

where $\xi(x, t)$ is a standard space-time white noise. The model solved in this present paper corresponds to $\sigma(q) = 2q^2$ and $D(q) = 1$. Averages of solutions of Eq. (L1)

over the noise can be obtained from the dynamical action $S[q, p] = \iint dx dt [p\partial_t q - \mathcal{H}(q, p)]$ with Hamiltonian $\mathcal{H}(q, p) = -D(q)\partial_x q\partial_x p + \frac{1}{2}\sigma(q)(\partial_x p)^2$, and where $p(x, t)$ is the response field. At large time these averages can be obtained from the solutions to the saddle-point equations $\partial_t q = \frac{\delta \mathcal{H}}{\delta p}$ and $\partial_t p = -\frac{\delta \mathcal{H}}{\delta q}$, which admit the conservation law $\frac{d}{dt} \mathcal{H}(p, q) = 0$.

We will focus below on a subclass of models within the MFT called quadratic models and show how the work of this present paper is relevant to solve them.

1. Mapping of quadratic models in the MFT to the coupled DNLS system

Consider here the quadratic MFT models which have a noise variance parameterized as

$$\sigma(q) = 2Aq(B - q) \quad (\text{L2})$$

and a diffusion constant $D(q) = 1$. This class contains both the SEP and the present model of diffusion in random medium. The MFT hydrodynamic equations (i.e., the saddle-point equations) read

$$\begin{aligned} \partial_t q &= \partial_x [\partial_x q - 2Aq(B - q)\partial_x p], \\ \partial_t p &= -\partial_x^2 p - A(B - 2q)(\partial_x p)^2. \end{aligned} \quad (\text{L3})$$

We introduce the generalized derivative Cole-Hopf transform

$$R(x, t) = A\partial_x p(x, t)e^{ABp(x, t)}, \quad Q(x, t) = q(x, t)e^{-ABp(x, t)}. \quad (\text{L4})$$

The variables $\{R, Q\}$ then verify the coupled DNLS system (A7) with $\beta = 1$,

$$\begin{aligned} \partial_t Q &= \partial_x^2 Q + 2\partial_x(Q^2 R), \\ -\partial_t R &= \partial_x^2 R - 2\partial_x(QR^2). \end{aligned} \quad (\text{L5})$$

2. Gauge transformation between NLS and DNLS and relation with the nonlocal transformation of Ref. [42]

a. Change of variable of Wadati and Sogo

Wadati and Sogo proved in 1982 [65] that the nonlinear Schrodinger equation and the derivative nonlinear Schrodinger equation were gauge equivalent. Indeed, consider the following systems in the conventions of Ref. [65], first the coupled NLS,

$$\begin{aligned} iq_{1t} + q_{1xx} - 2r_1q_1^2 &= 0, \\ ir_{1t} - r_{1xx} + 2r_1^2q_1 &= 0, \end{aligned} \quad (\text{L6})$$

and second the coupled DNLS,

$$\begin{aligned} q_{2t} - iq_{2xx} - (r_2q_2^2)_x &= 0, \\ r_{2t} + ir_{2xx} - (r_2^2q_2)_x &= 0. \end{aligned} \quad (\text{L7})$$

Wadati and Sogo showed that the following change of variables allows us to map the coupled DNLS system to the

coupled NLS system,

$$q_1 = \frac{q_2}{2} \exp\left(-i \int_{-\infty}^x r_2 q_2\right),$$

$$r_1 = (-ir_{2x} + r_2^2 q_2/2) \exp\left(i \int_{-\infty}^x r_2 q_2\right). \quad (\text{L8})$$

To show the relation with the nonlocal transformation of Ref. [42], one needs to relate the conventions of Wadati to the ones of this present work and of Ref. [42]. We first transform the time in Eqs. (L6) and (L7) as $t \rightarrow it$, and choose

$$q_1 = v, \quad r_1 = u,$$

$$q_2 = -2R, \quad r_2 = iQ. \quad (\text{L9})$$

We obtain that Eq. (L7) is the $\{R, Q\}$ system with $\beta = 1$ [that is, e.g., Eq. (11) with $g = 0$ or Eq. (A7)] and that Eq. (L6) is the $\{P, Q\}$ system with $g = -1$. This $\{P, Q\}$ system is precisely the equations verified by the functions $\{v, u\}$ of Ref. [42] (with $v = P$ and $u = Q$).

Now, considering the MFT for the SEP, we have shown in Eq. (L4) that the derivative Cole-Hopf transform of the MFT variables verify the DNLS $\{R, Q\}$ system. Performing the gauge transformation (L8) with our new variables thus leads to

$$u = (Q^2 R + \partial_x Q) \exp\left(2 \int_{-\infty}^x dy QR\right),$$

$$v = -R \exp\left(-2 \int_{-\infty}^x dy QR\right). \quad (\text{L10})$$

We can now go back to the variables q and p of the MFT using the generalized derivative Cole-Hopf transform (L4), and we obtain

$$u = (-Aq(B - q)\partial_x p + \partial_x q) \exp\left(-\int_{-\infty}^x dy A(B - 2q)\partial_y p\right), \quad (\text{L11})$$

$$v = -A\partial_x p \exp\left(\int_{-\infty}^x dy A(B - 2q)\partial_y p\right), \quad (\text{L12})$$

which is valid for any quadratic theory. This recovers the ‘‘generalized Cole-Hopf equations’’ obtained very recently in Ref. [42, Eqs. (10)–(11)] (which use the notations $H = p$ and $\varrho = q$). Note however the missing the factor A in the second equation in that work.

3. Stationary measure

The stochastic equation (L1) admits generically a family of stationary measures. For instance if one fixes the boundary conditions as $q(0) = q(L) = \varrho$, and if the problem is taken on a finite-size interval, the stationary measure is [2,26,64,66]

$$\mathcal{P}_{\text{eq}}(\{q(x)\}) \sim e^{-\int_0^L dx (f(q(x)) - f(\varrho) - (q(x) - \varrho)f'(\varrho))}, \quad (\text{L13})$$

where $f''(q) = \frac{2D(q)}{\sigma(q)}$. The linear term is determined so that the maximum probability is for $q = \varrho$.

Consider the model of diffusion in a random environment studied here in Eq. (2), with a more general amplitude for the noise. In that case one has $D(q) = 1$ and $\sigma(q) = 2\alpha q^2$, hence

$f''(q) = 1/(\alpha q^2)$. This leads to $f(q) = -\frac{1}{\alpha} \ln q + kq + c$, and to the stationary measure

$$\mathcal{P}_{\text{eq}}(\{q(x)\}) \propto e^{-\frac{1}{\alpha} \int_0^L dx (-\ln(q(x)/\varrho) + \frac{q(x)-\varrho}{\varrho})}. \quad (\text{L14})$$

4. Remark

The stationary measure (L14) is the analog in the continuum of a discrete measure on a lattice defined as a product of independent Γ variables at each site, i.e., $\prod_x w_x$, with PDF $p(w) \propto w^{\gamma-1} e^{-w}$. Indeed that measure appeared as a stationary measure in the β polymer problem. The fact that its one point distribution is a Γ variable was found in Ref. [18], and recently proved for the continuum model in Ref. [62, Prop. 5.4]. The fact that it is a product measure of Γ variables was conjectured recently in Ref. [67, discussion below Conjecture 1.14]. For the more general quadratic model parametrized as Eq. (L2), in particular for the SEP, the corresponding discrete stationary measures are instead factorized Bernoulli.

5. Remark

From a mathematical standpoint the precise meaning of Eq. (L13) is nontrivial, more generally the continuum analog of a discrete i.i.d. process is subtle [68] and some exotic noises appear in related Howitt-Warren stochastic flows [69].

6. Remark

For the diffusion model, one has $B = 0$ in Eq. (L2). Hence, $R = A\partial_x p$ and $Q = q$ satisfy the DNLS system with $\beta = 1$. By choosing here $A = -\alpha$ one can vary the exponent γ of the local Γ distribution to any value in the stationary measure.

7. Extension of Ref. [42] to quadratic MFT models with annealed initial condition and tracer away from the origin

Let us consider a model within the MFT where the noise variance is parametrized as (L2). We study here the annealed case where the initial condition of the hydrodynamic equations (L3) is fluctuating according to the stationary measure of the MFT [2,35,36]. We choose the initial condition as a local equilibrium configuration with two different densities on the positive and negative axis,

$$\mathcal{P}(q(x, 0)) \sim e^{-\sqrt{T}\mathcal{F}(q(x, 0))},$$

$$\mathcal{F}(q(x, 0)) = \int_{\mathbb{R}} dx \int_{\tilde{q}(x)}^{q(x, 0)} dz \frac{2D(z)}{\sigma(z)} [q(x, 0) - z], \quad (\text{L15})$$

with $\tilde{q}(x) = q_- \Theta(-x) + q_+ \Theta(x)$ is the step density profile.

We will be interested in the position X_t of a tracer initially located at position $X_0 = 0$ and at final position $X_1 = \xi$. Its position at any time is defined as

$$\int_0^{X_t} dx q(x, t) = \int_0^\infty dx [q(x, t) - q(x, 0)]. \quad (\text{L16})$$

If we focus on the generating function of X_1 or the current at the right of X_1 , i.e., $Z(\xi) = \int_\xi^\infty dx [q(x, 1) - q(x, 0)]$, then it was shown [26,35,36] that the mixed-time boundary

conditions of the hydrodynamic system (L2) read

$$p(x, 1) = \lambda \Theta(x - \xi), \quad (\text{L17})$$

$$p(x, 0) = \lambda \Theta(x) + \int_{\bar{q}(x)}^{q(x,0)} dr \frac{2D(r)}{\sigma(r)} \quad (\text{L18})$$

for some constant λ . Using the gauge transformation (L12) along with the same manipulations as the ones in Ref. [42, below Eqs. (14) and (15)] allows us to transform these boundary conditions for $\{p, q\}$ into simple boundary conditions for $\{u, v\}$,

$$u(x, 0) = \frac{\omega}{K} \delta(x), \quad v(x, 1) = K \delta(x - \xi). \quad (\text{L19})$$

for some constant K to be determined as in Ref. [42]. These boundary conditions have an asymmetry due to the presence of ξ that we can cancel using the same boost transformation as in Eq. (A10),

$$\begin{aligned} U(x, t) &= u(x - vt, t) e^{-\frac{1}{2}xv + \frac{v^2}{4}t}, \\ V(x, t) &= v(x - vt, t) e^{\frac{1}{2}xv - \frac{v^2}{4}t}. \end{aligned} \quad (\text{L20})$$

Note that this boost leaves the coupled NLS system (L6) invariant. We choose $v = -\xi$ so that

$$\begin{aligned} U(x, t) &= u(x + \xi t, t) e^{\frac{1}{2}x\xi + \frac{\xi^2}{4}t}, \\ V(x, t) &= v(x + \xi t, t) e^{-\frac{1}{2}x\xi - \frac{\xi^2}{4}t}, \end{aligned} \quad (\text{L21})$$

which yields for boundary conditions

$$U(x, 0) = \frac{\omega}{K} \delta(x), \quad V(x, 1) = K e^{-\frac{\xi^2}{4}} \delta(x). \quad (\text{L22})$$

One can then proceed as in this work to complete the scattering analysis and solve the large-deviation problem.

8. Discussion on the quench and annealed initial conditions

The quadratic models of MFT have been investigated through the spectrum of classical integrability in three works and two contexts of initial conditions:

(1) Reference [42] considered the SEP with an initial condition in the annealed class and solved the problem through the mapping to the coupled NLS $\{P, Q\}$ system and the use of its scattering theory. The remarkable feature of that work is that the annealed initial condition for the SEP admits a simple quenched δ, δ mixed-time boundary conditions interpretation in the coupled NLS $\{P, Q\}$ system.

(2) The present work as well as Ref. [40] considered the diffusion in random media, equivalent to the KMP model, with a quenched initial condition and solved the problem using the scattering theory of the coupled DNLS $\{R, Q\}$ system.

At this stage, the observation is that depending on whether the quench or annealed initial condition is considered, a specific integrable model might be more suited to obtain the exact solution of the problem. Since other gauge transformations between integrable models have been proposed in Ref. [65], it would be interesting to investigate whether mappings to other integrable models would allow us to answer new questions.

-
- [1] L. Bertini, A. De Sole, D. Gabrielli, G. Jona-Lasinio, and C. Landim, Macroscopic fluctuation theory, *Rev. Mod. Phys.* **87**, 593 (2015).
- [2] B. Derrida, Nonequilibrium steady states: Fluctuations and large deviations of the density and of the current, *J. Stat. Mech.: Theory Exp.* (2007) P07023.
- [3] B. Derrida, An exactly soluble nonequilibrium system: The asymmetric simple exclusion process, *Phys. Rep.* **301**, 65 (1998).
- [4] C. A. Tracy and H. Widom, Asymptotics in ASEP with step initial condition, *Commun. Math. Phys.* **290**, 129 (2009).
- [5] M. Kardar, G. Parisi, and Y.-C. Zhang, Dynamic Scaling of Growing Interfaces, *Phys. Rev. Lett.* **56**, 889 (1986).
- [6] L. Bertini and G. Giacomin, Stochastic burgers and KPZ equations from particle systems, *Commun. Math. Phys.* **183**, 571 (1997).
- [7] I. V. Kolokolov and S. E. Korshunov, Explicit solution of the optimal fluctuation problem for an elastic string in random potential, *Phys. Rev. E* **80**, 031107 (2009); Universal and nonuniversal tails of distribution functions in the directed polymer and KPZ problems, *Phys. Rev. B* **78**, 024206 (2008); Optimal fluctuation approach to a directed polymer in a random medium, **75**, 140201(R) (2007).
- [8] B. Meerson, E. Katzav, and A. Vilenkin, Large Deviations of Surface Height in the Kardar-Parisi-Zhang Equation, *Phys. Rev. Lett.* **116**, 070601 (2016).
- [9] N. R. Smith, B. Meerson, and A. Vilenkin, Time-averaged height distribution of the Kardar-Parisi-Zhang interface, *J. Stat. Mech.* (2019) 053207.
- [10] A. Krajenbrink and P. Le Doussal, Inverse Scattering of the Zakharov-Shabat System Solves the Weak Noise Theory of the Kardar-Parisi-Zhang Equation, *Phys. Rev. Lett.* **127**, 064101 (2021).
- [11] A. Krajenbrink and P. L. Doussal, Inverse scattering solution of the weak noise theory of the Kardar-Parisi-Zhang equation with flat and Brownian initial conditions, *Phys. Rev. E* **105**, 054142 (2022).
- [12] A. Shabat and V. Zakharov, Exact theory of two-dimensional self-focusing and one-dimensional self-modulation of waves in nonlinear media, *Sov. Phys. JETP* **34.1** (1972).
- [13] M. J. Ablowitz, D. J. Kaup, A. C. Newell, and H. Segur, The inverse scattering transform-Fourier analysis for nonlinear problems, *Stud. Appl. Math.* **53**, 249 (1974).
- [14] D. J. Kaup and A. C. Newell, An exact solution for a derivative nonlinear Schrödinger equation, *J. Math. Phys.* **19**, 798 (1978).
- [15] G. Barraquand and I. Corwin, Random-walk in β -distributed random environment, *Probab. Theory Relat. Fields* **167**, 1057 (2017).
- [16] P. Le Doussal and T. Thiery, Diffusion in time-dependent random media and the Kardar-Parisi-Zhang equation, *Phys. Rev. E* **96**, 010102(R) (2017).

- [17] I. Corwin and Y. Gu, Kardar-Parisi-Zhang equation and large deviations for random walks in weak random environments, *J. Stat. Phys.* **166**, 150 (2017).
- [18] T. Thiery and P. Le Doussal, Exact solution for a random walk in a time-dependent 1D random environment: The point-to-point β polymer, *J. Phys. A: Math. Theor.* **50**, 4 (2016).
- [19] G. Barraquand and M. Rychnovsky, Large deviations for sticky Brownian motions, *Electron. J. Probab.* **25**, 1 (2020).
- [20] G. Barraquand and P. Le Doussal, Moderate deviations for diffusion in time dependent random media, *J. Phys. A: Math. Theor.* **53**, 215002 (2020).
- [21] D. Bernard and P. Le Doussal, Entanglement entropy growth in stochastic conformal field theory and the KPZ class, *Europhys. Lett.* **131**, 10007 (2020).
- [22] G. Barraquand, Some integrable models in the KPZ universality class (Université Paris Diderot-Paris 7, 2015), <https://tel.archives-ouvertes.fr/tel-01167855>.
- [23] C. Kipnis, C. Marchioro, and E. Presutti, Heat flow in an exactly solvable model, *J. Stat. Phys.* **27**, 65 (1982)
- [24] L. Bertini, A. De Sole, D. Gabrielli, G. Jona-Lasinio, and C. Landim, Current Fluctuations in Stochastic Lattice Gases *Phys. Rev. Lett.* **94**, 030601 (2005).
- [25] L. Bertini, D. Gabrielli, and J. L. Lebowitz, Large deviations for a stochastic model of heat flow, *J. Stat. Phys.* **121**, 843 (2005).
- [26] B. Derrida and A. Gerschenfeld, Current fluctuations in one-dimensional diffusive systems with a step initial density profile, *J. Stat. Phys.* **137**, 978 (2009).
- [27] V. Lecomte, A. Imparato, and F. van Wijland, Current fluctuations in systems with diffusive dynamics, in and out of equilibrium, *Prog. Theor. Phys. Suppl.* **184**, 276 (2010).
- [28] P. L. Krapivsky and B. Meerson, Fluctuations of current in nonstationary diffusive lattice gases, *Phys. Rev. E* **86**, 031106 (2012).
- [29] L. Zarfaty and B. Meerson, Statistics of large currents in the Kipnis-Marchioro-Presutti model in a ring geometry *J. Stat. Mech.* (2016) 033304.
- [30] T. Bodineau and B. Derrida, Distribution of current in nonequilibrium diffusive systems and phase transitions *Phys. Rev. E* **72**, 066110 (2005)
- [31] J. Tailleur, J. Kurchan, and V. Lecomte, Mapping Nonequilibrium Onto Equilibrium: The Macroscopic Fluctuations of Simple Transport Models, *Phys. Rev. Lett.* **99**, 150602 (2007).
- [32] P. I. Hurtado and P. L. Garrido, Spontaneous Symmetry Breaking at the Fluctuating Level, *Phys. Rev. Lett.* **107**, 180601 (2011); A. Prados, A. Lasanta, and P. I. Hurtado, Nonlinear driven diffusive systems with dissipation: Fluctuating hydrodynamics *Phys. Rev. E* **86**, 031134 (2012); C. Gutiérrez-Ariza and P. I. Hurtado, The kinetic exclusion process: A tale of two fields *J. Stat. Mech.* (2019) 103203.
- [33] M. A. Peletier, F. H. J. Redig, and K. Vafayi, Large deviations in stochastic heat-conduction processes provide a gradient-flow structure for heat conduction *J. Math. Phys.* **55**, 093301 (2014).
- [34] O. Shpielberg, Y. Don, and E. Akkermans, Numerical study of continuous and discontinuous dynamical phase transitions for boundary-driven systems, *Phys. Rev. E* **95**, 032137 (2017).
- [35] A. Grabsch, A. Poncet, P. Rizkallah, P. Illien, and O. Bénichou, Closing and solving the hierarchy for large deviations and spatial correlations in single-file diffusion, [arXiv:2110.09269](https://arxiv.org/abs/2110.09269).
- [36] A. Poncet, A. Grabsch, P. Illien, and O. Bénichou, Generalized Correlation Profiles in Single-File Systems, *Phys. Rev. Lett.* **127**, 220601 (2021).
- [37] Since $\hat{\Phi}(Z)$ may not be convex it should be called a Legendre-Fenchel transform, which is not involutive [44].
- [38] We will keep β as a parameter but for the application to obtain $\Psi(z)$ it is understood that it is set to $\beta = -1$.
- [39] Comparing with Ref. [10] the “true” coupling constant is in fact $\hat{g} = \Lambda g = -z^{\frac{\xi}{2}} e^{-\frac{\xi^2}{4}}$.
- [40] Eldad Bettelheim, N. R. Smith, and B. Meerson, Inverse Scattering Method Solves the Problem of Full Statistics of Nonstationary Heat Transfer in the Kipnis-Marchioro-Presutti Model, *Phys. Rev. Lett.* **128**, 130602 (2022).
- [41] Wadati, Miki, K. Konno, and Y.-H. Ichikawa, A generalization of inverse scattering method, No. IPPJ-381. Nagoya Univ. (Japan). Inst. of Plasma Physics (1979).
- [42] K. Mallick, H. Moriya, and T. Sasamoto, Exact Solution of the Macroscopic Fluctuation Theory for the Symmetric Exclusion Process, *Phys. Rev. Lett.* **129**, 040601 (2022).
- [43] When the integrand has a jump at $q = 0$, one integrates respecting the symmetry $iq \rightarrow -iq$, equivalently one integrates on \mathbb{R}^- and take twice the real part.
- [44] H. Touchette, The large deviation approach to statistical mechanics, *Phys. Rep.* **478**, 1 (2009).
- [45] A. Krajenbrink and P. Le Doussal (unpublished).
- [46] P. Le Doussal, S. N. Majumdar, A. Rosso, and G. Schehr, Exact Short-Time Height Distribution in the One-Dimensional Kardar-Parisi-Zhang Equation and Edge Fermions at High Temperature, *Phys. Rev. Lett.* **117**, 070403 (2016).
- [47] For the KPZ equation the partition sum $Z_{\text{KPZ}} = e^{H_{\text{KPZ}}}$ is an unbounded random variable. As a result the rate function $\Psi(\bar{z})$ is undefined for $\bar{z} < -1$. The present convergence results show precisely how, in the large ξ limit, one goes from a bounded random variable Z to an unbounded one Z_{KPZ} .
- [48] A. Krajenbrink and P. Le Doussal, Simple derivation of the $(-\lambda H)^{5/2}$ large deviation tail for the 1D KPZ equation, *J. Stat. Mech.* (2018) 063210.
- [49] A. Krajenbrink, P. Le Doussal, and S. Prolhac, Systematic time expansion for the Kardar-Parisi-Zhang equation, linear statistics of the GUE at the edge and trapped fermions, *Nucl. Phys. B* **936**, 239 (2018).
- [50] A. Krajenbrink, Beyond the typical fluctuations: A journey to the large deviations in the Kardar-Parisi-Zhang growth model, Ph.D. thesis, PSL Research University, 2019.
- [51] I. Corwin (private communication).
- [52] Although it maps to the $\{P, Q\}$ system with $\delta - \delta$ initial conditions (as was the case in the study of the WNT of the KPZ equation with droplet initial condition) because of the highly nonlocal nature of the mapping it does not map SSEP observables to KPZ ones in any obvious way.
- [53] L.-C. Tsai, Integrability in the weak noise theory, [arXiv:2204.00614](https://arxiv.org/abs/2204.00614).
- [54] See, e.g., Sec. 3.3.1. in M. Dunajski, *Solitons, Instantons and Twistors* (Oxford University Press, Oxford, 2009).
- [55] A. V. Kisil, The relationship between a strip Wiener-Hopf problem and a line Riemann-Hilbert problem, *IMA J. Appl. Math.* **80**, 1569 (2015).
- [56] Chapter 1.3 in B. Noble, *Methods Based on the Wiener-Hopf Technique for the Solution of Partial Differential Equations*,

- International Series of Monographs on Pure and Applied Mathematics (Pergamon Press, New York, 1958), Vol. 7.
- [57] R. M. Corless, G. H. Gonnet, D. E. Hare, D. J. Jeffrey, and D. E. Knuth, On the Lambert W function, *Adv. Comput. Math.* **5**, 329 (1996).
- [58] A. Krajenbrink and P. Le Doussal, Exact short-time height distribution in the one-dimensional Kardar-Parisi-Zhang equation with Brownian initial condition, *Phys. Rev. E* **96**, 020102(R) (2017).
- [59] J. Yu, Edwards-Wilkinson fluctuations in the Howitt-Warren flows, *Stoch. Process. Appl.* **126**, 948 (2016).
- [60] M. Balázs, F. Rassoul-Agha, and T. Seppalainen, The random average process and random walk in a space-time random environment in one dimension, *Commun. Math. Phys.* **266**, 499 (2006).
- [61] C. Howitt and J. Warren, Consistent families of Brownian motions and stochastic flows of kernels, *Ann. Probab.* **37**, 1237 (2009).
- [62] D. Brockington and J. Warren, The bethe ansatz for sticky brownian motions, [arXiv:2104.06482](https://arxiv.org/abs/2104.06482).
- [63] K. Gawędzki and P. Horvai, Sticky behavior of fluid particles in the compressible Kraichnan model, *J. Stat. Phys.* **116**, 1247 (2004).
- [64] H. Spohn, *Large Scale Dynamics of Interacting Particles* (Springer, New York, 1991).
- [65] M. Wadati and K. Sogo, Gauge transformations in soliton theory, *J. Phys. Soc. Jpn.* **52**, 394 (1983).
- [66] L. Bertini, A. De Sole, D. Gabrielli, G. Jona-Lasinio, and C. Landim, Toward a nonequilibrium thermodynamics: A self-contained macroscopic description of driven diffusive systems, *J. Stat. Phys.* **135**, 857 (2009).
- [67] G. Barraquand and M. Rychnovsky, Random walk on nonnegative integers in β -distributed random environment, *Commun. Math. Phys.* (2022), doi: [10.1007/s00220-022-04536-1](https://doi.org/10.1007/s00220-022-04536-1).
- [68] B. Tsirelson and S. Limit, *Noise, Stability*, Lectures on Probability Theory and Statistics (Springer, Berlin, 2004), pp. 1–106.
- [69] Y. L. Jan and O. Raimond, Sticky flows on the circle and their noises, *Probab. Theory Relat. Fields* **129**, 63 (2004); The noise of a Brownian sticky flow is black, [arXiv:math/0212269](https://arxiv.org/abs/math/0212269).